FUNCTIONAL ROLE OF CBX2 IN THE PATHOGENESIS OF HEPATOCELLULAR CARCINOMA

WANG YIXIANG

PhD

The Hong Kong Polytechnic University

2025

The Hong Kong Polytechnic University

Department of Applied Biology and Chemical Technology

Functional role of CBX2 in the pathogenesis of hepatocellular carcinoma

Wang Yixiang

A thesis submitted in partial fulfilment of the requirement for the degree of Doctor of Philosophy

April 2025

CERTIFICATE OF ORIGINALITY

I hereby declare that this thesis is my own work and that, to the best of my knowledge and belief, it reproduces no material previously published and written, nor material that has been accepted for the award of any other degree or diploma, except where due acknowledgement has been made in the text.

Student Name: Wang Yixiang

Signed:

Abstract

Chromobox 2 (CBX2) is an essential component of the canonical Polycomb Repressive Complex 1 (cPRC1), which plays a role in epigenetic regulation and gene silencing. Earlier findings suggested that aberrant expression of CBX2 is associated with poor prognosis in hepatocellular carcinoma (HCC). However, the underlying mechanisms remain elusive. We confirmed that CBX2 is overexpressed in a subpopulation of HCC patients. While CBX2 expression is low in non-tumorous liver cell lines, it is overexpressed to varying levels in most HCC cell lines examined. CBX2-overexpressing and -knockout cell models were generated to determine the functions of CBX2 in HCC pathogenesis. We found that growth and migratory ability of HCC cells are directly correlated with CBX2 expression levels. Gene knockout of CBX2 also profoundly reduced HCC tumor growth *in vivo*. Transcriptomic and bioinformatics analyses further suggested that genes of the metabolic pathways are enriched in the CBX2-knockout cells. Concordantly, cell growth inhibition of CBX2 knockout cells were associated with reduction in rate of glycolysis and oxidative phosphorylation, with a concomitant reduction in ATP and NAD^+ level. Bioinformatics analysis and functional screen led to the identification of phosphoenolpyruvate carboxykinase 2 (PCK2), a mitochondrial enzyme that catalyzes the conversion of oxaloacetate to phosphoenolpyruvate in the gluconeogenic pathway, was induced in CBX2 knockdown cells and responsible for the growth-inhibition found in these cells. Importantly, knockdown of PCK2 in CBX2-knockout cells restored the rate of glycolysis and NAD^+ level, and completely rescued the cell growth defects due to CBX2 deficiency. Interestingly, overexpression of PCK1, the cytosolic from of PCK, did not have any effect on CBX2-knockout cells. Together these data suggested that PCK2 potentially regulates cell growth through yet-unknown activity. Our findings uncovered a novel functional role of CBX2-PCK2 regulatory axis in HCC growth, revealed a novel target for the development of novel HCC therapeutics.

Acknowledgment

First and foremost, I would like to extend my deepest gratitude to Prof. Ko Chi Bun, Ben, my supervisor, for his guidance, patience and expertise thorough my whole PhD project. I am grateful to him for providing my with an opportunity to study in the Hong Kong Polytechnic University and work in his research team in the Department of Applied Biology and Chemical Technology. I would like to express my gratitude to Dr. Ben Ko for his careful guidance in the process of completing this thesis, and I am really appreciate his support and assistance to me during my whole PhD study.

Also, I am grateful and thankful to Prof. Zhao Yanxiang and Prof. Lee Kin-wah, Terence and their lab for kind assistance for my project. I also express my appreciation to Prof. Zhang Yaojun and Dr. Wang Juncheng from Guangzhou Sun Yat-seq University Cancer Centre, for providing the HCC specimens. My sincere thanks to my colleague, Dr. Zhang Yajing, Dr. Chan Wing Chueng, Dr. Chueng Yuk Kim, Dr. Liu Hang, Mr Liu Mingkang, Miss Chau Po Ki and Miss Zhao Siming for their collaboration and insightful feedback on this project. Lastly, I am indebted my parents and girlfriend for their emotional support during my PhD study. I thank everyone who contributed directly or indirectly to this project.

Table of Content

List of Abbreviations

CBX2	Chromobox 2
cPRC1	Canonical Polycomb Repressive Complex 1
HCC	Hepatocellular carcinoma
PCK2	Phosphoenolpyruvate carboxykinase 2
HBV	Hepatitis B virus
HCV	Hepatitis C virus
NAFLD	Non-alcoholic fatty liver disease
RAF	Rapidly accelerated fibrosarcoma
EMT	Epithelial-mesenchymal transition
MMPs	Matrix metalloproteinases
ECM	Extracellular matrix
PKM2	Pyruvate kinase isozymes M2
CSC	Cancer stem cell
TCA cycle	Tricarboxylic acid cycle
OXPHOS	Oxidative phosphorylation
ROS	Reactive oxygen species
AMPK	AMP-activated protein kinase
PGC-1α	Peroxisome proliferator-activated receptor gamma coactivator 1-alpha
SIRT1	Sirtuin-1
NADPH	Nicotinamide adenine dinucleotide phosphate
NAD^+	Nicotinamide adenine dinucleotide
HK	Hexokinase
PFK	Phosphofructokinase
PKs	Pyruvate kinases

G-6-P	Glucose-6-phosphate
F-6-P	Fructose-6-phosphate
F-1,6-BP	Fructose-1,6-bisphosphate
PEP	Phosphoenolpyruvate
2-DG	2-Deoxy-D-Glucose
FCCP	Carbonyl cyanide-p-trifluoromethoxyphenylhydrazone
G6Pase	Glucose-6-phosphatase
PEPCK	Phosphoenolpyruvate carboxykinase
OAA	Oxaloacetate
PC	Pyruvate carboxylase
PCK1	Phosphoenolpyruvate carboxykinase 1
PCK2	Phosphoenolpyruvate carboxykinase 2
NAM	Nicotinamide
NAMPT	Nicotinamide phosphoribosyltransferase
FAO	Fatty acid oxidation
TP53	Tumor protein P53
SMAD6	SMAD family member 6
PTMs	Post-translational modifications
H2Bub	Monoubiquitylation of H2B
H2Aub	Monoubiquitylation of H2A
HATs	Histone acetyltransferases
HDACs	Histone deacetylases
RTKs	Receptor tyrosine kinases
EGF	Epidermal growth factor
EZH2	Enhancer of zeste 2 polycomb repressive complex

PcG	Polycomb Group
PREs	Polycomb response elements
CMMs	Cell memory modules
PRC1	Polycomb Repressive Complex 1
PRC2	Polycomb Repressive Complex 2
PhoRC	Pho-repressive complex
PR-DUB	Polycomb repressive deubiquitinase
PCGF	Polycomb group ring finger protein
RING1/2	Really interesting new gene 1 and 2
CBX	Chromobox
PHC	Polyhomeotic-like protein
EED	Embryonic ectoderm development
SUZ12	Suppressor of zeste 12
HMT	Histone methyltransferase
HIF-1α	Hypoxia-inducible factor 1-alpha
ITRs	Inverted terminal repeats
WNK	With-no-lysine (K) kinase
WTIP	Wilms' tumor protein 1 interacting protein
YAP	Yes-associated protein
GOT2	Glutamic-oxaloacetic transaminase

1 Introduction

1.1 HCC

HCC ranks the sixth most prevalent cancer globally and is the third leading cause of cancer-related mortality(1). Originating from mature hepatocytes, HCC accounts for 85%-90% of all primary liver cancer cases(2). It is particularly prevalent in Sub-Saharan Africa and Southeast Asia, where it constitutes over 50% of liver cancer incidences in these regions. HCC is often diagnosed at an advanced, inoperable stage, and its prognosis remains poor. Beyond surgical resection, alternative interventions like transarterial chemoembolization, systemic therapy, targeted therapy, and immune checkpoint therapy offer limited life extension for patients with advanced HCC (3). Moreover, systemic therapy is poorly tolerated by patients with significant liver dysfunction. Despite this, immune checkpoint therapy has shown notable efficacy, and the combination of molecular and targeted therapies with immunotherapy presents promising avenues for research.

1.2 Epidemiology and Risk Factors

Notably, Asia accounts for approximately 72% of HCC occurrences, where China reporting the highest incidence rate at 18.3%, largely attributed to its vast population (4). The variability in HCC incidence across regions is influenced by distinct risk factors, including Hepatitis B virus (HBV) and Hepatitis C virus (HCV) infections. HBV and HCV infection accounts for 50% and 20% of all HCC cases respectively (5). Besides viral infections, alcohol consumption and smoking are recognized risk factors for HCC. In addition, nearly 1% of patients with non-alcoholic fatty liver disease (NAFLD) and cirrhosis develop HCC annually, indicating a rising concern of HCC pathogenesis (6). Recent epidemiological research has also highlighted a potential link between diabetes and HCC, particularly in patients with NAFLD (7).

1.3 Approved Drugs for HCC

Currently, several medications such as cisplatin, gemcitabine, and sorafenib have been approved for clinical use in treating HCC(8-10). These drugs effectively inhibit tumor growth, but long-term use may lead to drug resistance in cancer cells (11-13).

Cisplatin's effectiveness stems from its molecular structure, which contains chloride atoms. These atoms are released and replaced by water molecules, generating a positive charge that reacts with nucleophilic sites on DNA and proteins. This reaction causes cross-linking between adjacent guanines on the same DNA strand, inhibiting DNA replication and transcription, and ultimately disrupting the normal cell cycle, leading to cell death. Nonetheless, cisplatin also affects normal, healthy dividing cells, resulting in side effects such as nephrotoxicity, neurotoxicity, nausea, and ototoxicity (14).

Gemcitabine is transported into cells via nucleoside transporters and is then phosphorylated into gemcitabine monophosphate by deoxycytidine kinase. This process inhibits DNA synthesis by incorporating gemcitabine monophosphate into DNA strands. However, it also harms dividing cells, both cancerous and healthy cells (15).

Sorafenib, recognized as an effective treatment for liver cancer, acts as a kinase inhibitor, targeting several protein kinases including vascular endothelial growth factor receptor, platelet-derived growth factor receptor, and rapidly accelerated fibrosarcoma (RAF) kinases (16). It down-regulates the expression of cell cycle control protein called Cyclin D1, and enhances the DNA replication, recombination and repair, cell adhesion, metabolism, and transport in liver cancer (16). Despite its high efficacy, sorafenib may still induce side effects such as fatigue, rash, diarrhea and osteonecrosis, and even result in drug resistance in HCC (17).

1.4 Pathogenesis of HCC

Previous study indicated that the development of HCC involves a cascade of molecular alternations. These include dysregulation of inflammatory cytokines and chemokines, gene mutations and alternation in epigenetics, changes in micro-environment, aberrant regulation of liver cell stemness and dysregulation of signaling pathways (18) . These changes lead to inflammation and fibrosis of the liver, resulting in chronic hepatitis and cirrhosis, and predispose HCC development (19, 20). In the case of HBV and HCV infection, the virus promotes interleukin-6 production and secretion in inflammation associated cells, leading to activation of the STAT3 signaling pathway, resulting in epithelial-mesenchymal transition (EMT) (21). EMT represents a critical transformation process enabling transformed cells to acquire malignant characteristics, notably invasiveness and migration capabilities. Throughout this process, cells lose their epithelial attributes, such as apicobasal polarity and extracellular adhesion, transitioning into a mesenchymal phenotype (22). EMT is also associated with drug resistance, posing challenges in cancer management (23). The matrix metalloproteinases (MMPs) protein family play a pivotal role in degrading extracellular matrix (ECM) structural proteins, facilitating cell proliferation, migration, and invasion (24). Elevated levels of MMPs, including MMP1, MMP2, MMP3, MMP7, and MMP8, are observed in HCC, marking a significant indicator of malignancy (25).

Besides, HCC pathogenesis was also accompanied by abnormal expression of essential metabolic enzyme, such as pyruvate kinase isozymes M2 (PKM2). Previous study showed that PKM2 is elevated in HCC and drives HCC progression by inducing an immunoosuppressive microenvironment(26). It has also been reported that PKM2 can sustain the cancer stem cell (CSC) microenvironment, promoting cancer stemness and metastasis. CSCs, or tumor-initiating cells, marked by $CD34^{+}$, demonstrate the ability to form progenitor

colonies. CD34 is a transmembrane protein that initially identified as a biomarker for hematopoietic stem cell progenitors. Previous research has indicated that CD34 is implicated in HCC, where it is associated with tumor angiogenesis, metastasis, and resistance to conventional therapy (27). These CD34-positive cells enhance self-renewal capabilities and promote tumor initiation compared to CD34-negative cells (28). Hence, it is essential to underscore the critical role of CSCs in tumor heterogeneity and hierarchy, beyond genetic and epigenetic influences (29, 30). CSCs have been detected in various cancers, including lung, pancreatic, breast, prostate, colon, glioma, and liver cancers, where they are associated to malignancy and recurrence (31). Characteristically, CSCs contribute to drug resistance and relapse post-therapy by evading drug action through mechanisms such as DNA damage repair, drug efflux protein activation, EMT, and self-renewal capabilities (32). They also counteract DNA damage effect with chemotherapy through hypoxia and abnormal angiogenesis (33), CSCs take advantage of improperly DNA repair pathway, exploiting them to overcome the chemotherapy induced cell death (34). CSCs also maintain a low differentiation state, perpetuating drug resistance and posing significant challenges to cancer therapy. In HCC, liver cancer stem cells (LCSCs) enhance primary cancer proliferation and secondary cancer metastasis (35). Several biomarkers, including EpCAM, CD133, CD44, CD13, CD90, CD24, and OV6, have been validated in LCSCs, offering strategies for cancer stem cell targeting and recurrence prevention (36). For instance, cells expressing $EpCAM^{+}CD45^{-}$ have been shown to initiate tumor formation in mouse models, implicating the role of EpCAM in carcinogenesis (37). Besides, CD133, a cell surface glycoprotein, is implicated in various biological pathways, including cell self-renewal and therapeutic resistance, and is considered a biomarker in liver cancer (38). Increased CD133 expression correlates with poor prognosis and higher recurrence rates in HCC patients (39). Recent advancements have introduced precision drugs targeting specific markers to eliminate cancer stem cells, such as VB4-845,

which inhibits tumor sphere formation with high EpCAM expression, and measles viruses shown to effectively target $CD133^+$ tumor cells.

1.5 Oxidative Phosphorylation and Warburg Effect in HCC

The liver plays a pivotal role in regulating metabolic processes, including detoxification, glycogen storage, and secretion of metabolic hormones. Due to its high mitochondrial density, the liver is central to metabolic activities such as beta-oxidation, the tricarboxylic acid cycle (TCA cycle), ketogenesis, respiratory activities, and ATP synthesis through oxidative phosphorylation (OXPHOS). These processes may undergo significant alterations in the context of HCC development (40). Recent studies have indicated that disruptions in mitochondrial metabolic pathways, caused by mitochondrial DNA damage, can lead to an increase in reactive oxygen species (ROS) within mitochondria, known as "ROS mito-flashes," and mitochondrial depolarization (41). These phenomena have been observed in various human cancers, including HCC (42). Furthermore, research has shown that AMP-activated protein kinase (AMPK) enhances ATP production from OXPHOS, thereby modulating cellular metabolic pathways. AMPK also influences the oxidative response of mitochondria by activating the peroxisome proliferator-activated receptor gamma coactivator 1-alpha (PGC-1α), a crucial regulator of the tumor promoter sirtuin-1 (SIRT1). The activation of SIRT1 by PGC-1α is believed to enhance the invasive and migratory capabilities of HCC cells by boosting biosynthesis activities and ATP production (43).

Due to the high demand for nutrients and energy required for uncontrolled cell proliferation, invasion, and migration, cancer cells must adapt their ATP supply and various material sources through a process called metabolic reprogramming. This process remodels catabolic and anabolic metabolism in tumor tissue, compared to non-tumor tissue, to create a cancer cell micro-environment and support tumor growth (44). Under normal conditions, ATP is

primarily generated from glucose, fatty acid, and amino acid catabolism through processes such as glycolysis, the TCA cycle, OXPHOS, and beta-oxidation. During these processes, glucose, fatty acids, and proteins are broken down into macromolecules, which are then converted to ATP to fulfill the cell's energy demands. Especially OXPHOS, occurring mainly in mitochondria, is the primary process of energy supply. However, cancer cells tend to produce ATP through conversion of pyruvate to lactate under normal oxygen conditions, a phenomenon known as aerobic glycolysis, or the Warburg effect. Warburg effect was first discovered by Otto Warburg and colleagues in the 1920s and has been extensively studied in recent decades (45). Although aerobic glycolysis is less efficient for ATP generation compared to OXPHOS, the significant higher rate of glucose metabolism in cancer cells through aerobic glycolysis provides a greater amount of ATP for cancer cell development in a given period (46). Recent evidence shows that cancer cells increase ATP production by altering the activity of NA^+/K^+-ATPase pumps in the cell membrane, leading to a rapid increase in aerobic glycolysis while mitochondrial oxidation remains constant (47). Additionally, the higher demand for glucose as a carbon source in aerobic glycolysis promotes the synthesis of nucleotides, lipids, and proteins through branching pathways. For example, phosphoglycerate dehydrogenase can divert carbon molecules from glucose into de novo serine biosynthesis (48). Increased aerobic glycolysis may also support de novo lipid synthesis by reducing nicotinamide adenine dinucleotide phosphate (NADPH) equivalents in the oxidative branch of the pentose phosphate pathway (49). Another proposed mechanism supporting biosynthesis pathways in the Warburg effect is the regeneration of nicotinamide adenine dinucleotide (NAD^+) from NADH during the conversion of pyruvate to lactate. In aerobic glycolysis, NAD^+ is converted into NADH by glyceraldehyde phosphate dehydrogenase, and the regeneration of NAD^+ during lactate production helps maintain the

NAD^+ pool for glycolysis, thus allowing rapid biosynthesis to support cancer cell growth and development (50).

There are three key enzymes essential for aerobic glycolysis: hexokinase (HK), phosphofructokinase (PFK), and pyruvate kinases (PKs). The abnormal expression of these enzymes significantly influences the progression of HCC. HK is responsible for converting glucose to glucose-6-phosphate (G-6-P), and recent studies have shown that HK2, the most efficient isoform of HK, is regulated by multiple signaling pathways, including the PI3K/Akt/HIF-1α axis, the β-catenin/c-Myc signaling pathway and STAT3 signaling pathway (51). Thus, recent studies support that HK2 is a highly promising target for HCC treatment.

As the second rate-limiting enzyme of glycolysis, PFK converts fructose-6-phosphate (F-6-P) to fructose-1,6-bisphosphate (F-1,6-BP) and plays an essential role in the regulation of glycolysis in HCC(51). Increased PFK-1 activity has been validated to promote glycolysis and proliferation in HCC (52). Lastly, the final rate-limiting enzyme, PKs, catalyzes the conversion of phosphoenolpyruvate (PEP) to produce ATP. One isoform of PKs, called PKM2, is highly upregulated in cancer cells and is associated with poor prognosis (53). HCC cells can activate glucose uptake and increase oxidative stress with high PKM2 expression levels (54). Previous studies have reported that inhibitors such as compound 3k and shikonin, which target the formation of PKM2, can inhibit the growth of HCC, providing new therapeutic targets for HCC treatment (55).

Except for these inhibitors, multiple molecular drugs targeting different glycolytic enzymes have been discovered, including 2-Deoxy-D-Glucose (2-DG), 3-PO, FX11, and lonidamine, which provide a novel dimension for HCC therapy (53-55). For example, 2-DG, a glucose

analog, can inhibit both glucose uptake and the activity of HK2 (56). Previous study showed that combination of 2-DG with sorafenib suppressed the growth and motility of HCCs more effectively than 2-DG or sorafnib alone (57). Additionally, lonidamine, a small-molecule anticancer drug, can inhibit both HK2 and the mitochondrial pyruvate carrier, thereby strongly suppressing glycolysis and mitochondrial activity (58). Recent evidence revealed that post-treatment with lonidamine could increase the cytotoxicity of some anti-tumor drugs by inhibiting cell damage repair (59).

Besides, gluconeogenesis is a crucial metabolic pathway for generating energy from non-carbohydrate sources such as lactate, glutamine, alanine, and glycerol during fasting states(60). The liver releases energy to muscle, adipose tissue, and other extra-hepatic tissues to maintain circulation and metabolism in energy-limited conditions (61). Recent research indicates that gluconeogenesis is absent in malignant human hepatocytes and also suggests that promoting a switch from glycolysis to gluconeogenesis may inhibit tumor growth and induce apoptosis (62), providing a novel clinical approach for HCC therapy.

Most steps in gluconeogenesis are the reverse of glycolysis, except three unique steps that utilize distinctive enzymes, including fructose-1,6-bisphosphatase, glucose-6-phosphatase (G6Pase), and phosphoenolpyruvate carboxykinase (PEPCK). Fructose-1,6-bisphosphatase converts fructose 1,6-bisphosphate to fructose 6-phosphate, while G6Pase generates glucose from glucose-6-phosphate (63). These two enzymes are responsible for late-stage gluconeogenesis, whereas PEPCK catalyzes the conversion of oxaloacetate (OAA) to PEP in an early step following the carboxylation of lactate to pyruvate by pyruvate carboxylase (PC) (64). PEPCK not only participates in gluconeogenesis but also contributes to cataplerosis in the TCA cycle. Compounds entering the TCA cycle can be utilized by PEPCK to fulfill the demands of gluconeogenesis and other metabolic pathways, including serine synthesis, and

the pentose phosphate pathway (65). Increasing evidence suggests that tumor cells exploit PEPCK to meet their high energy demands, and abnormal PEPCK expression compared to adjacent non-tumorous tissue is observed in many cancer types (64). PEPCK has two isoforms, PEPCK1 (PCK1) and PEPCK2 (PCK2), located in the cytosol and mitochondria, respectively. Overexpression of PCK1 is noted in colon cancer and melanoma, while significantly higher levels of PCK2 are found in lung, breast, and bladder cancers(66). However, in gluconeogenic organs such as the liver and kidney, the expression of both PEPCK isoforms is negligible. PEPCKs are considered a tumor suppressor, inhibiting glycolysis and the TCA cycle to prevent energy generation for liver and kidney's tumor growth (64).

1.6 NAD^+ and $NADP^+$ in HCC

NAD^+ is a coenzyme involved in various metabolic pathways, including glycolysis, TCA cycle and OXPHOS. It is generally produced through three pathways: the de novo synthesis pathway, the Preiss-Handler pathway, and the salvage pathway. The de novo synthesis pathway and the Preiss-Handler pathway used tryptophan and nicotinic acid respectively. They were regarded as two inefficient methods to synthesis NAD^+, because the two processes are highly energy-consuming. The salvage pathway, using nicotinamibe riboside as a starting material, is less energy-consuming (Fig. 1-1). NAD^+ is primarily consumed by sirtuins, glycohydrolases, and poly(ADP-ribose) polymerase respectively (67). Nicotinamide (NAM), a byproduct of these consumption reactions, is recycled back to NAD^+ by nicotinamide phosphoribosyltransferase (NAMPT) to replenish the NAD^+ pool. Liver is the organ that heavily relied on the salvage pathway and supplying NAD^+ to peripheral tissues, while other organs relied on circulating NAM made by the liver (68).

A growing body of research suggests that impaired NAD^+ production and degradation are strongly associated with carcinogenesis and tumor growth (69). In the salvage pathway, NAMPT is a key enzyme for NAD^+ production, and its upregulation in cancer leads to abnormal NAD^+ accumulation and resistance to NAMPT inhibitors in clinical settings (70). Although NAD^+ levels vary depending on glucose levels, age, calorie intake, exercise, etc., the concentrations of NAD^+ in the cytosol and nucleus are similar, while the mitochondrial NAD^+ pool is much higher and considered as an independent storage due to the mitochondrial membrane's impermeability to NAD^+ and NADH (71). Until now, no definite NAD^+ transporter has been identified in mammalian cells (72, 73). However, researchers recently identified solute carrier family 25 member 51 as a potential mitochondrial NAD^+ transporter, although the detailed molecular mechanism remains unclear (74, 75). It is worth noting that cytosolic NAD^+ levels vary across cell types and are higher in hepatocytes and astrocytes compared to others (76). Additionally, T cells with relatively lower CD38 expression showed higher NAD^+ levels and inhibit tumor activity, suggesting NAD^+ may be involved in the anti-tumor immune response (77).

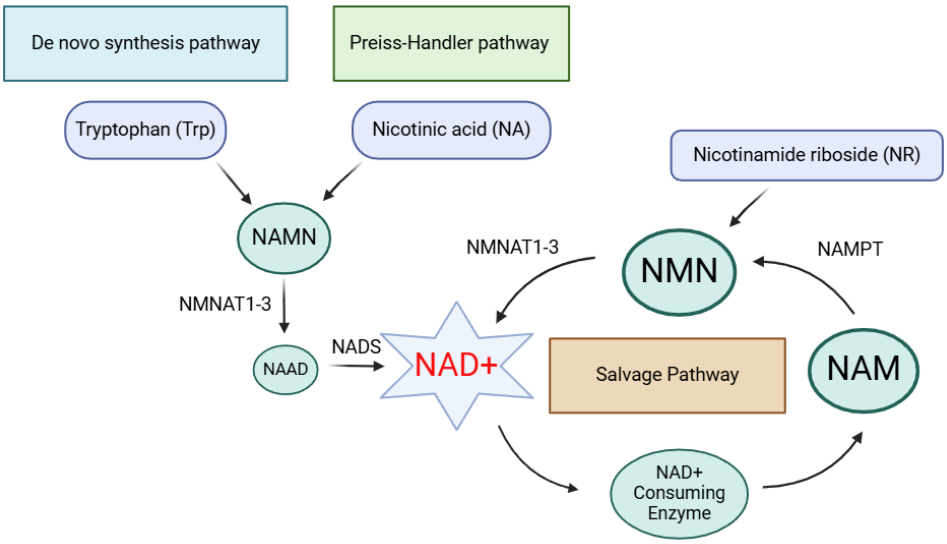

Figure. 1-1 NAD^+ synthesis pathway (Figure generated using BioRender).

Besides NAD^+, $NADP^+$ is another essential coenzyme. It is converted from NAD^+ through the transfer of a phosphate group of from ATP on to the 2-hydroxyl group of the adenosine ribose moiety, so the structure of $NADP^+$ highly resembles NAD^+. However, while NAD^+ is mostly involved in catabolic reactions, $NADP^+$ is primarily involved in anti-oxidative effect and anabolic reactions (78). $NADP^+$ levels are regulated by multiple signaling pathways, such as the PPP pathway, cytosolic and mitochondrial NADP-dependent isocitrate dehydrogenase, glutamine metabolism, and fatty acid oxidation (FAO) (79). Recent evidence suggested that $NADP^+$ was primarily reduced to NADPH in the PPP, enabling cancer cells to survive high levels of ROS (80). As ROS plays a pivotal role by not only inducing cell death but also increasing cancer risk when cells have insufficient antioxidative defenses, cancer cells ensure ROS levels are restrict in dynamic range that allows cell proliferation without cell damage (80). Increasing ROS production is reported to be associated with the stimulation of proliferation and cell survival by up-regulating antioxidant transcription factors and reprogramming NADPH metabolism (81).

1.7 Genetic Alteration and HCC

Genetic alterations are closely linked to the occurrence and development of HCC. These include mutations and amplification of proto-oncogenes; mutations and deletion of tumor suppressor genes; and gene alternations in critical pathways such as the cell cycle, cell adhesion, apoptosis, and differentiation (82). The most frequently mutated genes in HCC include telomerase reverse transcriptase, catenin beta 1, tumor protein P53 (TP53), axin1 and AT-rich interaction domain 1A and 2, while the rest of the mutations account for less than 10% of all HCC cases (83). Most HCCs develop from gene mutations that primarily affect the abnormal regulation of major biological activities, including the maintenance of telomeres, the Wnt/β-catenin pathway, the P53 pathway, the cell cycle, the RAS/MAPK/ERK pathway,

the AKT/mTOR pathway, epigenetic regulation, chromatin remodelling, oxidative stress, and angiogenesis (83).

1.7.1 DNA Methylation and HCC

DNA methylation primarily occurs at cytosine bases (C) followed by guanine (G), known as CpG sites. In the human genome, 70-80% of CpG sites are methylated, mainly located in regions with low CpG density or repetitive DNA sites. Generally, methylation of promoter regions causes gene repression, while methylation within gene bodies suggests gene activation. This pattern is commonly observed in various cancer types, including HCC (84). Previous research has identified three types of abnormal DNA methylation mechanisms related to HCC. Firstly, hypermethylation of CpG islands in promoter regions of tumor suppressor genes could lead to gene repression and loss of function. Besides, gene instability and oncogene activation caused by low methylation levels in genes and repetitive DNA sites cause hypomethylation in these regions, which can activate oncogenes and cause genomic instability. Lastly, aberrant activity of DNA methyltransferases can disrupt normal methylation patterns, contributing to carcinogenesis (85). Over the past few decades, scientists have identified many genes with high levels of methylation in HCC, including cyclin dependent kinase inhibitor 2A, Ras association domain family member, adenomatous polyposis coli, and SMAD family member 6 (SMAD6). Conversely, few hypomethylated genes have been described, such as insulin like growth factor 2, C-C motif chemokine ligand 20, and NAD(P)H quinone dehydrogenase 1 (86).

1.7.2 Epigenetic Regulation of Histone and HCC

Genetic information is largely identical in every cell of a eukaryote, but gene expression patterns can be tissue- and organ-specific, enabling cells to play different roles depending on their location. Maintaining appropriate cellular function relies on a balance of stability and reversibility in gene expression. The nucleosome, the basic unit of chromatin in eukaryotes,

consists of genomes tightly wrapped around octamers of core histone proteins. These nucleosomes must be packed about ten thousand folds to fit into the nucleus while providing DNA accessibility for proteins involved in transcription, replication, and repair (87).

Nucleosome properties can be changed through various mechanisms. For example, replacement of canonical core histones with specialized variants, which allows the genome to adapt to different functional requirements (88). Previous research indicated that two similar H3 family, including canonical H3 and replacement H3.3, exist in most eukaryotes. And previous study showed that H3.3, which differed from the canonical H3, may result in the dissociation of H2A-H2B and H2A.Z-H2B dimers and reduce the stability of histone in genome (89). Besides, Chromatin remodeling enzymes could also alter the binding sites of histones on DNA, making the DNA more or less accessible for transcription processes. In mammal, SWI/SWF remodeling enzymes are responsible for the alteration of reconstituted chromatin' structure and the BRG1 ATPase, which is a catalytic subunit of SWI/SWF remodeling enzymes, was determined to regulate the P53 in cancer (90). It was reported that the formation of a loop of enhancer and promoter site of MYC locus with the BRG1 dependent chromatin remodeling led to the activation of MYC expression in small cell lung cancer(91). Covalent chemical modifications of histones, including various modifications such as methylation, acetylation, phosphorylation, and ubiquitylation, have recently attracted significant scientific interest due to the discovery of hyperacetylated histones in highly active genes (92). And aberrant histone methylation, acetylation, phosphorylation, and ubiquitylation are the most commonly observed in cancers including HCC(93).

1.7.3 Histone Methylation

Histone methylation occurs on all basic residues: arginines, lysines, and histidines (94). On the ε-amine group of lysines, methylation can be categorized into three groups: monomethylated (me1), dimethylated (me2), or trimethylated (me3). Recently, the most

studied histone methylation sites include H3 lysine 4 (H3K4), H3K9, H3K27, H3K36, H3K79, and H4K20. Histone methylation was originally considered a slower process compared to other post-translational modifications (PTMs) and thought to be irreversible (95). However, the discovery of H3K4 demethylase, lysine-specific demethylase 1A, revealed that histone methylation is reversible (96). The balance between methyltransferases and demethylases has been identified as a key regulator of gene expression. Although some methylation events are stably maintained in the genome, others may be mediated in specific contexts, such as differentiation processes and environmental response activities.

The effect of methylation depends on the context. For example, H3K4me3 is commonly regarded as an active transcriptional marker, while H3K27me3 is associated with repressed chromatin. Nevertheless, some modified histones show opposing activities in different situations, including transcriptional activation and repression. For instance, H3K4me2 and H3K4me3 can be also linked to transcriptional repression when bound by the PHD-domain-containing co-repressor protein inhibitor of growth family member 2 (97). In summary, although methylation is crucial for various biological processes and disruption of its function leads to developmental defects, diseases, or aging, many questions remain. Further research is required to fully understand the mechanisms and effects of histone methylation.

1.7.4 Histone Ubiquitylation

Over the past three decades, histone ubiquitylation has been identified as a crucial modification involved in transcriptional regulation and DNA repair (98). In 1975, histone H2A was first discovered to be modified by ubiquitin in cells. To date, H2A and H2B are regarded as two of the most abundantly modified proteins in the nucleus, with approximately 50% of H2A and 2% of H2B being ubiquitylated (99).

Recent research has highlighted the role of monoubiquitylation of H2A and H2B in transcriptional regulation. Monoubiquitylation of H2A is primarily associated with the gene suppression, while monoubiquitylation of H2B (H2Bub) is generally linked to gene activation. Abnormalities in these modifications can lead to carcinogenesis, and many ubiquitylating enzymes have been identified as oncogenes or tumor suppressors (99, 100). For example, monoubiquitylation of H2A (H2Aub) and H2Bub levels showed dramatically decreased in prostate and breast tumors, respectively (101, 102). Despite these findings, the precise mechanisms by which histone ubiquitylation contributes to these actions remain elusive. Further studies are needed to unravel these mechanisms, with the potential to significantly impact the identification and development of cancer therapies in the future.

1.7.5 Histone Acetylation and Phosphorylation

Histone acetylation is mediated by the opposing actions of histone acetyltransferases (HATs) and histone deacetylases (HDACs). HATs are responsible for adding acetyl groups, while HDACs catalyze their removal (103). Histone acetylation and deacetylation were first identified in the globin gene of chicken erythrocytes, which remain bound to chromatin when the gene is inactive. Compared to histone methylation, histone acetylation is more closely associated with potential gene activity rather than the transcriptional process itself.

When the positively charged lysine residues of histone N-termini are acetylated, the affinity of DNA for the histones decreases. This acetylation allows the N-termini to be released from the nucleosome, leading to nucleosome unfolding and increased accessibility for transcription factors (104). Increased histone acetylation following neuronal activity is crucial for maintaining gene expression levels essential for long-term synaptic plasticity and memory (105). However, little is known about this modification during memory formation in other brain cells. Therefore, more refined research is needed to investigate the role of histone acetylation in other cell types.

1.7.6 Histone Phosphorylation

Recent research has identified that the serine, threonine, and tyrosine residues of histones can be phosphorylated by various protein kinases and dephosphorylated by phosphatases. This chemical modification has been proven to be involved in DNA damage repair, transcription regulation, and chromatin compaction.

For DNA damage repair, the phosphorylation of H2AX is essential. Phosphorylation at serine 139 of the H2AX variant histone occurs in all phases of the cell cycle and participates in various DNA damage response pathways, including non-homologous end joining, homologous recombination, and replication-coupled DNA repair (106-109). However, the same phosphorylation events can be implicated in multiple cellular processes. For example, H4S1ph in yeast is involved not only in chromatin compaction and nucleosome stabilization but also in DNA repair, transcription, and sporulation.

Therefore, histone phosphorylation plays diverse roles in biology and should not be considered in isolation. Further research is needed to identify the mechanisms of recruitment of specific histone variants to chromatin domains in each biological process.

1.8 Signaling Pathway and HCC

1.8.1 Wnt/β-Catenin Pathway

Among all the molecular pathways implicated in the pathogenesis of HCC, the Wnt/β-catenin pathway is one of the most frequently activated. This pathway is involved in embryonic development, adult homeostasis, and regeneration. Aberrant activation of this pathway contributes to various cancers, including gastrointestinal cancer, leukemia, melanoma, breast cancer, and HCC (110, 111).

The Wnt/β-catenin pathway can be divided into the canonical and non-canonical Wnt pathways, which form a concomitant and mutual network of regulation. The canonical Wnt pathway is typically inactivated in adult tissues, as its activation leads to the degradation of β-catenin, a linker between E-cadherin and the cytoskeleton involved in cell adhesion (112). Aberrant activation of the Wnt/β-catenin pathway can result in activation of cell differentiation and lead to liver diseases, including the malignant development of HCC (113).

Additionally, a ligand called WNT5a plays a crucial role in the non-canonical Wnt/β-catenin pathway. WNT5a can activate the canonical Wnt/β-catenin pathway as well as multiple protein kinases and transcription factors (114). Recent findings have shown that WNT5a expression is reduced in HCC, and its overexpression inhibits tumor growth, migration, and colony formation ability in HCC, suggesting that WNT5a acts as a tumor suppressor in HCC (115).

1.8.2 P53 Pathway

P53, a nuclear transcriptional regulator protein essential for the cell cycle, is the most frequently mutated gene in many cancers. Mutation of P53 and disruption of normal P53 function promote tumor inhibition and advancement, so mutated P53 might function as a tumor suppressor by competing with wild-type P53. In HCC, the combination of P53 with the oncogenic protein murine double minute 2 is activated, leading to the suppression of P53 activity and the activation of the downstream JAK/STAT signaling pathway, promoting tumor cell proliferation (116).

Previous research has also suggested that HBV may block the P53 pathway by binding to P53, causing inhibition of cell apoptosis (117). Conversely, HCV may activate P53 in the cytoplasm and decrease P21 expression through epigenetic regulation, thereby promoting

cancer cell proliferation. HCV may even activate the expression of p73, a suppressor protein in the P53 family, resulting in the development of HCC (118).

1.8.3 RAS/MAPK/ERK Pathway

Activation of the MAPK/ERK pathway depends on signal transduction from extracellular receptors on the cell surface, such as receptor tyrosine kinases (RTKs) or G protein-coupled receptors (119). Improper activation of this pathway can result in abnormal cell behavior, including increased cell proliferation, cell dedifferentiation, and inhibition of cell survival, eventually leading to carcinogenesis. Although the importance of the RAS/MAPK/ERK pathway in the pathogenesis of HCC has been overlooked in the past few decades due to the low frequency of RAS mutations in HCC, frequent activation of this pathway is present in HCC patients (120). Increased levels of epidermal growth factor (EGF) and transforming growth factor alpha are found in HCC, which can bind to the EGF receptor and subsequently trigger RTKs involved in the MAPK/ERK pathway (121). Moreover, non-coding RNAs, including microRNAs and long non-coding RNAs, have been validated as regulators of the MAPK/ERK pathway in recent research. For example, the activity of the MAPK/ERK signaling pathway is reduced by miR-4510 and miR-30a through the suppression of RAS and RAF, respectively. In contrast, an opposite effect is observed with the application of miR-330-5p and miR-487, which target sprouty and sprouty-related protein with enabled/VASP homology-1 domain in HCC (122).

1.8.4 AKT/mTOR Pathway

The PI3K/AKT/mTOR pathway is a hallmark of cancer, which is involved in the regulation of essential cellular process, including cell survival, cell cycle, metabolism, motility and angiogenesis (123). In low nutrient environment, the body prefer to activate of mTOR to keep the stable energy supply and cell material. Large amounts of proteins, lipids, and nucleotides are required to respond to cancer cells' demand for growth and division.

Therefore, aberrant regulation of mTOR pathway often occurs in tumors and is essential in regulating metabolism. As the main function of liver is maintenance of body metabolism, HCC patients with over activated mTOR pathway suggested to become more aggressive and shown as a marker of poor prognosis (124). Activation of AKT/mTOR pathway promote the reprograming of metabolic pathway in cancer cell environment, including glucose, lipid, amino acid, and oxidative metabolism in HCC (111). The different protein binds to mTOR protein could divided mTOR complex into mTOR complex 1 (mTORC1) and mTOR complex 2 (mTORC2) (125). Activation of mTROC1 lead to the phosphorylation of ribosomal S6 kinase 1 and eukaryotic translation inhiation factor 4E-binding protein-1, while activation of mTORC1 phosphorylate AKT, then lead to the increase of AKT activity. This phosphorylated AKT have been strongly demonstrated to associate with the C-myc activation and further promote the development of HCC (111).

1.9 Epigenetic Readers and Chromatin Regulation

It is well-known that chromatin is composed of nucleosomes wrapped around an octamer of histone proteins. Histone modification is achieved through the recognition of PTMs by proteins that harbor specific recognition sites. These proteins, known as epigenetic readers, are involved in the recruitment of remodeling complexes and the compaction of chromatin. Defective regulation of the expression and binding activity of epigenetic readers can alter the distribution and localization of histone marks on genes, resulting in abnormal chromatin-associated biological processes and eventually contributing to malignant cancer (126).

Recent findings have identified that the expression levels of 11 methyltransferases and demethylases, such as euchromatin histone lysine methyltransferase 2 (EHMT2), Su(var) enhancer of zeste (SET) domain bifurcated histone lysine methyltransferase 1, SET domain

containing 2, and enhancer of zeste 2 polycomb repressive complex 2 (EZH2), are associated with the development of HCC (127). For example, EHMT2, which regulates the methylation of lysine 9 in histone 3 (H3K9me2) and other non-histone proteins, is deregulated in various cancers. Its reduction is associated with the EMT process (128).

1.9.1 Polycomb Group (PcG) Proteins

Polycomb Group (PcG) proteins were first identified as epigenetic repressors of homeotic gene (Hox) expression in Drosophila melanogaster (129). PcG proteins encode a family of evolutionarily conserved epigenetic regulators that bind to specialized, switchable modular DNA elements known as polycomb response elements (PREs) or cell memory modules (CMMs) and core promoters (130, 131). PREs mediate the silencing of neighboring genes, and CMMs refer to the ability of cells to remember and propagate their gene expression programs throughout development (132, 133). Evidence also suggests that PcG proteins control anterior-posterior segment identity, differentiation, and body development planning. Several complexes with different components and structural configurations have been identified (134). In Drosophila, five PcG-containing complexes have been identified: polycomb repressive complex 1 (PRC1), polycomb repressive complex 2 (PRC2), pho-repressive complex (PhoRC), dRing-associated complex, and polycomb repressive deubiquitinase (PR-DUB) complex. Subsequently, PRC1 and PRC2 were identified in vertebrates (135). These protein complexes regulate various biological processes, including cell fate and lineage decisions, cellular memory, stem cell function, and tissue homeostasis (136).

In embryonic development, PcG proteins, along with other epigenetic regulators, coordinate transcriptional programs by repressing the expression of specific genes in a temporal manner. This regulation bestows specific identity and function to particular cells (137). Moreover,

PcG proteins also assist mature differentiated cells in maintaining their specific gene expression patterns, thereby controlling cell fate and memory (129, 138).

1.9.2 Polycomb Repressive Complexes

PcG proteins, through association with other proteins, form multi-subunit protein complexes known as PRCs. PRCs regulate the epigenetic status of chromatin and maintain it in a transcriptionally inactive state. PRCs are divided into two groups, namely PRC1 and PRC2, based on their protein composition. PRC1 and PRC2 are responsible for different epigenetic modifications: PRC1 catalyzes the monoubiquitylation of histone H2A at lysine 119 (H2AK119Ub1), while PRC2 catalyzes the trimethylation of histone H3 at lysine 27 (H3K27me3) (134).

During the mammalian embryonic development, PcG proteins selectively repress gene expression and ceullar differentiation and lineage. It have been reported that mouse model of mutant PcG protein exhibited phenotype alteration during the development of embryo (139). However, positive correlations between the expression or mutation of PcG proteins and various cancers have been identified in multiple cancer types, including breast, ovarian, and prostate cancers (134). Abnormal PcG expression or mutation is associated with the inactivation of tumor suppressors or the activation of proto-oncogenes. This includes the suppression of cyclin-dependent kinase inhibitors and the activation of c-myc genes, resulting in the loss of cell identity, enhanced proliferative ability, and resistance to apoptosis (134, 140, 141). Moreover, aberrant PcG expression leads to increased cell migration and invasion (142). Recent findings further suggest that PcG proteins are responsible for stem cell renewal and lineage commitment, indicating a potential role in the maintenance of CSCs (143).

PRC1 is composed of polycomb group ring finger protein (PCGF), really interesting new gene 1 and 2 (RING1/2), chromobox (CBX), and polyhomeotic-like protein (PHC). The

RING1/2 subunits are the core components of PRC1, to which other molecules are tethered. PRC1 exists in various forms. There are six members of the PCGF protein family, and RING1/2 binds to one of these PCGF proteins to form the RING-PCGF complex, which regulates the activity of the PHC and CBX subunits. The complete complex can recognize H3K27me3 via the chromodomain of CBX (144). On the other hand, a non-canonical PRC1 variant is formed when the RING1-PCGF complex interacts with RING1 and Ying Yang 1 binding protein, rather than PHC and CBX. This non-canonical PRC1 has a higher capacity for ubiquitinating H2A and possesses various complexes (145).

Polycomb PRC2 is composed of EZH2, embryonic ectoderm development (EED), suppressor of zeste 12 (SUZ12), and retinoblastoma-binding protein 4. In mammals, EZH2 is responsible for the catalysis of H3K27me3 but requires activation by other factors. SUZ12 regulates the histone methyltransferase (HMT) activity of PRC2, while EED controls the substrate specificity of the EZH2 complex, targeting various histones such as H3K27 or H1K26. Furthermore, PRC2 contributes to the inactivation of the X chromosome, maintaining stem cell fate and imprinting (136).

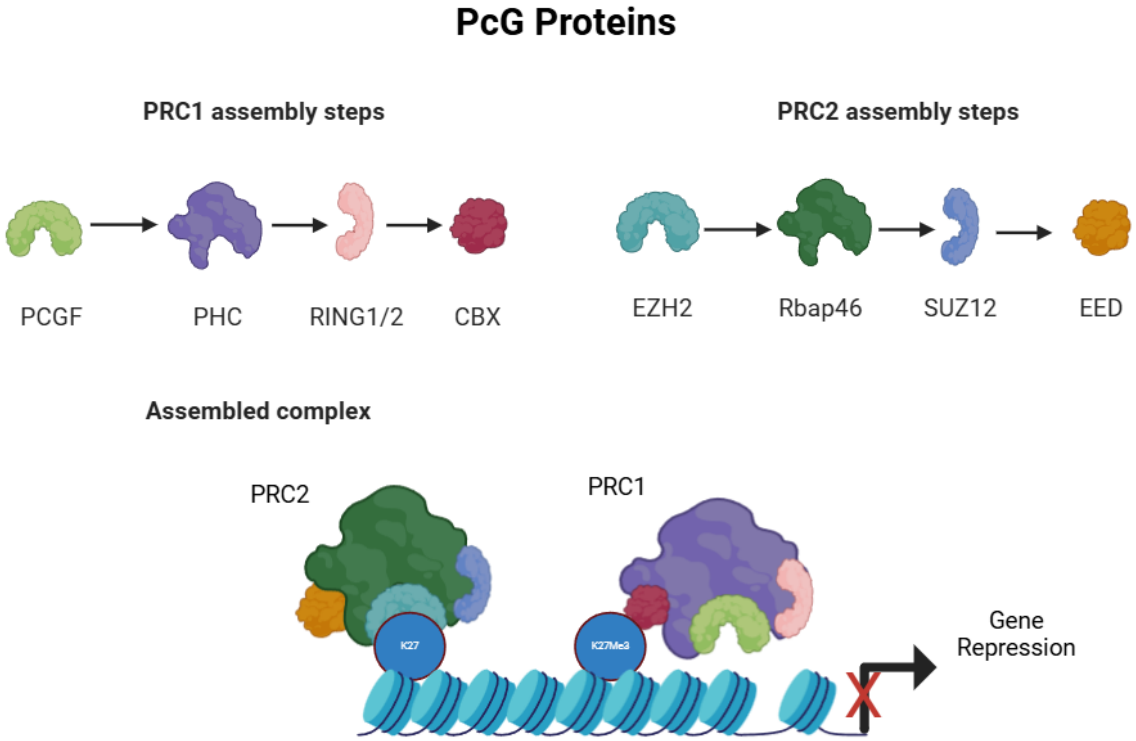

Figure. 1-2 Polycomb repressive complexes (Figure generated using BioRender).

A new PcG protein complex named PhoRC has recently been identified (146). It is consisted of the sequence-specific DNA-binding transcription factor YY1 and a Scm-like protein with four malignant brain tumor domains. The complex specifically binds to mono- and di-methylated H3K9 and H4K20 peptides. Some studies suggest that PhoRC may guide PRC1 and PRC2 to target genes during gene inactivation, but the underlying mechanism remains controversial (147).

1.9.3 PcG Protein and Cancer

Both DNA methylation and histone modifications impact gene expression by influencing chromatin structure and DNA accessibility. Abnormal chromatin structure can lead to aberrant gene expression and genomic instability, resulting in cellular transformation and malignant growth. Abnormal PcG expression may contribute to the renewal of cancer stem cells and the formation of cancer cells. Previous study have shown that loss of PRC1

impaired the liver cancer stem cell self-renewal, and inhibitor targeting PRC1 induce similar phenotypes in PRC1 deletion HCC cells. Alteration of PRC activity is associated with dysregulation of PcG protein expression (148). This is supported by recent findings that overexpression of SUZ12 in hematological malignancies and various solid tumors, including liver, breast, prostate, bladder, oral cavity, and colon cancer, is associated with altered PRC2 activity (149).

Mutations and deletions in the EZH2 gene, which inactivate the methyltransferase activity of EZH2, are associated with B cell lymphomas, follicular lymphomas, and myelodysplastic and myeloproliferative disorders (150). Upregulation of EZH2 has been found in various human cancers and is associated with tumor aggressiveness across multiple cancer types (151). EZH2 is composed of the EED interaction domain, domain 1, domain 2, Cysteine-rich domain, and the SET domain (152). In combination with EED/ESC and SUZ12 proteins, the SET domain of EZH2 contributes to methylation activity and has been identified to directly methylate various target molecules, including GATA4, STAT3, and β-catenin (153).

EZH2 also contributes to epigenetic regulation by binding directly to the promoter regions of target genes, as validated in c-Myc and Notch (154, 155). Accumulating evidence has revealed that EZH2 is involved in various signaling pathways, including the Wnt/β-catenin pathway, MAPK/ERK pathway, Notch signaling pathway, and PI3K/AKT and exhibits both tumor suppressor and promoter qualities pathway (153),. In breast cancer, EZH2 expression is abundant in tumor tissue and is closely associated with the bi- and tri-methylation of lysine 36 of histone 3, resulting in the repression of E-cadherin expression in cancer cells via the Notch signaling pathway. This indicates that elevated EZH2 expression induces tumor initiation and drives metastatic progression (156). However, in lung cancer, EZH2 possesses

tumor-suppressive roles by repressing the expression of insulin-like factors, which are activators of ERK and AKT amplification (157).

1.9.4 Chromobox Protein Family

Both PRC1 and PRC2 induce covalent post-translational histone modifications, resulting in epigenetic reprogramming. While PRC1 catalyzes the monoubiquitylation of histone H2A at lysine 119 (H2AK119Ub1), PRC2 catalyzes the trimethylation of histone H3 at lysine 27 (H3K27me3) (134). These two post-translational modifications of histones are associated with transcriptional silencing. During this process, the PRC2 complex is first recruited to chromatin. Subsequently, the Ezh2 protein, a histone methyltransferase, catalyzes the formation of H3K27me3 through its SET catalytic domain. H3K27me3 then functions as a binding site for the CBX protein of the PRC1 complex. The CBX protein consists of a chromodomain that has a high affinity for H3K27me3 (158). The interaction of CBX with H3K27me3 anchors the PRC1 complex to chromatin. The RING1B subunit, an E3 ubiquitin ligase in the complex, catalyzes the formation of H2AK119Ub. Ultimately, these events lead to chromatin folding and compaction and the cessation of transcription (159).

There are eight CBX proteins in humans, but only five are found in the PRC1 complex: CBX2, CBX4, CBX6, CBX7, and CBX8. All of them contain an N-terminal chromodomain for the recognition of methylated H3. Each CBX protein recognizes H3K27me3 with varying affinities. CBX2 can bind H3K9me3 or H3K27me3, while CBX4 has more affinity for H3K9me3. CBX7 strongly recognizes both modifications, but CBX6 has weak affinity for H3K27me3 (158).

Considering the similarity of the C-terminal domain, HP1 proteins consist of the remaining CBX proteins in the family, including CBX1, CBX3, and CBX5. The chromatin-binding domain of HP1 CBX proteins recognizes histone H3 lysine 9 dimethylation (H3K9me2) or

H3K9me3, resulting in transcriptional deactivation and gene repression (160). In this process, all three CBX proteins in the HP1 family recognize and bind to the H3K9me2/3 mark site and then recruit methyltransferase suppressors to methylate nearby H3K9 residues. This leads to new methylation marks for HP1 protein recognition, producing a positive feedback loop that compacts chromatin and represses gene expression (161).

1.9.5 Chrombox Protein Family in Cancer

Compared to adjacent normal tissue, CBX1, CBX2, CBX3, CBX4, CBX5, and CBX8 proteins are highly expressed in most cancers, including breast cancer, head and neck squamous carcinoma, non-small cell lung cancer, gastric cancer, and urinary bladder cancer (83). In HCC, the decision of differentiation or self-renewal depends on the molecular composition of PRC1(162). It is well noted that all CBX proteins have been suggested to be tumor-promoting factors in most cancers (83). However, CBX7 is suggested to have the potential for tumor-suppressive activity in breast cancer (163). Recent studies show that CBX7 determines the pluripotency of embryonic stem cells with PH1 in PRC1. When CBX7 is active, CBX2, CBX4, and CBX8 expression are repressed to avoid premature cell differentiation. When CBX7 expression is reduced during differentiation, CBX2, CBX4, and CBX8 are activated (164). Recent research showed that CBX7 inhibits the binding of Twist1, a transcription factor regulating cell migration and invasion, to the promoter site of epithelial cell receptor potein tyrosine kinase A2, resulting in the suppression of tumor growth and metastasis (165). Unlike other CBX proteins, CBX4 is a SUMO E3 ligase responsible for maintaining the stemness of human epidermal cells by preventing senescence and cell differentiation (166). CBX4 can sumoylate the hypoxia-inducible factor 1-alpha (HIF-1α), promoting the transcription of HIF1α and VEGF (167). High expression of CBX4 has been reported to be associated with poor overall survival in HCC patients, suggesting that CBX4 may be an independent prognostic factor in HCC patients with drug resistance due to its

stemness maintenance ability (168). To date, CBX2, CBX4, and CBX7 are the main targets of investigation, so the functional role of CBX8 in carcinogenesis remains elusive. Recent evidence suggests that CBX8 activates MMP-2 activity by suppressing with-no-lysine (K) kinase (WNK) 2, which acts as a tumor suppressor in lung and breast cancer, resulting in increased cell migration and invasion (169). CBX8 is also suggested to inhibit cyclin dependent kinase inhibitor 2C and promote tumor growth and metastasis in lung cancer (170).

1.9.6 CBX2

CBX2 is essential for PRC1 targeting to H3K27me3-rich domains genome-wide. The PRC1 complex associated with H3K27me3 chromatin invariably harbors CBX2 (159). CBX2 contains two characteristic domains of CBX proteins: a chromodomain in the N-terminal and a PcBox at the C-terminal. Unlike other CBX proteins, CBX2 has a unique structure called the AT hook, responsible for reorganizing AT-rich sequences in the genome. These sequences mark sites for other epigenetic readers, such as high mobility group AT-hook and methyl CpG binding protein 2 proteins (171). Notably, the binding activity of the AT hook does not rely on the trimethylation of lysine 27 of Histone 3 and can guide CBX2 to bind directly to chromatin, allowing CBX2 to regulate gene expression without H3K27me3 (172). Furthermore, phosphorylation of serine 42 of the CBX2 chromodomain by casein kinase 2 switches the CBX2 binding affinity from H3K9me3 to H3K27me3, providing a flexible mechanism for CBX2 epigenetic regulation in different microenvironments (173).

Elevated expression of CBX2 has been found in various cancers, including prostate, breast, and lung cancers(174-176). Upregulation of CBX2 is negatively associated with the overall survival rate in several cancers, including HCC. RNA sequencing analysis indicates that CBX2 expression may serve as an independent prognostic indicator for HCC overall survival (177). Furthermore, evidence suggests that CBX2 promotes the expression of Wilms' tumor

protein 1 interacting protein (WTIP) to inhibit the phosphorylation of Yes-associated protein (YAP), which provokes the Hippo pathway to reprogram cancer cells into cancer stem cells (178). A previous study showed that knockdown of CBX2 directly regulates the expression of the cyclin-dependent kinase inhibitor p21 and the INK4A/ARF locus (179). CBX2 has also been validated to contribute to the inhibition of the expression of the differentiation gene SRY-box transcriptional factor during embryonic stem cell development (164).

Studies on CBX proteins reveal the complex roles of this protein family in tumor biology, emphasizing that their functions are cell type- and organ-specific. While the precise roles of CBX proteins remain unclear, clinical data support that CBX2 acts as an oncogene in multiple cancers. However, the functional role of CBX2 in metabolic mechanisms and carcinogenesis in HCC is still elusive. Further research is required to validate the direct or indirect targets of aberrant CBX2 regulation in the recurrence, development, and drug resistance of HCC.

Hence, in this study, we aimed to elucidate the functional role of CBX2 in carcinogenesis in HCC *in vivo* and in vitro. Also, we aim to investigate the effect of CBX2 regulation in liver cancer cell characteristics, such as proliferation, migration and invasion. Moreover, we also try to explore the molecualr mechanism of CBX2 in HCC to elucidate the relationship between CBX2 and cancer metabolism, including glycolysis, gluconeogenesis and OXPHOS and validate the putative target of CBX2.

2. Methodology

2.1 Antibody, plasmid, and reagent

CBX2 (ab80044) was from abcam, PCK1 (12940) and PCK2 (6924S) was from Cell Signaling Technology, beta-Actin (A5441) was from Sigma.

Nicotinamide (HY-B0150) was from MedChemExpress, PrimeScript RT Master Mix, SYBR Premix Ex Taq II kits and RNAiso Plus (#9109) were from Takara. ViaFect™ Transfection Reagent (#E4982) was from Promega. Gibco™ Opti-MEM™ I Reduced Serum Medium Lentivirus plasmid pLenti-CRISPRv2-Cas9, Transponase system Piggybac was from Addgene,

Lactate Assay Kit (MAK064) and Pyruvate Assay Kit (MAK071-1KT) were from Sigma, PEP Assay Kit (ab204713) and OAA Assay kit (ab83428) were from Abcam; Glycerol-Glo Assay (J3150), CellTiter-Glo® Luminescent Cell Viability Assay (G7570) and NAD/NADH-Glo™ Assays (G9071) were from Promega.

shRNA in experiments

shCTRL:CAACAAGATGAAGAGCACCAA

shGALNT3: GCTCTATTCTTCACCTGCAAT

shGCNT3: CCAGTACTGTAGGAATATCTT

shCA4: GATGCACATAGTACATGAGAA

shPCK2: GTAGAGAGCAAGACGGTGATT

2.2 Cell and HCC Specimens

PHH, PLC5, and Hep3B cells were sourced from the American Type Culture Collection. Huh7 cells were obtained from the Health Science Research Resources Bank (Osaka, Japan). Thirty pairs of HCC and adjacent tissues were collected from the laboratory of Professor Zhang Yaojun at the Sun Yat-sen University Cancer Centre in Guangzhou, China.

2.3 Cell Culture

Cells were cultured in growth medium supplemented with 10% fetal bovine serum (Gibco), and maintained in a humidified incubator at 37 °C with 5% CO2. All cells were authenticated by short tandem repeat profiling analysis.

2.4 CBX2 CRISPR/Cas9 System

LentiCRISPRv2 is a vector system that contains two expression cassettes: hSpCas9 and a chimeric guide RNA. This vector can be digested with BsmBI, allowing an annealed pair of oligos to be cloned into a single guide RNA scaffold. The oligos are designed based on the target site sequence (20 bp) and must be flanked by a 3 bp NGG PAM sequence at the 3' end. The sgRNA for CBX2 was designed using the Benchling online tool (https://www.benchling.com/crispr).

CBX2 sgRNA CRISPR/Cas9 Lentivector sequence 1:

CACCGTGACTGGCGGCGGGCGCCG

CBX2 sgRNA CRISPR/Cas9 Lentivector sequence 2:

CACCGAGGTGCAGAACCGGAAGAG

2.5 Lentivirus Packaging and Transduction

For lentivirus packaging, HEK293FT cells were transfected with 5 µg CBX2 sgRNA CRISPR/Cas9 vector 1, 5 µg CBX2 sgRNA CRISPR/Cas9 vector 12, 10.5 µg of pLP1, 10.5 µg of pLP2 and 9.0 µg pVSVG, using calcium phosphate transfection. After

48h-72h of transfection, medium containing the lentivirus was collected. For cells transduction, medium containing the lentivirus was mixed with 8μg/ml hexadimethrine bromide (Polybrene) and incubated with HCC cells. After two days, cells were replaced with fresh medium containing 15μg/ml puromycin (Gibco) , for selection of cells with target gene integration.

2.6 DNA Transfection

Cells were transfected with a DNA vector using ViaFect™ Transfection Reagent (Promega). Cells were seeded one day prior to transfection, achieving 70%-80% confluence on the day of the procedure, with approximately 15×10^4 adherent cells in each well of a 6-well plate. 2 μg of plasmid DNA were added to Opti-MEM medium and mixed thoroughly. The DNA was then combined with ViaFect™ Transfection Reagent in a 3:1 ratio. The mixture was incubated at room temperature for 20 minutes before being added to the cells.

2.7 Western Blotting

Cells were harvested and lysed by using RIPA lysis buffer (50 mM Tris-HCl, pH 7.4, 150 mM NaCl, 0.5% sodium deoxy-cholate, 1% Nonidet P-40, 0.1% SDS, 1 mM EDTA, 2 mM sodiumorthovanadate, 50 mM sodium fluoride, 10 mg/ml aproti- nin, 10 mg/ml leupeptin, 1 mM PMSF) supplemented with Protease Inhibitor Cocktail (Roche). Protein concentration was determined using Protein Assay Kit (BioRad) with bovine serum albumin (Sigma) as the standard. Thirty mg protein samples were mixed with SDS loading buffer (10% SDS, 50% glycerol, 0.01% bromophenol blue, 7% DTT, 50 mM Tris pH 6.8) and was resolved by

SDS-polyacrylamide electrophoresis. The protein was transferred to a nitrocellulose membrane and immunoblotted with antibodies as indicated. Blots were developed with ECL Western blotting reagents (Thermo Fisher Scientific).

2.8 Proliferation, Migration and Invasion Assay

In the proliferation assay, 3000 cells were seed in to each well and were count every day by using the hemocytometer under microscope. Cells were harvested and counted for six days manually after cells were stained with Trypan blue stain. Cell migration assay: Cells were starved for 6 hours before the migration assay by changing the medium to DMEM only (serum free) and was passage into the Millicell® Inserts system with DMEM only medium. DMEM contained with 10%FBS was added in the bottom of the wells and cells were fixed after incubation at 37°C for 21 hours. Crystal violet was used to stain, and the migrated cells were counted under the light microscope. Cell invasion assay: Before seeding the cells in the Millicell® Inserts system, the inserts was coated by Matrigel. Cells were starved for 6 hours before the invasion assay by changing the medium to DMEM only (serum free) and passage into the coated Millicell® Inserts system with DMEM only medium. DMEM contained with 10%FBS was added in the bottom of the wells and cells were fixed after incubation at 37°C for 21 hours. Crystal violet was used to stain, and the migrated cells were counted under the light microscope.

2.9 RNA Extraction

Cells were washed with PBS and 300ul of TRIzol Plus was added to each well of 6 wells plate. The reagent was swirled around in plate to ensure surface was covered and then transferred to the 1.5ml centrifuge tube. After 5 minutes incubation at room temperature, 60

ul of chloroform was added to solution, mixed and kept at room temperature for 5 minutes. Then centrifuged at 14,000 RPM for 15 minutes at 4 degree, and isolated the RNA at the top layer without touching the middle layer. Measure the amount of RNA solution and an equal amount of Isopropanol was added, mixed and kept in room temperature for 10 minutes. Then centrifuge again at 13,000 RPM for 10 minutes at 4 degrees to precipitate the RNA. Washed with cold 70% ethanol twice and airdried. The completely dry RNA pellet was eluted with RNase free water and stored in -20 degree.

2.10 RT-qPCR

cDNA was synthesized from RNA using the PrimeScript RT Master Mix (TaKaRa). The cDNA was then mixed with SYBR Premix Ex Taq II kits (TaKaRa) and subjected to qPCR analysis using the Applied Biosystems QuantStudio 7 Flex Real-Time PCR System (University Research Facility in Life Sciences, The Hong Kong Polytechnic University, Hong Kong). PCR was conducted with the following cycle parameters: an initial denaturation at 95° C for 2 minutes, followed by 40 cycles of denaturation at 95° C for 30 seconds, and a final extension step at 60° C for 30 seconds. Melting curve analysis was performed by heating the samples to 95° C for 15 seconds, followed by cooling to 60° C for 1 minute.

Primers used in this experiment:

GALNT3

Forward: 5'-TCTACTGAGCCGCAACTGTG-3'

Reverse: 5'-GGTCCAAGATCTCGGTGCAA-3'

GCNT3:

Forward: 5’-CACGCTACCTCCCAAGTGTT-3’

Reverse: 5’-CTGTCAGAGTTACAGGGTTTGC-3’

CA4:

Forward: 5’-TTTCTGGTGGAGGCTGGAAC-3’

Reverse: 5’-TTTTAATCATGCCTAAAGTCCCAC-3’

PCK2:

Forward: 5’-CCAGGCCTCAGCACCTTAAT-3’

Reverse: 5’-GTGCTTGGAGCCCAATACCT-3’

2.11 Cell Cycle Analysis Assay

Cells was harvested from six well plates and then washed twice with cold PBS. 70% cold ethanol was dropwise in the cell pellet and vortex to ensured all cells were fixed without cell clumps. After 30 minutes fixation, cells was washed twice with cold PBS again and 50 ul of 100ug/ml RNase was added in per 1 ml solution to eliminate RNA. Then 200ul of 50 ug/ml propidium iodide (PI) was added to stain DNA and procced to flow cytometric analysis within one hour. All samples were filter with 0.4um filter paper before loading to flow cytometric machine and 5X105 number of single cell excluding cell doublets were analysed.

2.12 Cell Apoptosis Assay

Cells were harvested from six well plates and then washed twice with cold PBS. And then cells were resuspended with 1X binding buffer (10mM HEPES,140mM NaCl, 2.5mM CaCl2).

100ul of samples was transferred to 1.5ml tube and stained with Annexin V and PI for 15 minutes in room temperature at dark. Then top up to 500ul with 1X binding buffer to each tube and proceed to flow cytometric analysis within one hour. All samples were filter with 0.4um filter paper before loading to flow cytometric machine and 5X105 number of single cell excluding cell doublets were analysed.

2.13 Metabolic Intermediate Measurement

In all metabolic intermediate assay, 5000 cells were seeded in the day prior to assay in all measurement. The amount of Lactate, pyruvate, PEP, OAA, Glycerol-3-phosophate, ATP and the ratio of NAD^+/NADH were measured by the commercial kits and the procedure was followed the instruction provided by the supplier.

2.14 Transfection of SoNar System and Quantification of NAD^+/NADH Ratio

Cells were transfected with DNA vector by using ViaFect™ Transfection Reagent (Promega). Cells were seeded one day before transfection. Cells were 70%-80% confluent on the day of transfection, with around 15×10^4 adherent cells in each well of a 6-well plate. 2μg of plasmid including SoNar coding sequence was added to the Opti-MEM medium and mixed well. Plasmid was mixed with ViaFectTM Transfection Reagent in a 3:1 ratio. The mixture was incubated at at room temperature for 20 minutes before adding to the cells. Cells were examined under a fluorescent microscope 48 hours after transfection.

2.15 Measurement of ECAR and OCR

7 x10^3 cells were seeded in each well on Seahorse XF Microplate at the day prior to assay, and microplate were removed from 37-degree, 1% CO2 incubator and kept in 37-degree incubator without CO2 supply for one hour. Then the measurement approach was followed the instruction from Agilent Company and all used compounds was prepared freshly. For OCR measurements, oligomycin, FCCP, and rotenone/antimycin-A were injected into the plates to inhibit ATP synthase (complex V), disrupt mitochondrial potential, and shut down mitochondrial respiration, respectively. For ECAR measurements, glucose, oligomycin, and 2-deoxy-glucose (2-DG) were injected into the plates after one hour of glucose starvation to test cellular glycolytic capacity under different conditions.

2.16 Xenograft Nude Mice Tumor Model

Wild Type and CBX2 knock out 1x10^7 Cancer cells were subcutaneous injected with Matrigel (1:1) into left and right flank to establish xenograft nude mice tumor models. The size of tumors was measured for 27 days upon tumor inoculation. In the drug therapy effectiveness investigation, when the size of tumors reach 25-30 cubic mm, mice was used for drug treatment for 3 weeks. Tumors size were monitored each three days to determine the growth of tumor and the drug sensitivity. At the end of experiment, mice was scarified by cervical dislocation under anaesthesia. Tumors were divided into three parts for IHC staining, RNA extraction and protein extraction.

2.17 RNA-sequencing

Total RNAs were extracted from cells and subjected to whole transcriptome shotgun sequencing (RNA-seq) analysis. RNA-seq was conducted by Novogene. The quality of the raw reads was checked using the Fastqc program. After removing the index and adapter sequences, high-quality trimmed reads were mapped against the human reference genome (GRCh38 p12 Gencode v30) using Hisat. Gene expression levels indicated by FPKM were calculated using StringTie.

2.18 Differential Expression Analysis

Differential expression analysis was performed by comparing two groups (each with two biological replicates) using the DESeq R package (version 1.18.0). DESeq employs statistical procedures to determine differential expression in numerical gene expression data using a model based on a negative binomial distribution. The resulting P-values were adjusted using Benjamini and Hochberg's method to control for false discovery rates. Genes with a fold change greater than 1.5 and an adjusted P-value of less than 0.05 were classified as differentially expressed.

2.19 KEGG Enrichment Analysis of Differentially Expressed Genes

KEGG (http://www.genome.jp/kegg/), which categories DEGs to understand high-level functions and utilizes of the biological system, was performed using KOBAS software (http://kobas.cbi.pku.edu.cn).

2.20 Preparation of Quality Control (QC) Samples and Samples for Metabolomics

QC samples were prepared by dividing 15 × 10^6 cells in PBS (500 μL) into three aliquots for replicates. Each QC aliquot underwent the same sample preparation process as the experimental samples. Five replicate injections of the same QC aliquot were performed before the analysis, and one QC aliquot was injected after every four sample runs to ensure the stability and reliability of the instrument.

The aliquoted samples underwent methanol extraction, followed by vortexing for 60 seconds and overnight deproteinization. The samples were then centrifuged at 14,000 rpm at 4°C for 15 minutes. The resulting supernatant was dried under a gentle stream of nitrogen (N_2). Prior to injection into the mass spectrometry (MS) system, the samples were reconstituted in a 100 μL mixture of methanol and water (50:50, v/v).

2.21 UPLC-Orbitrap-MS/MS Analysis

A 3 μL aliquot of the sample was introduced into a Waters ACQUITY UPLC system for separation using a Waters ACQUITY UPLC HSS T3 Column (1.8 μm, 2.1 mm × 100 mm) in conjunction with an HSS T3 pre-column (1.8 μm, 2.1 mm × 5 mm, Waters Corporation, Milford, MA). The mobile phase consisted of a mixture of solvent A (0.1% formic acid in water, v/v) and solvent B (0.1% formic acid in acetonitrile, v/v), with a flow rate of 0.30 mL/min following the elution gradient detailed below: 0–1 min: 5% B; 1–1.5 min: 35% B; 1.5–3 min: 50% B; 3–6.5 min: 55% B; 6.5–8.5 min: 95% B; 8.5–10.5 min: 95% B; 10.5–11 min: 95%; and 11–14 min: 95% B. A 3-minute post-run duration was assigned for thorough equilibration, with the column maintained at 40°C and the sample chamber at 4°C.

For mass spectrometry analysis, a Thermo Orbitrap Fusion Lumos Tribrid Mass Spectrometry system (Thermo Fisher Scientific, Waltham, MA, USA) was utilized, featuring a heated electrospray ion source (H-ESI) operating in both positive (+ESI) and negative (-ESI) ion modes. The H-ESI settings included a spray voltage of 3500 V for positive ESI and 2300 V for negative ESI, with sheath gas set at 35 arbitrary units, nebulizer auxiliary gas at 10 arbitrary units, and sweep gas at 3 arbitrary units. Additionally, the ion transfer tube temperature was maintained at 300°C, while the vaporizer temperature was set to 320°C.

A full scan MS analysis was conducted over the mass range of 70–1200 m/z at a resolution of 120,000, utilizing an automatic gain control (AGC) target of 2.0 × 10^5 and a maximum injection time of 50 ms.

3. Results

3.1 CBX2 expression is elevated in HCC

To assess whether PRC1 components are altered in HCC, we examined the mutational frequencies of cPRC1 genes, including RING1 (encoding RING1A), RNF2 (encoding RING1B), PCGF2, BMI1 (encoding PCGF4), PHC1/2/3, and CBX2/4/6/7/8, in a large-scale genomic dataset (TCGA, PanCancer Atlas) of cancer patients. Similar to the earlier studies, we found that these genes are mutated in multiple cancer types, where gene amplification is the major mutation found in these cancers (Fig. 3-1A). Importantly, these genes were also amplified in a cohort of HCCs comprising 353 patient samples (Fig. 3-1A). Among genes of the cPRC1, RNF2, CBX4, CBX2, and CBX8 were amplified in a subset (4 to 7%) of HCC specimens (Fig. 3-1B).

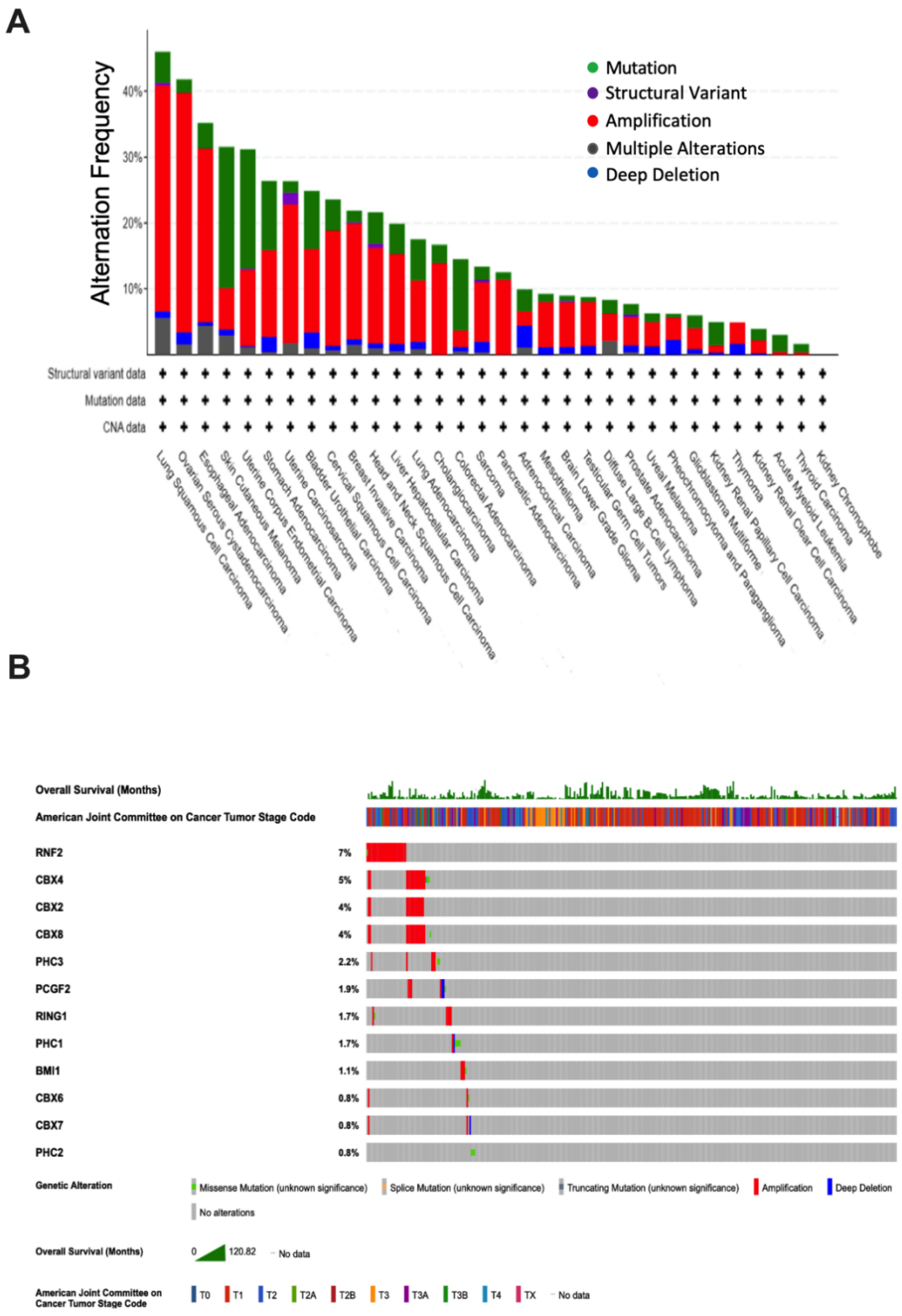

Figure. 3-1 A) Illustration of mutational frequency of components in the cPRC1 complex of human cancer data set. B) Mutational frequency of cPRC1 complex in a cohort of HCC patients comprised of 353 cases.

In this cohort of HCC, significant overexpression of CBX2 was observed in the tumors, compared to the non-tumorous tissues (Fig. 3-2A). In addition, high expression of CBX2 was associated with poor prognosis of the patients (Fig. 3-2B). Given the high heterogeneity of HCC in terms of mutational landscapes, CBX2 alterations may play a specific pathological role in a subgroup of HCCs. The overexpression of CBX2 protein was confirmed in twenty-three paired clinical HCC specimens collected from our locality (Fig. 3-2C). CBX2 was also expressed at different levels in various HCC cell lines (PLC5, Hep3B, Huh7, HepG2, MHCC97L, SNU387, SNU398, SNU423). Among others, Hep3B cells expressed CBX2 at the highest level (Fig. 3-2D). In contrast, CBX2 expression was very low or negligible in three independent primary hepatocytes, but it was expressed in transformed liver cell lines (Fig. 3-2D). Together, these data showed that CBX2 expression is low in primary hepatocytes, but become elevated during HCC oncogenesis, suggesting that CBX2 may play functional roles in HCC pathogenesis.

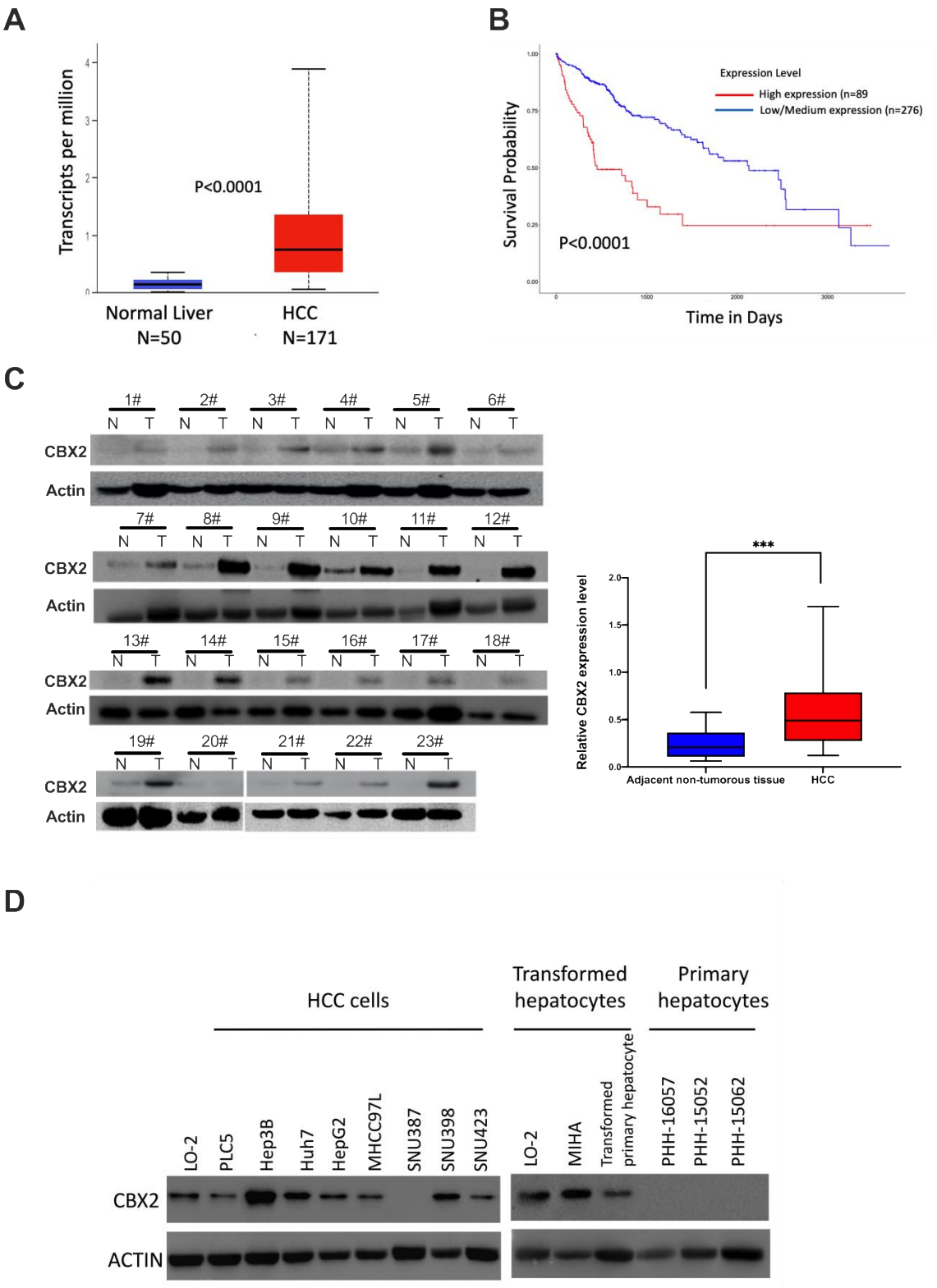

Figure. 3-2 A) Expression level of CBX2 in HCCs compared to non-turmorous livers. B) Kaplan-Meier analysis of HCC patient with high and low CBX2 expression levels. C) Left, Western blot analysis of CBX2 expression in 23 paired HCCs and adjacent non-tumorous livers. Right, Quantification of CBX2 expression in HCC versus non-tumorous livers. ***, P<0.001 (by t - test). D) Western blot analysis of CBX2 protein expression in HCC cell lines, transformed liver cells, and primary hepatocytes.

3.2 CBX2 is essential for proliferation, migration, and invasion of HCC cells

CBX2 knockout HCC cell lines were generated to study the role of CBX2 in HCC pathogenesis. CRISPR-Cas9 vectors were generated by designing guide RNAs (gRNAs) targeting exon 1 and exon 4 of CBX2 (Fig. 3-3A), respectively, followed by transfection into Huh7 and Hep3B cells. CBX2 knockout cells were selected in the presence of puromycin (15μg/ml). CBX2 knockout Huh7 (Huh7 KO) and Hep3B (Hep3B KO) cells exhibited profound reduction in CBX2 protein expression respectively, whereas cells transfected with the blank vector (Hep3B CTRL and Huh7 CTRL) did not (Fig. 3-3B). These data suggested that the gRNAs effectively knockout CBX2 gene. To further investigate the effect of CBX2 expression in HCC pathogenesis, CBX2 was ectopically expressed in a transformed primary hepatocyte (PHH) cell line through stable integration of a CBX2 transgene driven by a CMV promoter. A piggyBac (PB) transposon system was employed to facilitate stable integration of the CBX2 transgene, flanked by transposon-specific inverted terminal repeats (ITRs) and mediated by the co-expression of a transposase that recognizes ITRs. Cell populations successfully integrated with the transgene were selected by the addition of puromycin(2.5μg/ml). Western blot analysis showed that PHH cells expressing the empty vector (PHH CTRL) do not express CBX2. However, PHH transfected with the CBX2-expressing transgene (PHH OE) showed a significant increase in CBX2 expression (Fig. 3-3B).

To investigate the pathogenic function of CBX2 gene in HCC cells, we first determined the proliferation of Huh7 CTRL and Hep3B CTRL cells versus their CBX2 knockout counterpart (Huh7 KO and Hep3B KO cells) respectively. Huh7 KO and Hep3B KO cells exhibited a significant reduction in the rate of cell proliferation over a period of 5 days compared the Huh7 CTRL and Hep3B CTRL cells respectively (Fig. 3-3C), suggesting that CBX2 is an

essential gene for HCC cell growth. Similarly, the proliferation of PHH OE is significantly higher than the PHH CTRL over a period of 5 days (Fig. 3-3D), suggesting that the expression of CBX2 facilitates proliferation of hepatocytes. To determine the mechanisms underlying the cell growth phenotypes, Hep3B CTRL and KO cells were analyzed by fluorescence activated cell sorting analysis. Cell cycle analysis revealed that Hep3B KO cells showed a significant increase in proportion of cells at G1 phase of the cell cycle (Fig. 3-3E). However, no difference in cell death between Hep3B KO and CTRL could be observed (Fig. 3-3F). Together, these data suggested that depletion of CBX2 resulted in G1 cell cycle arrest, leading to retarded cell growth.

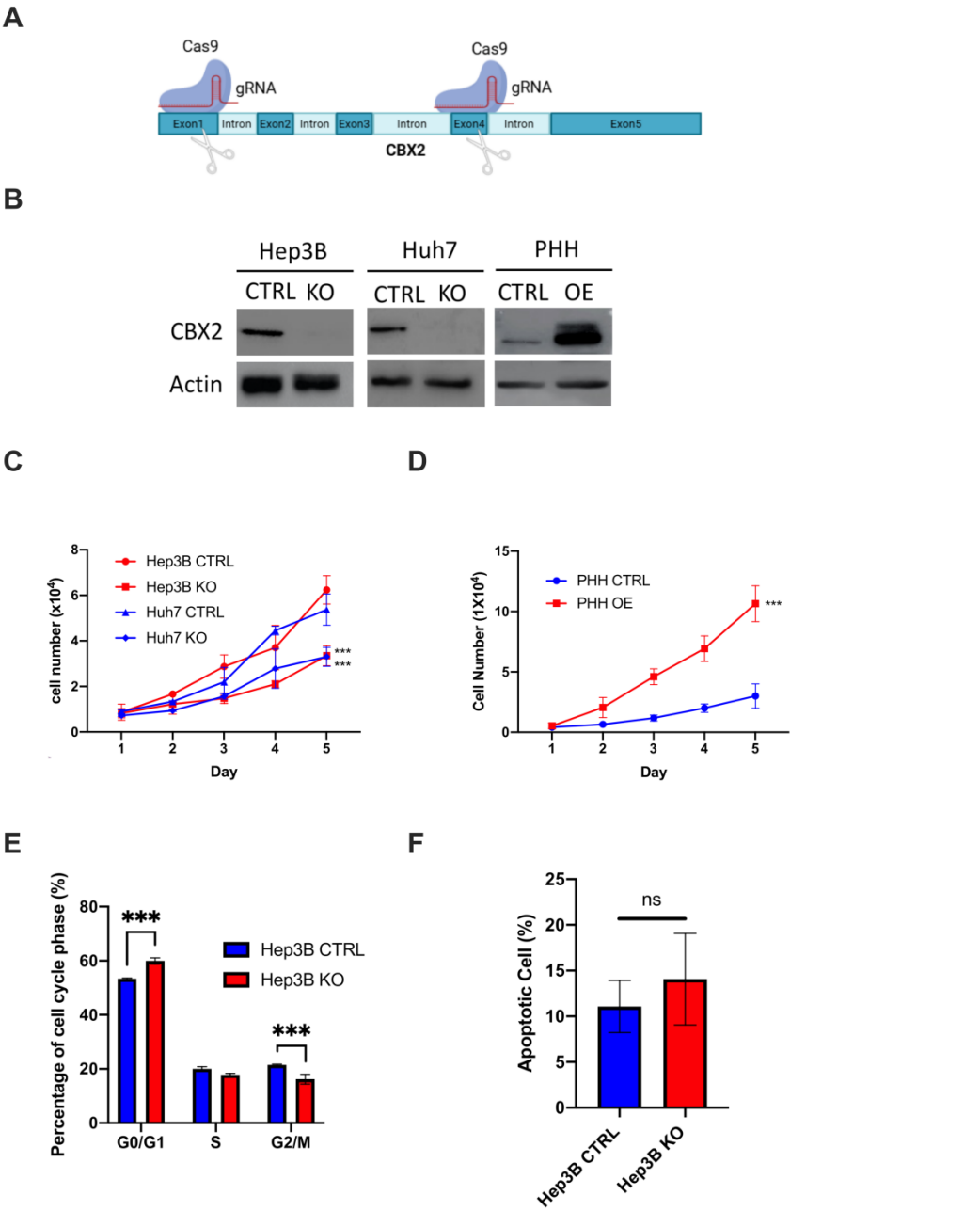

Figure. 3-3 A) Illustration of CRISPR-Cas9 mediated CBX2 knock out in Hep3B and Huh7 cells. B) Western blot analysis of CBX2 protein expression in Hep3B CTRL versus Hep3B KO, Huh7 CTRL versus Huh7 KO, and PHH OE versus PHH CTRL cells respectively. C) Cell proliferation assays of Hep3B and Huh7 cells in the presence or absence of CBX2 respectively. ***, $P < 0.001$ (by 2 - way ANOVA), between Hep3B CTRL versus Hep3B KO, and Huh7 CTRL versus Huh7 KO cells at day 5, respectively. D) Cell proliferation assays of PHH OE versus PHH CTRL cells, ***, $P < 0.001$ (by 2 - Way ANOVA), between PHH OE and PHH CTRL at day 5. E) Cell cycle analysis of Hep3B CTRL versus Hep3B KO cells. ***, $P< 0.001$ (by 2 - Way ANOVA). F) Apoptosis analysis of Hep3B CTRL versus Hep3B KO cells. ns, no significant difference.

Next, the functional role of CBX2 in HCC cell metastasis was investigated. In the transwell assays, Hep3B KO and Huh7 KO cells showed a significant reduction in migration ability compared with Hep3B CTRL and Huh7 CTRL cells respectively (Fig. 3-4). Similarly, in the transwell invasion assays, Hep3B KO and Huh7 KO cells showed a significant reduction in invasion ability compared with Hep3B CTRL and Huh7 CTRL cells respectively (Fig. 3-4). In contrast, PHH OE cells showed a profound enhancement in cell migration and invasion ability (Fig. 3-4). Together, these data suggested that CBX2 expression is crucial for the migration and invasion ability of the HCC cells and non-tumorous hepatocytes.

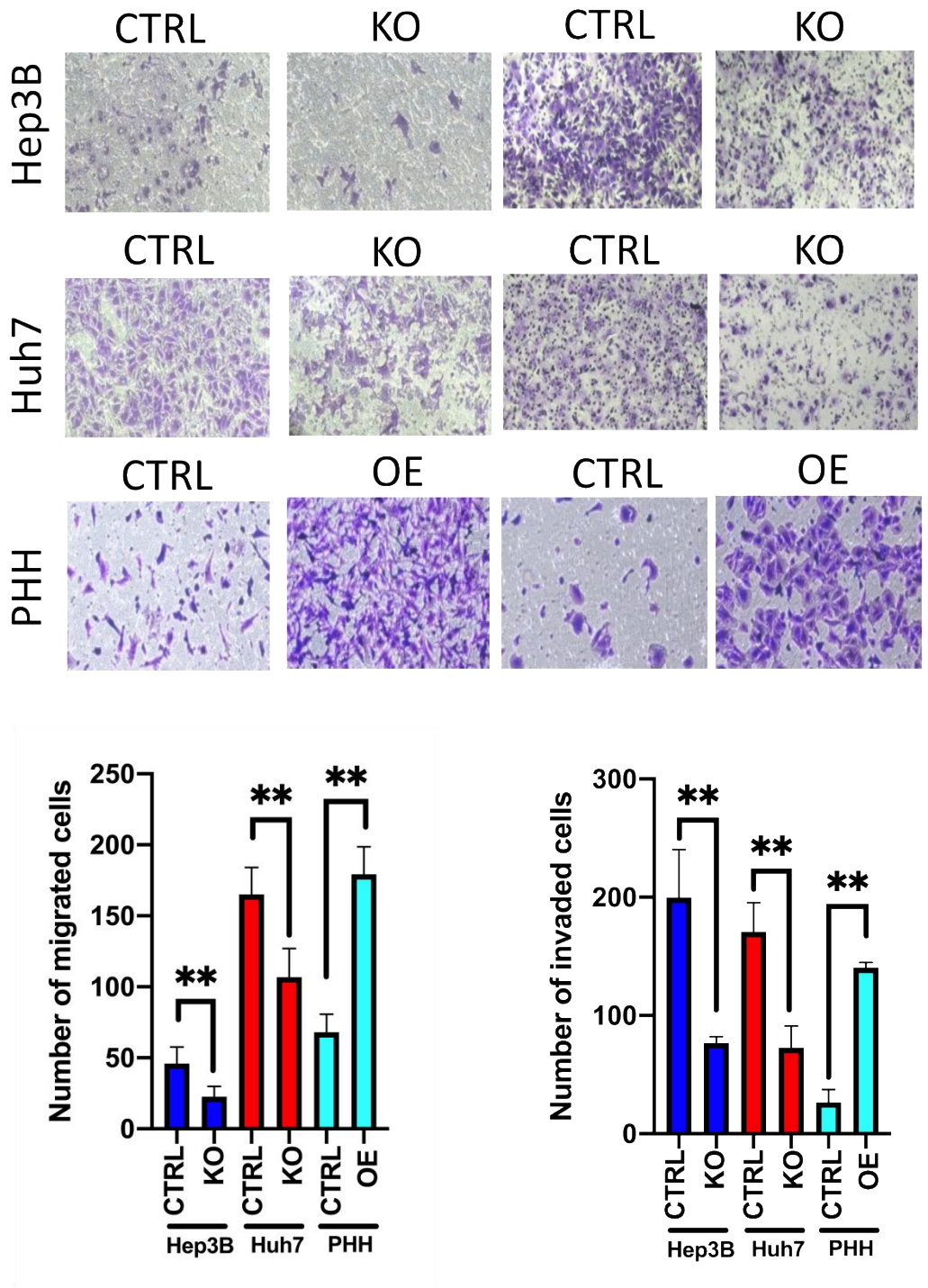

Figure. 3-4 Migration and invasion assays of Hep3B CTRL versus Hep3B KO cells, Huh7 CTRL versus Huh7 KO, and PHH OE versus PHH CTRL cells respectively. Top, representative figure of crystal violet staining of Hep3B and Huh7 CTRL and KO cells, PHH CTRL and OE cells in migration and invasion assay. Bottom, quantification of crystal staining of Hep3B and Huh7 CTRL and KO cells, PHH CTRL and OE cells in migration (left) and invasion (right) assay. **, $P < 0.05$ (by t - test).

To further investigate if CBX2 regulates HCC growth *in vivo*, xenograft mouse tumor model was established using Hep3B KO and Hep3B CTRL cells respectively. Subcutaneous inoculation of Hep3B CTRL cells into nude mice established palpable tumor in 22 out of 28 attempts (78.6%) (22/28), whereas inoculation of Hep3B KO cells only established palpable tumor in 11 out of 28 attempts (39.29%). Compared with tumors formed by the Hep3B CTRL cells, tumors formed by Hep3B KO cells demonstrated a profound reduction in tumor size over a period of 21 days (Fig. 3-5A and Fig. 3-5B). At the end of the experiment, analysis of the dissected tumors showed that tumors formed by Hep3B KO cells exhibited a significant reduction in tumor volume (Fig. 3-5C) and weight (Fig. 3-5D). Therefore, consistent with the cell analysis, CBX2 is essential for HCC tumor growth *in vivo*.

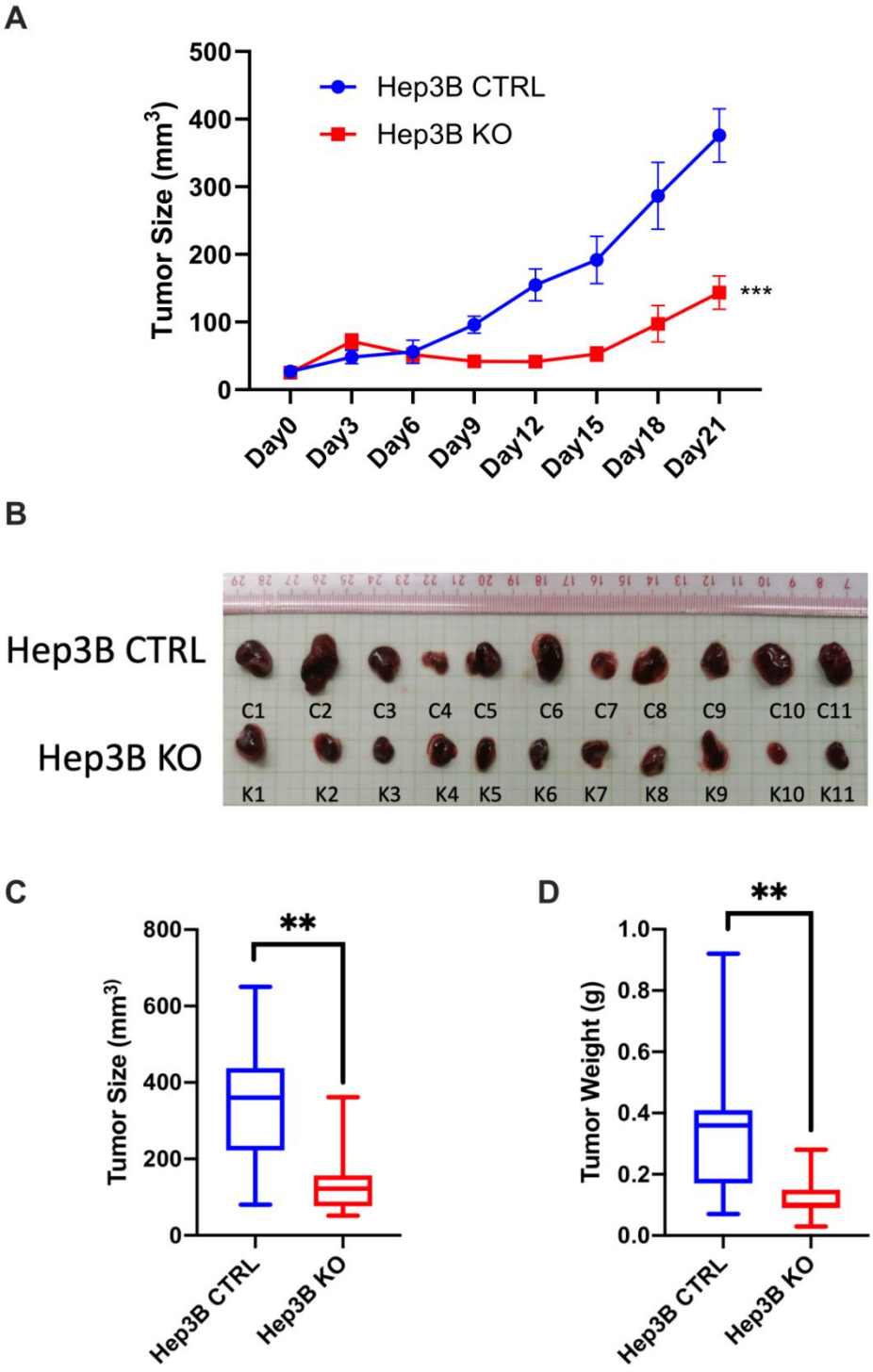

Figure. 3-5 A) Growth of xenograft tumors after subcutaneous implantation of Hep3B KO and Hep3B CTRL cells. ***, P< 0.001 (by 2 - way ANOVA), between Hep3B KO versus Hep3B CTRL cells at day 21. B) Photographs of the harvested tumors. C) Tumor size and D) tumor weight of xenograft tumors harvested from Hep3B CTRL and KO cells at day 21 respectively. **, P<0.05 (by t - test).

3.3 CBX2 regulates gene expressions related to metabolism

To further understand the functional role of CBX2 in HCC, RNA sequencing analysis was conducted using Hep3B KO and Hep3B CTRL cells, and Huh7 KO and Huh7 CTRL cells respectively. Differentially expressed genes (DEGs) (fold change ≥ 1.5 and q value ≤ 0.05) were identified using DESeq2. Hep3B KO, Hep3B CTRL, Huh7 KO and Huh7 CTRL cells showed distinct gene expression patterns (Fig. 3-6A). Volcano plot revealed that, compared to Hep3B CTRL cells, there were 517 genes up-regulated and 446 genes down-regulated Hep3B KO cells. On the other hand, compared to Huh7 CTRL cells, there were 296 genes up-regulated and 56 genes down-regulated in Huh7 KO cells respectively (Fig. 3-6B).

Among these DEGs, 36 up-regulated (Table. 1) and 5 down-regulated genes were commonly altered in both CBX2 knockout cell lines (Fig. 3-7A). We analyzed and compared the significantly enriched KEGG pathways among the common altered genes to identify processes that were commonly regulated by CBX2. Among others, genes with functions related to metabolic pathways were significantly enriched among these DEGs (Fig. 3-7B), suggesting that CBX2 may play a role in metabolic regulation.

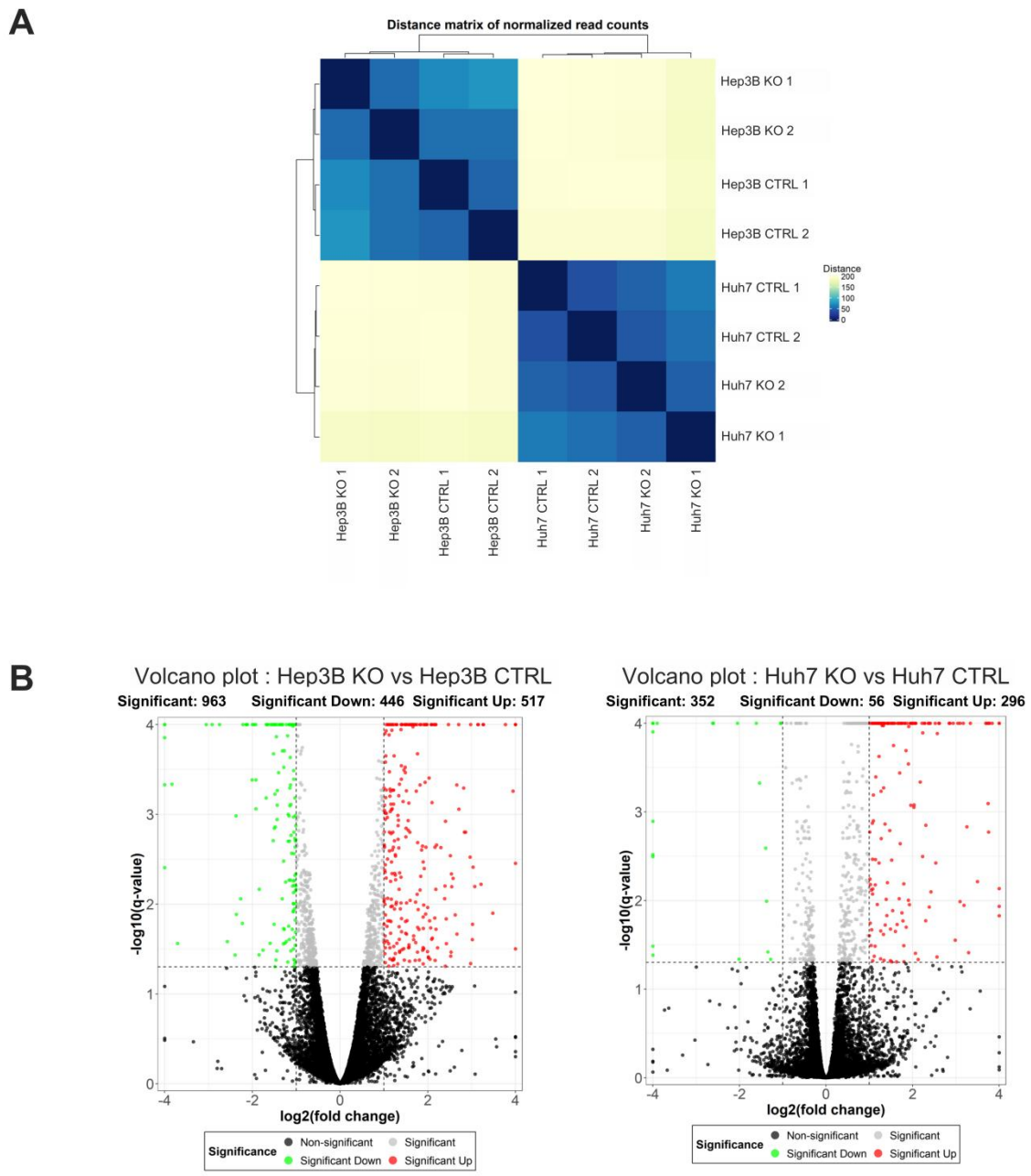

Figure. 3-6. A) Sample distance matrix of Hep3B CTRL, Hep3B KO, Huh7 CTRL and Huh7 KO cells. B) Volcano Plot and DEGs of Hep3B CTRL versus Hep3B KO cells, and Huh7 CTRL versus Huh7 KO cells.

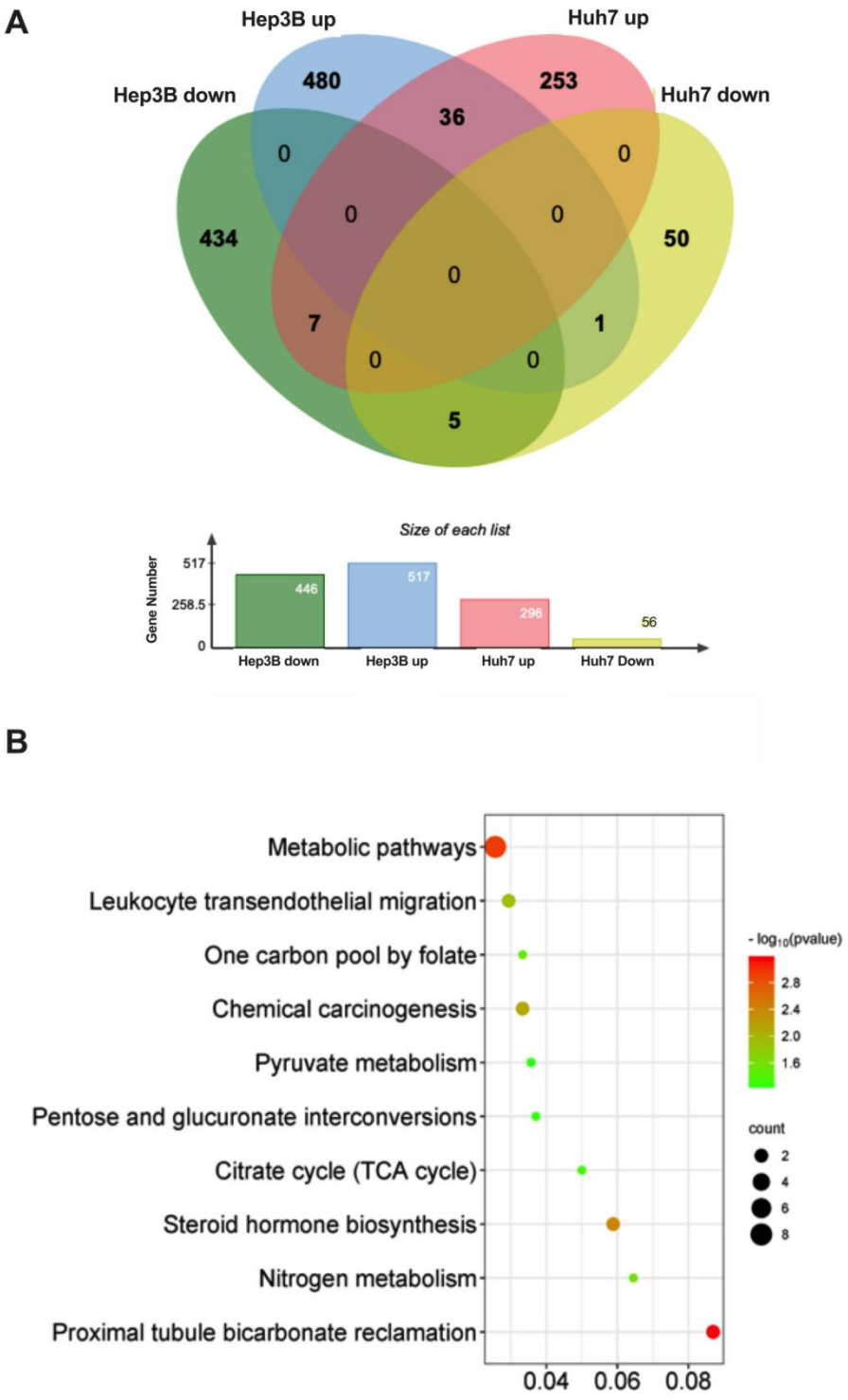

Figure. 3-7 A) Top, Venn diagram of commonly up-regulated and down-regulated genes in both Hep3B KO and Huh7 KO cells. Bottom, number of up-regulated (Hep3B up) and down-regulated (Hep3B down) genes of Hep3B CTRL versus Hep3B KO cells, and number of up-regulated (Huh7 up) and down-regulated (Huh7 down) genes of Huh7 CTRL versus Huh7 KO cells. B) KEGG pathway enrichment analysis of the commonly up-regulated genes in Hep3B KO and Huh7 KO cells.

GENE NAME	DESCRIPTION
ACSM2A	acyl-CoA synthetase medium chain family member 2A
AKR1C2	aldo-keto reductase family 1 member C2
AL713998.1	novel transcript
ALDH1L2	aldehyde dehydrogenase 1 family member L2
APOL6	apolipoprotein L6
ARL2BP	ADP ribosylation factor like GTPase 2 binding protein
BNIP5	BCL2 interacting protein 5
BTN3A2	butyrophilin subfamily 3 member A2
CA4	carbonic anhydrase 4
CDX2	caudal type homeobox 2
COL14A1	collagen type XIV alpha 1 chain
DUOX2	dual oxidase 2
FP565260.2	novel protein
GALNT3	polypeptide N-acetylgalactosaminyltransferase 3
GCNT3	glucosaminyl (N-acetyl) transferase 3, mucin type
HAMP	hepcidin antimicrobial peptide
HMCN1	hemicentin 1
LBP	lipopolysaccharide binding protein
LGSN	lengsin, lens protein with glutamine synthetase domain
LUM	lumican
MAT1A	methionine adenosyltransferase 1A
MUC13	mucin 13, cell surface associated
NDRG1	N-myc downstream regulated 1
P4HA1	prolyl 4-hydroxylase subunit alpha 1
PARM1	prostate androgen-regulated mucin-like protein 1
PCK2	phosphoenolpyruvate carboxykinase 2, mitochondrial
SAA2	serum amyloid A2

SERPINA3	serpin family A member 3
SH3BP2	SH3 domain binding protein 2
SIAE	sialic acid acetylesterase
SULT1B1	sulfotransferase family 1B member 1
TTC39B	tetratricopeptide repeat domain 39B
TXNIP	thioredoxin interacting protein
UBE2L6	ubiquitin conjugating enzyme E2 L6
UCA1	urothelial cancer associated 1
UGT2B4	UDP glucuronosyltransferase family 2 member B4

Table 1. Gene list of 36 commonly up-regulated gene in both CBX2 knockout cell lines (Hep3B and Huh7).

3.4 CBX2 regulates HCC metabolisms through maintaining NAD+/NADH ratio

To further explore the role of CBX2 in metabolism, we determined extracellular acidification rate (ECAR) and oxygen consumption rate (OCR) of Hep3B and Huh7 CTRL and KO cells using Seahorse Analyzer. OCR analysis revealed that knockout of CBX2 gene did not significantly alter oxygen consumption profile in Hep3B (Fig. 3-8A) and Huh7 (Fig. 3-8B) cells in response to different treatments. However, the maximal respiration and spare respiration were significantly elevated in Hep3B KO (Fig. 3-8A) and Huh7 KO (Fig. 3-8B) cells respectively, suggesting that the CBX2 knockout cells might developed better resistance to metabolic stress. On the other hand, Hep3B KO and Huh7 KO cells exhibited a significant reduction in ECAR compared to their respective control cells (Fig. 3-8C and D). Glycolysis and glycolytic capacity were reduced in Hep3B KO (Fig. 3-8C) and Huh7 KO cells (Fig. 3-8D) respectively, suggesting that CBX2 regulates glycolytic pathway of HCC cells.

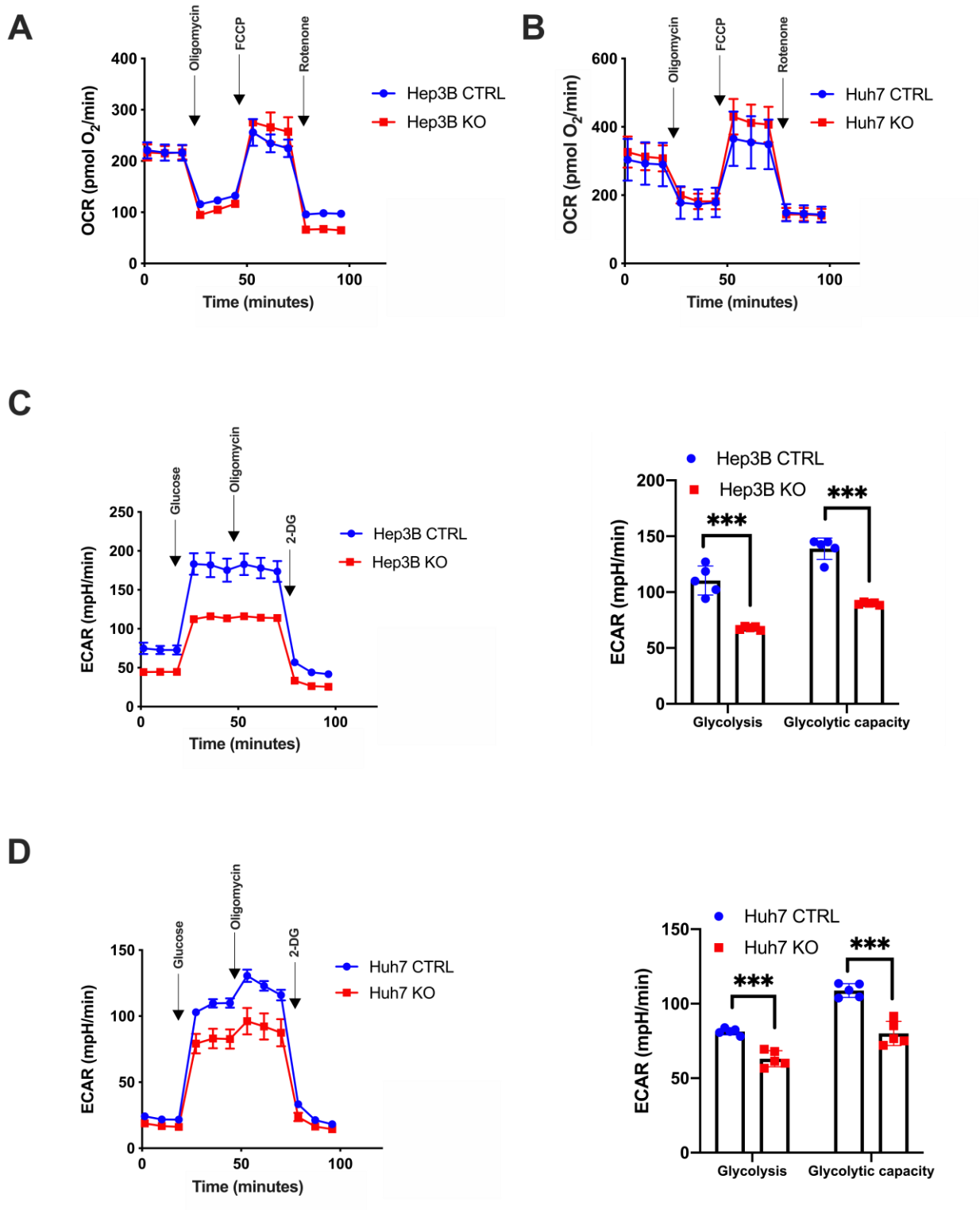

Figure. 3-8 A) Oxidative phosphorylation measurement in Hep3B KO and Hep3B CTRL cells. B) Oxidative phosphorylation measurement in Huh7 KO and CTRL cells. C) Glycolysis measurement in Hep3B KO and CTRL cells. ***, $P < 0.001$ (by t - test). D) Glycolysis measurement in Huh7 KO and CTRL cells. ***, $P < 0.001$ (by t - test).

Consistent with the putative role of CBX2 in glycolysis, Hep3B KO and Huh7 KO cells exhibited a significant reduction in the level of ATP (Fig. 3-9A) and lactate (Fig. 3-9B) respectively, compared with their respective control cells. Concordantly, Hep3B KO and Huh7 KO cells also demonstrated a significant reduction and induction of NAD^+ level (Fig. 3-9C) and NADH level (Fig. 3-9D) respectively resulting in significant reduction of NAD^+/NADH ratio in these cells (Fig. 3-9E).

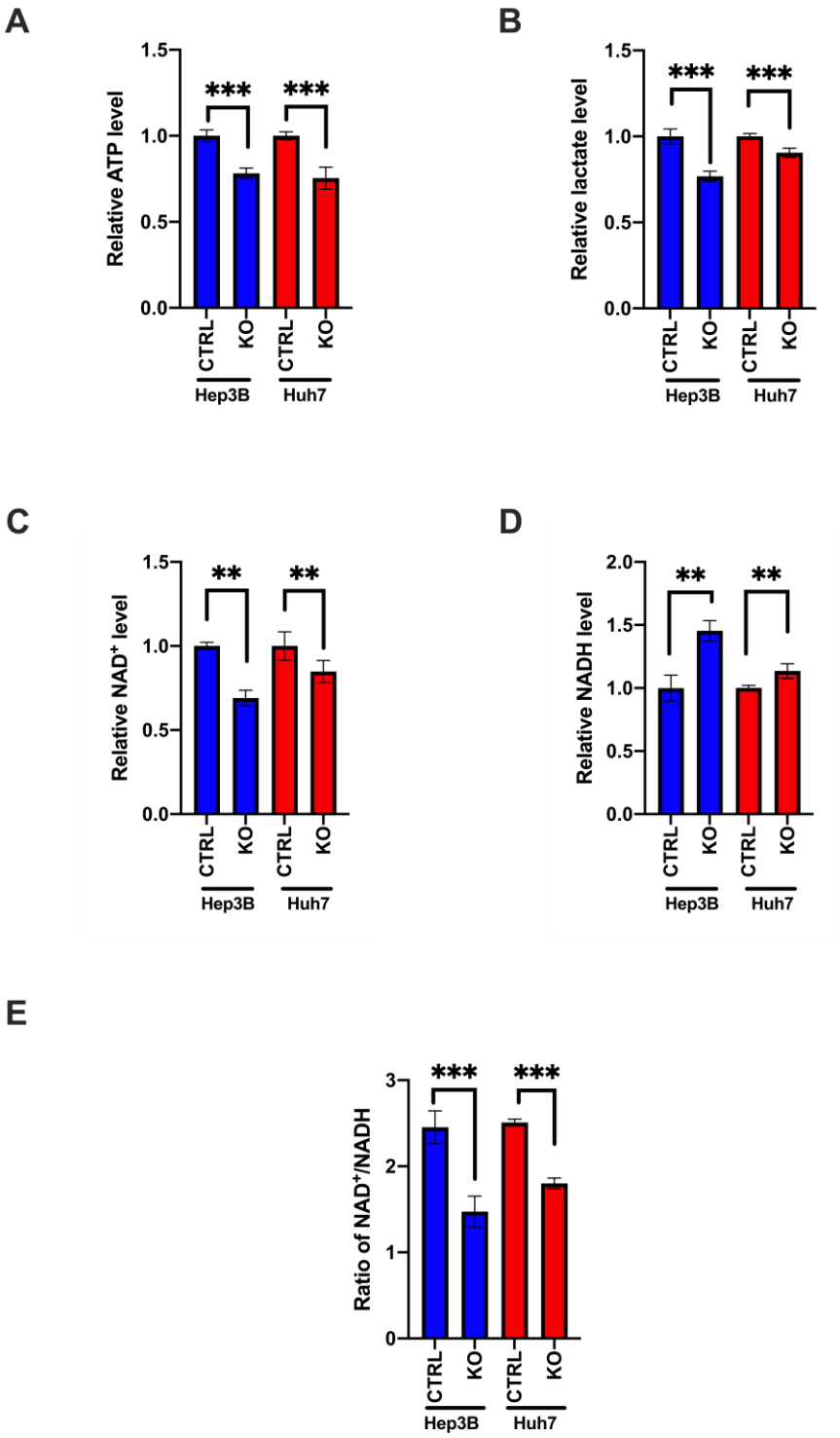

Figure. 3-9 A) ATP level in Hep3B KO versus Hep3B CTRL cells, and Huh7 KO versus Huh7 CTRL cells. ***, $P < 0.001$ (by t - test). B) Lactate level in Hep3B KO versus Hep3B CTRL cells, and Huh7 KO versus Huh7 CTRL cells. ***, $P < 0.001$ (by t - test). C) NAD^+ level in Hep3B KO versus Hep3B CTRL cells, and Huh7 KO versus Huh7 CTRL cells. **, $P < 0.05$ (by t - test). D) NADH level Hep3B KO versus Hep3B CTRL cells, and Huh7 KO versus Huh7 CTRL cells. **, $P < 0.05$ (by t - test). E) NAD^+/NADH level in Hep3B KO

versus Hep3B CTRL cells, and Huh7 KO versus Huh7 CTRL cells. ***, $P < 0.001$ (by t - test).

NAD^+ and NADH level, among other functions, are detrimental to the rate of glycolytic and oxidative phosphorylation, which was carried out in the cytoplasm and mitochondria respectively. To elucidate the origin of NAD^+ and NADH alternation, we determined NAD^+/NADH ratio using a highly responsive genetically encoded NAD^+/NADH sensor known as SoNar (180). SoNar is generated by chimeric fusion of cpYFP and the NADH binding domain of the Rex protein from Thermus aquaticus(181). SoNar exhibits differential fluorescence excitation property upon binding to NAD^+ (ex: 485nm/em: 530nm) and NADH (ex: 420nmn/em: 530nm) respectively, and generates fluorescence in a ratiometric manner. Furthermore, SoNar can be further modified for specific targeting to the cytoplasm (ct-SoNar) and mitochondria (mt-SoNar) respectively, allowing quantitative determination of NAD^+/NADH ratio at specific cellular compartment (180, 182). We found that ct-SoNar detected a rapid decline of NAD^+/NADH ratio in cytosol in Hep3B KO compared to CTRL cells (Fig. 3-10A and B), and mt-SoNar also detected a profoundly reduction of NAD^+/NADH in mitochondria (Fig. 3-10A and C) upon CBX2 deletion. As cytoplasmic NAD^+/NADH ratio is essential for glycolytic flux, these findings are concordant with the role of CBX2 in glycolysis and further suggested that CBX2 may play a role in the regulation of NAD^+/ NADH levels.

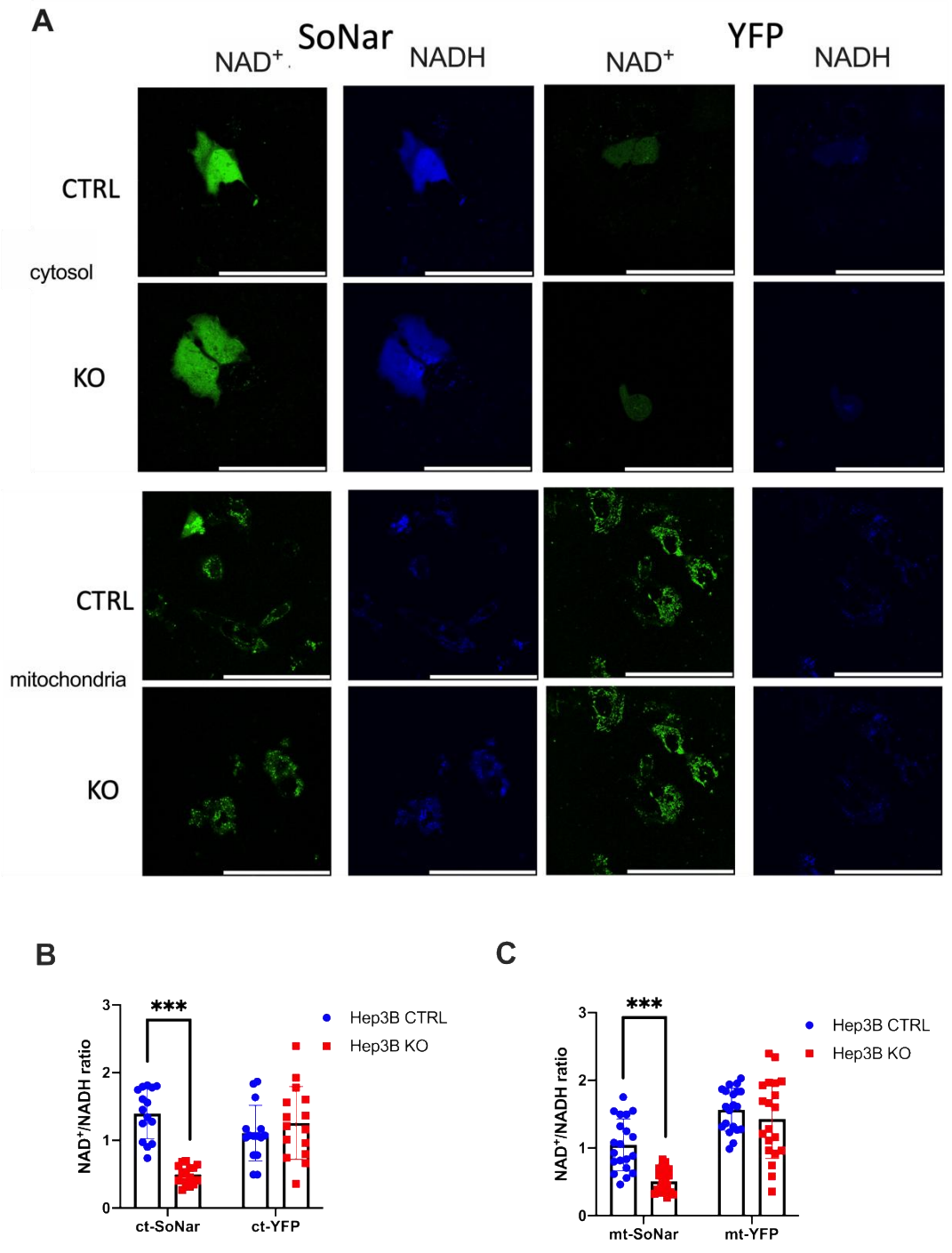

Figure. 3-10 NAD^+/NADH level measurement in Hep3B KO and CTRL cells using the SoNar System. A) Top: Image of the fluorescent signal in Hep3B KO and CTRL cells transfected with the ct-SoNar biosensor and ct-YFP vector. Bottom: Image of the fluorescent signal in Hep3B KO and CTRL cells transfected with the mt-SoNar biosensor and mtYFP vector. B) Quantification of NAD^+/NADH ratio in Hep3B KO and CTRL cells transfected with the ct-SoNar, using ct-YFP as an internal control. ***, $P < 0.001$ (by t - test). C) Quantification of NAD^+/NADH ratio in Hep3B KO and CTRL cells transfected with mt-SoNar, using mt-YFP as internal control. ***, $P < 0.001$ (by t - test).

To further elucidate if the cell growth inhibition in CBX2 KO cells is a consequence of the reduction in NAD^+/NADH ratio, we determined if NAM, a precursor of NAD^+ of the salvage pathway, rescues the proliferation of Huh7 KO and Hep3B KO cells respectively. NAM (0.5 mM) effectively restored the growth of Hep3B KO (Fig. 3-11A) and Huh7 KO (Fig. 3-11B) cells to a level similar to their corresponding control cells. In contrast, the addition of NAM did not promote the growth of Hep3B CTRL (Fig. 3-11A) and Huh7 CTRL (Fig. 3-11B) cells respectively. On the other hand, the addition of NAM significantly increased ATP levels in Hep3B KO (Fig. 3-11C) and Huh7 KO cells (Fig. 3-11D) respectively, but not in Hep3B CTRL (Fig. 3-11C) and Huh7 CTRL (Fig. 3-11D) cells. Together, these data suggested that CBX2 regulates cellular ATP level through maintaining NAD^+/NADH ratio.

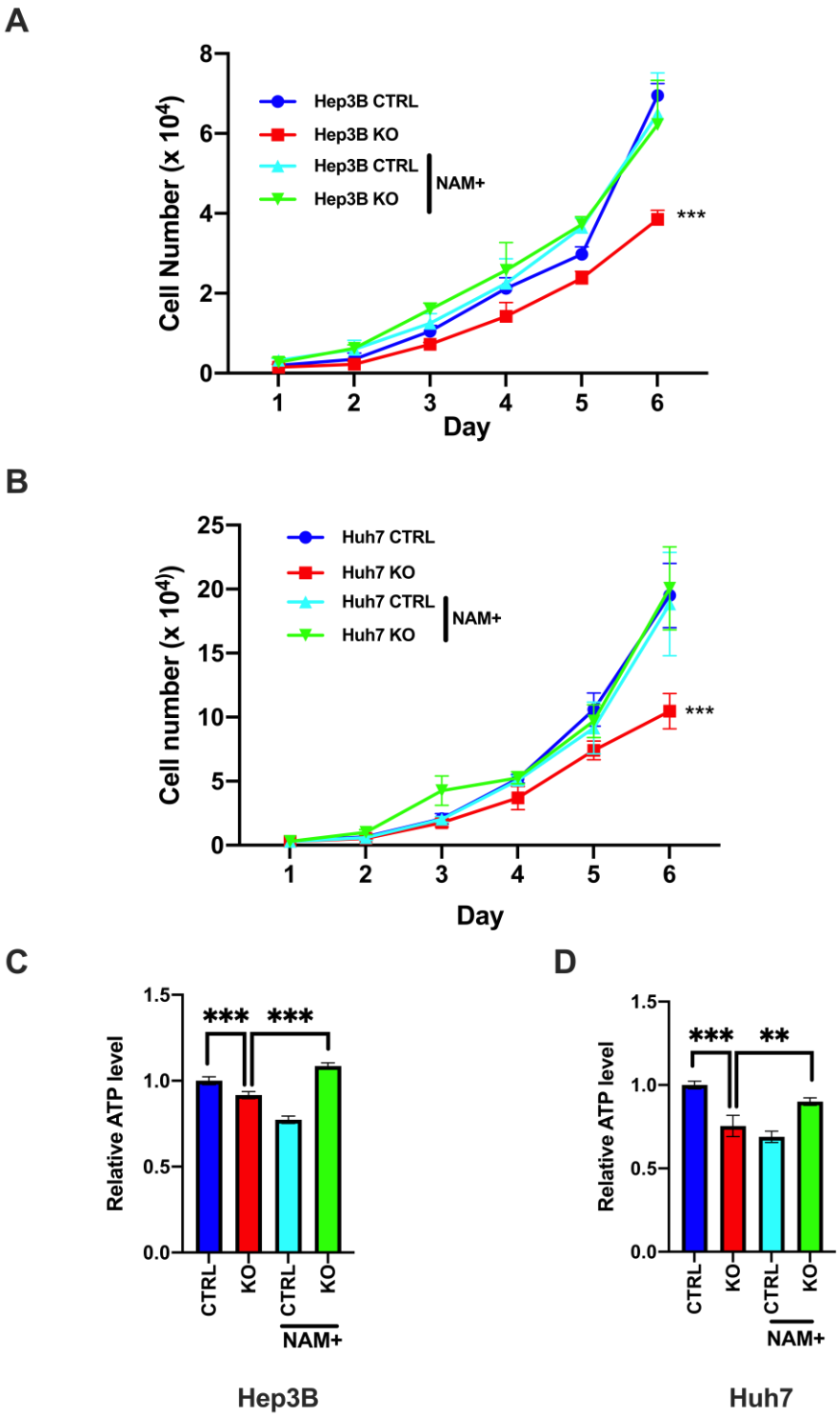

Figure. 3-11 A) Cell proliferation assay of Hep3B KO and CTRL cells with and without NAM (0.5 mM) supplementation. ***, $P < 0.001$ (by 2 - way ANOVA), compared with Hep3B CTRL cells. B) Cell proliferation assay in Huh7 KO and CTRL cells with and without NAM (0.5 mM) supplementation. ***, $P < 0.001$ (by 2 - way ANOVA), compared with Huh7 CTRL cells. C) ATP level measurement in Hep3B KO and CTRL cells with and without NAM (0.5 mM) supplementation. ***, $P < 0.001$ (by t - test). D) ATP level measurement in Huh7 KO and CTRL cells with and without NAM (0.5 mM) supplementation. **, $P < 0.05$; ***, $P<0.001$ (by t - test).

3.5 Upregulation of PCK2 mediates the effect of CBX2 deficiency in HCC cell growth

Because PRCs are involved in gene repressions (183), we hypothesized that gene knockout of CBX2 might induce expression of the target genes. Accordingly, examination of the genes represented in the term "metabolic pathway" (Fig. 3-7B) identified eight genes (ACSM2A, CA4, GALNT3, GCNT3, MAT1A, PCK2, P4HA1, and UGT2B4) that were commonly up-regulated in both Hep3B KO and Huh7 KO cells, suggesting that they might be putative targets of CBX2. Differential regulation of these genes by CBX2 was analyzed by quantitative RT-PCR analysis of Hep3B CTRL and KO cells respectively. Among others, four (CA4, GALNT3, GCNT3, and PCK2) genes were confirmed to be significantly up-regulated in Hep3B KO cells (Fig. 3-12A) suggesting that these upregulated genes potentially mediate the cell growth and metabolic phenotypes in the CBX2 knockout cells.

We further hypothesized that any gene(s) responsible for mediating the activity of CBX2 on cell growth and metabolism, upon its depletion, will rescue cell growth and metabolic phenotypes found in the CBX2 knockout cells. Accordingly, we conduct a shRNA screen of the candidate genes (CA4, GALNT3, GCNT3, and PCK2) using Hep3B KO cells. Transfection of shRNA against CA4 (shCA4), GALNT3 (shGALNT3), PCK2 (shPCK2) and GCNT3 (shGCNT3) into Hep3B KO cells, resulted in the repression of these genes respectively (Fig. 3-12B). Transfection of shCA4, shGALNT3, or shGCNT3, led to further suppression of cell proliferation of the Hep3B KO cells (Fig. 3-12C). Nevertheless, shPCK2 completely restored the proliferation of Hep3B KO cells to a rate similar to the Hep3B CTRL cells (Fig. 3-12C). These data suggested that overexpression of PCK2 in Hep3B KO cells mediates the cell growth suppression.

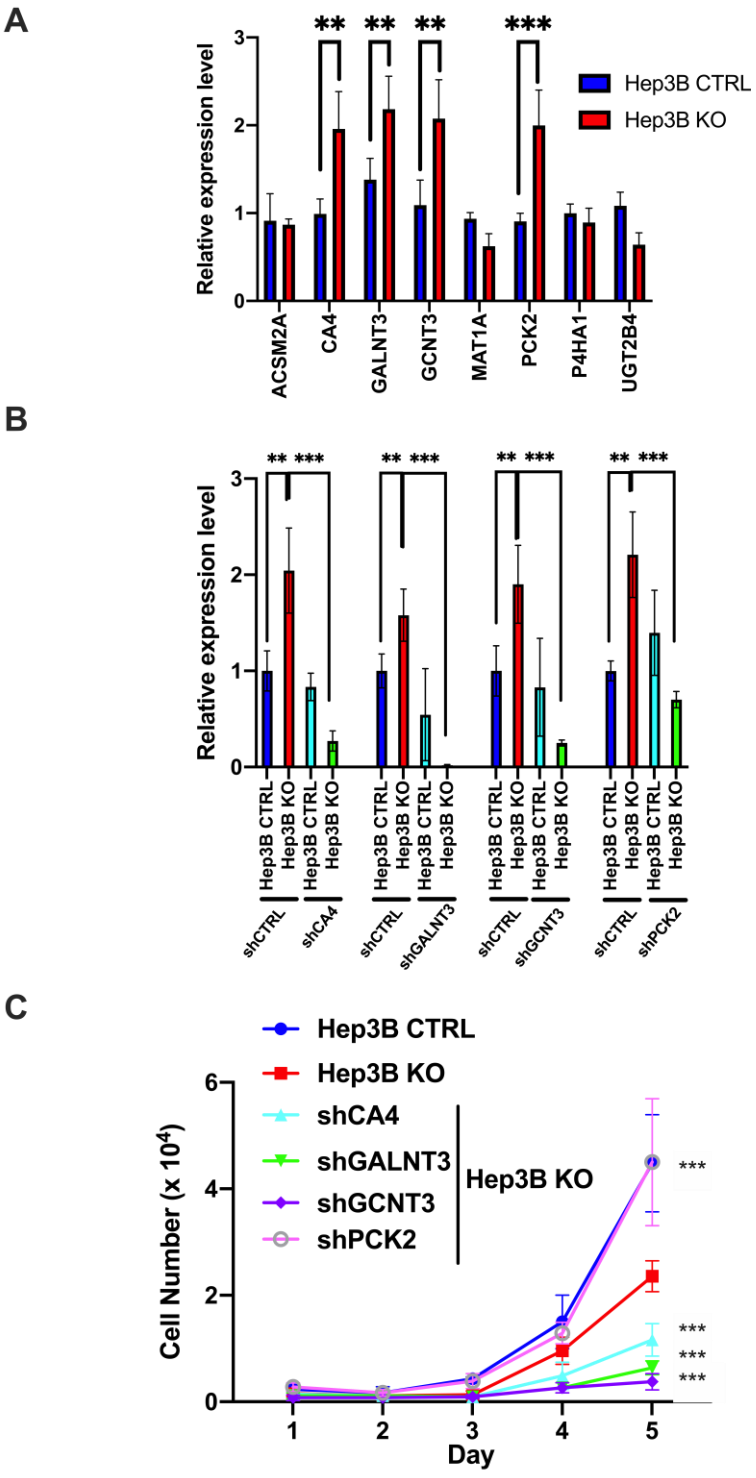

Figure. 3-12 A) Real - time quantitative PCR analysis of gene expressions in Hep3B KO and CTRL cells. **, $P < 0.05$; ***, $P < 0.001$ (by 2 - way ANOVA). B) Real - time quantitative PCR analysis of gene expressions in Hep3B KO and CTRL cells in response to shRNA - mediated gene knockdown of the indicated genes. **, $P < 0.05$; ***, $P < 0.001$ (by 2 - way ANOVA). C) Cell proliferation of Hep3B KO cells in response to shRNA - mediated gene knockdown of the indicated genes. ***, $P < 0.001$(by 2 - way ANOVA), compared with Hep3B KO cells at day 5.

Phosphoenolpyruvate carboxykinases (PCKs) are a rate-limiting enzymes in gluconeogenesis(184). There are two PCKs isoforms, namely the PCK1 and PCK2, representing the cytoplasmic and mitochondrial isoform respectively. Together they are responsible for the conversion of OAA to PEP, which is the intermediate of the gluconeogenesis pathway. To further understand the role of PCK2 in the regulation of HCC cell growth, we first determined the expression of PCK1 and PCK2 in HCC cells with or without CBX2. We found that PCK1 is expressed in the Hep3B and Huh7 CTRL cells respectively, whereas its expression was repressed in the corresponding KO cells (Fig. 3-13A). In contrast, PCK2 was expressed at a very low level in Hep3B and Huh7 CTRL cells, whereas its expressed was increased abundantly upon the knockout of CBX2 (Fig. 3-13A). Transfection of shPCK2 into Hep3B KO cells repressed PCK2 expression, whereas similar treatment did not alter PCK2 expression in Hep3B CTRL cells (Fig. 3-13B). Furthermore, transfection of shPCK2 promoted cell growth in Hep3B KO cells, it has no effect on the growth of Hep3B CTRL cells (Fig. 3-13C). On the other hand, transfection of shPCK2 into Huh7 KO cells also repressed the PCK2 expression (Fig. 3-13D) and partially restored the proliferation of Huh7 KO compared to Huh7 CTRL cells (Fig. 3-13E). Together, these data suggested that PCK2 is a specific mediator of CBX2 in the regulation of HCC cells proliferation.

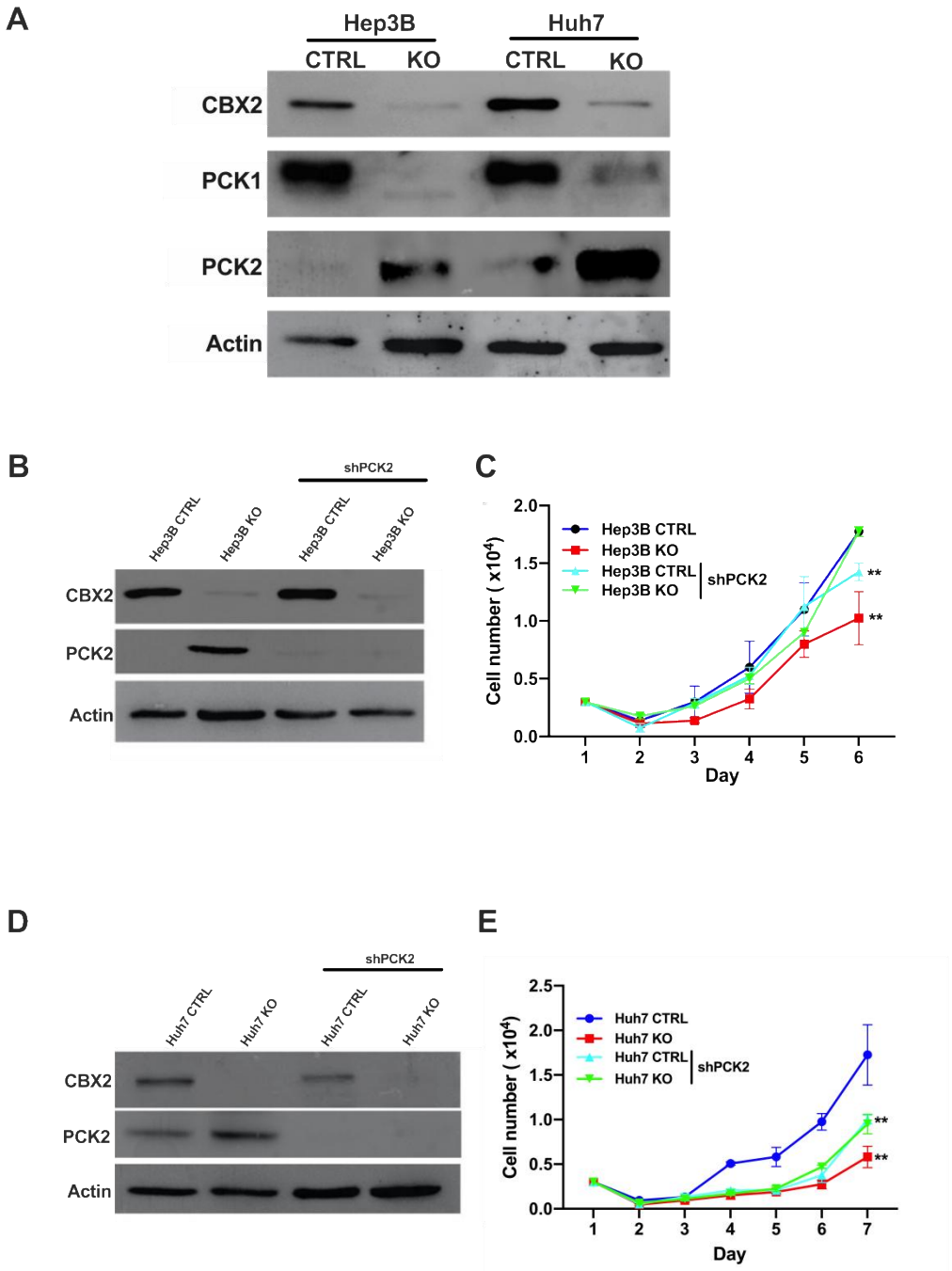

Figure. 3-13 A) Expression levels of CBX2, PCK1 and PCK2 in Hep3B CTRL versus KO, and Huh7 CTRL versus KO cells. B) Expression levels of CBX2 and PCK2 in Hep3B KO and CTRL cells transfected with shPCK2. C) Proliferation assay of Hep3B KO and CTRL cells transfected with shPCK2. **, $P < 0.05$ (by 2 - way ANOVA), compared with Hep3B CTRL cells at day 6. D) Expression levels of CBX2 and PCK2 in Huh7 KO and CTRL cells transfected with shPCK2. E) Proliferation assay of Huh7 KO and CTRL cells transfected with shPCK2. **, $P < 0.05$ (by 2 - way ANOVA), compared with Huh7 CTRL cells at day 7.

Next, we determined the level of PEP in Hep3B CTRL and KO cells and found that PEP was increased significantly in Hep3B KO, compared with Hep3B CTRL cells (Fig. 3-14A). In addition, transfection of shPCK2 to Hep3B KO cells restored NAD^+/NADH ratio of the cells to a level similar to that in Hep3B CTRL cells, but the same treatment did not affect NAD^+/NADH ratio of Hep3B CTRL cells (Fig. 3-14B). Transfection of shPCK2 to Hep3B KO cells also restored ECAR to the level similar to that of the Hep3B CTRL cells (Fig. 3-14C), resulted in the restoration of glycolysis and glycolytic capacity of the Hep3B cells (Fig. 3-14D).

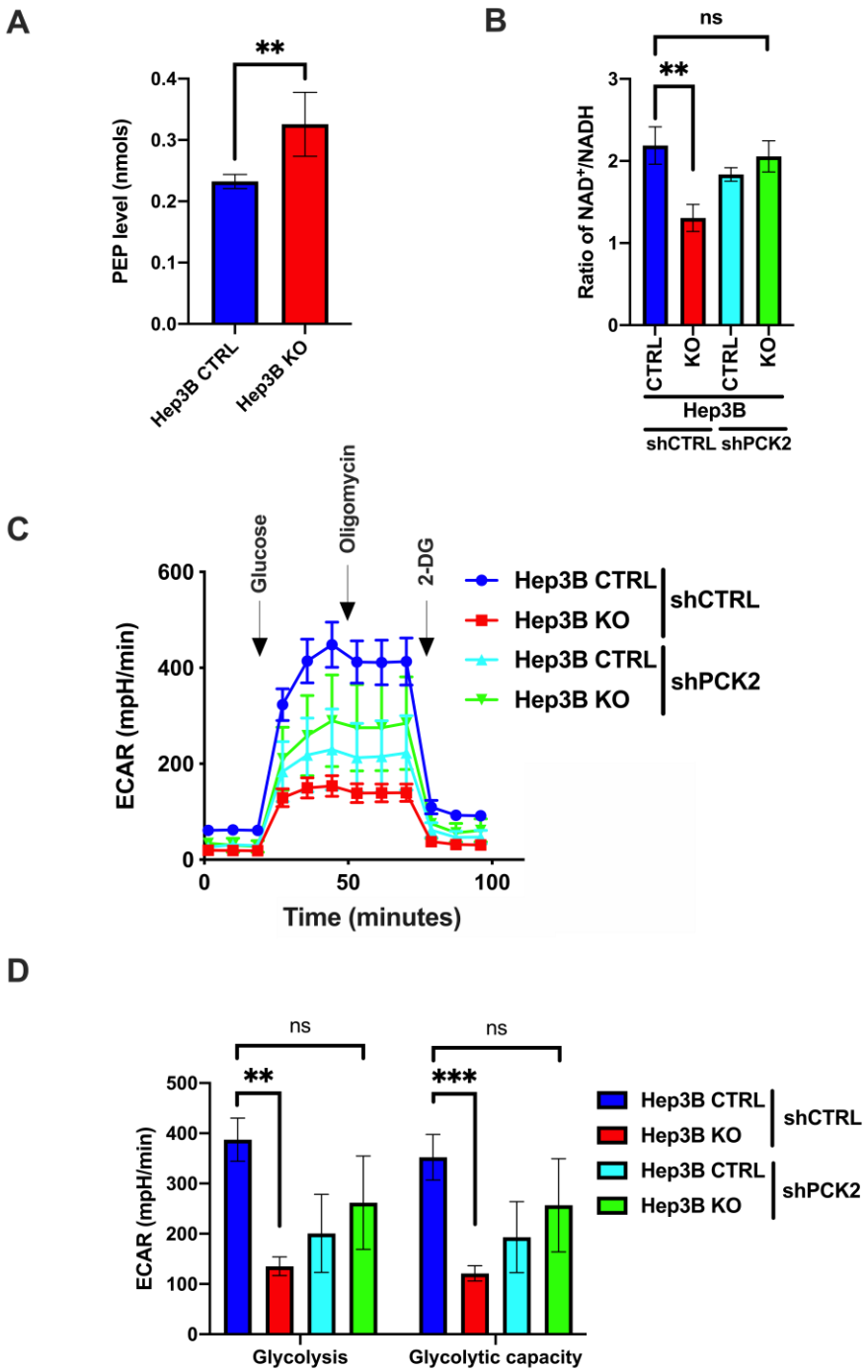

Figure. 3-14 A) PEP level measurement in Hep3B KO versus CTRL cells. **, $P < 0.05$ (by t - test). B) Measurement of the NAD^+/NADH level in Hep3B KO cells transfected with shCTRL and shPCK2 vector. **, $P < 0.05$; ns, no significant difference (by 2 - way ANOVA). C) ECAR measurement of Hep3B KO and CTRL cells transfected with shCTRL and shPCK2 vector. D) Analysis of glycolysis and glycolytic capacity of Hep3B KO cells transfected shCTRL and shPCK2 vector. **, $P < 0.05$; ***, $P < 0.001$; ns, no significant difference (by 2 - way ANOVA).

To further investigate the role of PCK1 and PCK2 in the CBX2-dependent HCC cell growth, we ectopically expressed PCK1 and PCK2 in Hep3B CTRL and KO cells respectively using the PiggyBac transposon system. Western blotting results showed that Hep3B CTRL and KO cells transfected with PiggyBac vector expressing PCK1 (PB PCK1) resulted a profound increase in PCK1 expression in these cells respectively, compared to cells transfected with the PiggyBac vector alone (PB CTRL)(Fig. 3-15A). On the other hand, Hep3B CTRL and KO cells transfected with PiggyBac vector expressing PCK2 (PB PCK2) resulted in the overexpression of PCK2 in these cells transfected with the PiggyBac vector alone (PB CTRL) (Fig. 3-15A). Next, the effect of PCK1 and PCK2 overexpression on HCC cell growth was determined. Ectopic expression of PCK1 (PB PCK1) in Hep3B CTRL and KO cells respectively did not lead to any change in the proliferation rate of these cells. On the other hand, ectopic expression of PCK2 in Hep3B CTRL cells significantly inhibited the proliferation of these cells, whereas ectopic expression of PCK2 in Hep3B KO cells did not affect the proliferation of these cells (Fig. 3-15B). Together, these data suggested that the proliferation of HCC cells is specifically inhibited by the induction of PCK2, but not PCK1.

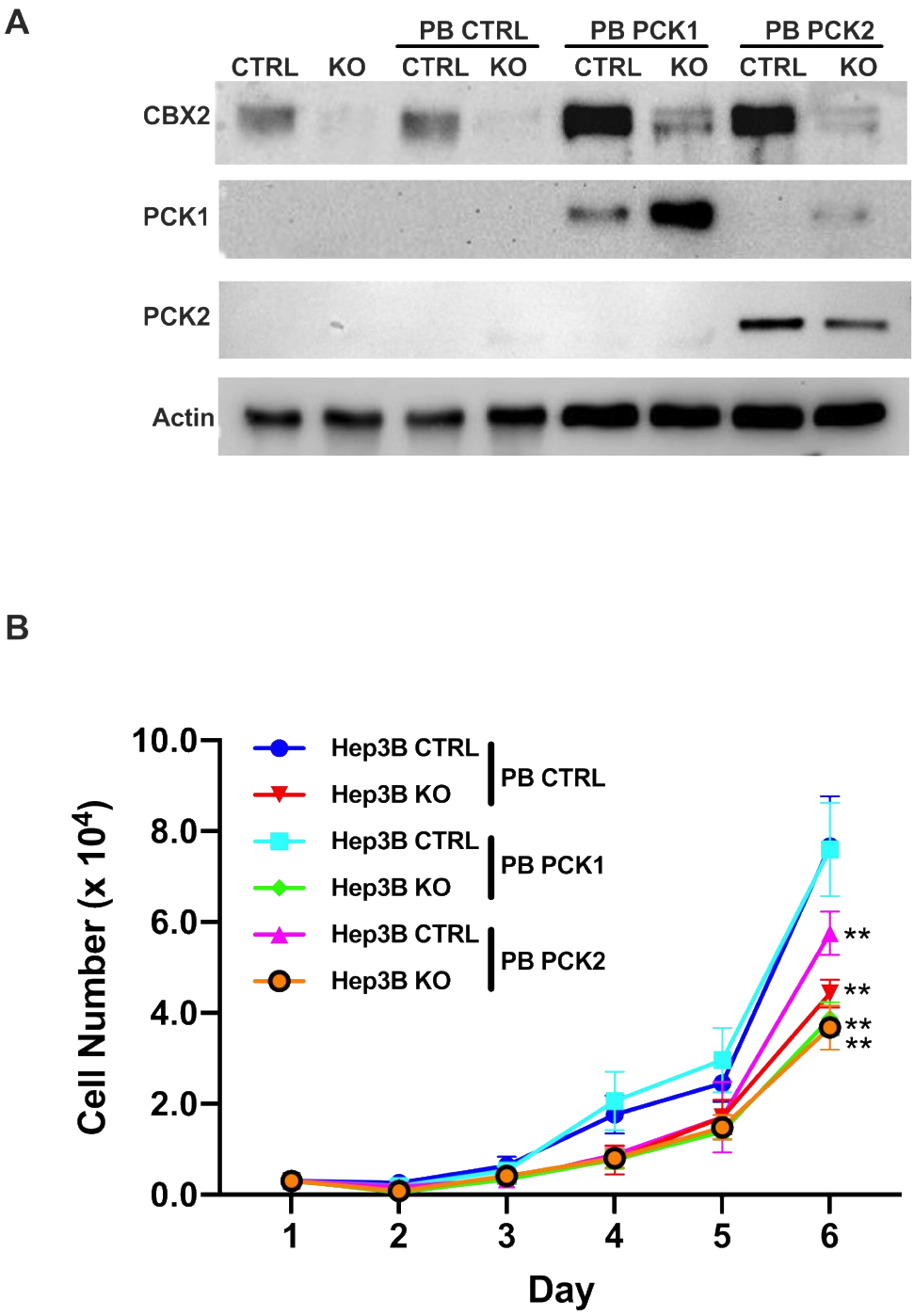

Figure. 3-15 A) Expression levels of CBX2, PCK1, and PCK2 in Hep3B CTRL and KO cells transfected with PB CTRL, PB PCK1 or PB PCK2 vector. B) Proliferation assay of Hep3B CTRL and KO cells transfected with PB CTRL, PB PCK1 or PB PCK2 vector. **, $P < 0.05$ (by 2 - way ANOVA), compared with Hep3B CTRL transfected with PB CTRL vector at day 6.

3.6 CBX2 enhance glycolysis and TCA cycle flux

PEP, a key cytoplasmic intermediate of gluconeogenesis, is generated from mitochondria and cytoplasmic OAA through PCK2 and PCK1 respectively (185) (Fig. 3-16). The induction of PCK2 in CBX2-depleted cells suggested that OAA will be removed from the TCA cycle to fuel gluconeogenesis. To determine if the level of TCA intermediates were altered in CBX2 knockout cells, we conducted mass spectrometric analysis of CBX2-proficient and -deficient cells. Metabolic analysis revealed that there is a significant reduction in the level of all TCA intermediates in Hep3B KO cells compared with Hep3B CTRL cells. These included alpha-ketoglutarate, succinate, fumarate, malate and citrate respectively (Fig. 3-17A and B). Previous studies showed that mass spectrometric analysis failed to identify cellular OAA, probably due to its immediate conversion to other metabolites(186). Because OAA is preferentially converted to aspartate by glutamic-oxaloacetic transaminase (GOT2), the level of aspartate was used as proxy for OAA in previous study(187-189). Similarly, we failed to identify OAA at a detectable level in the Hep3B CTRL and KO cells. However, aspartate was significantly reduced in Hep3B KO cells, compared to Hep3B CTRL (Fig. 3-17B), suggesting that OAA level is reduced in CBX2 KO cells.

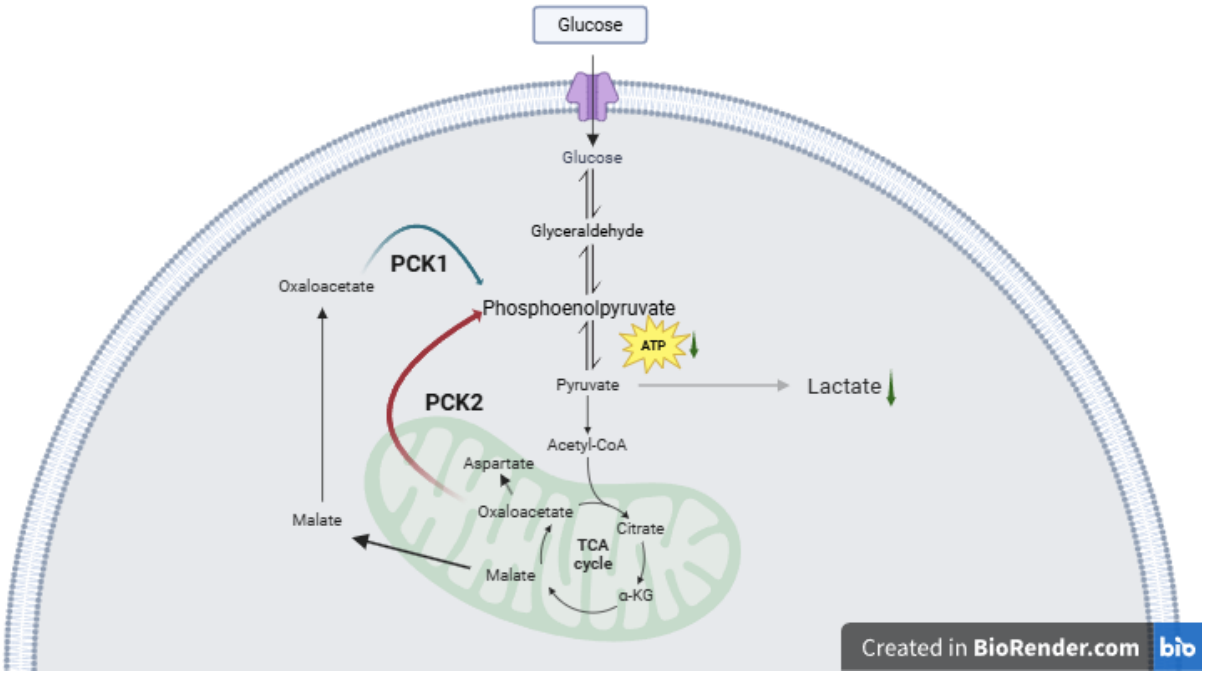

Figure. 3-16 The function of PCK1 and PCK2 (Figure generated using BioRender).

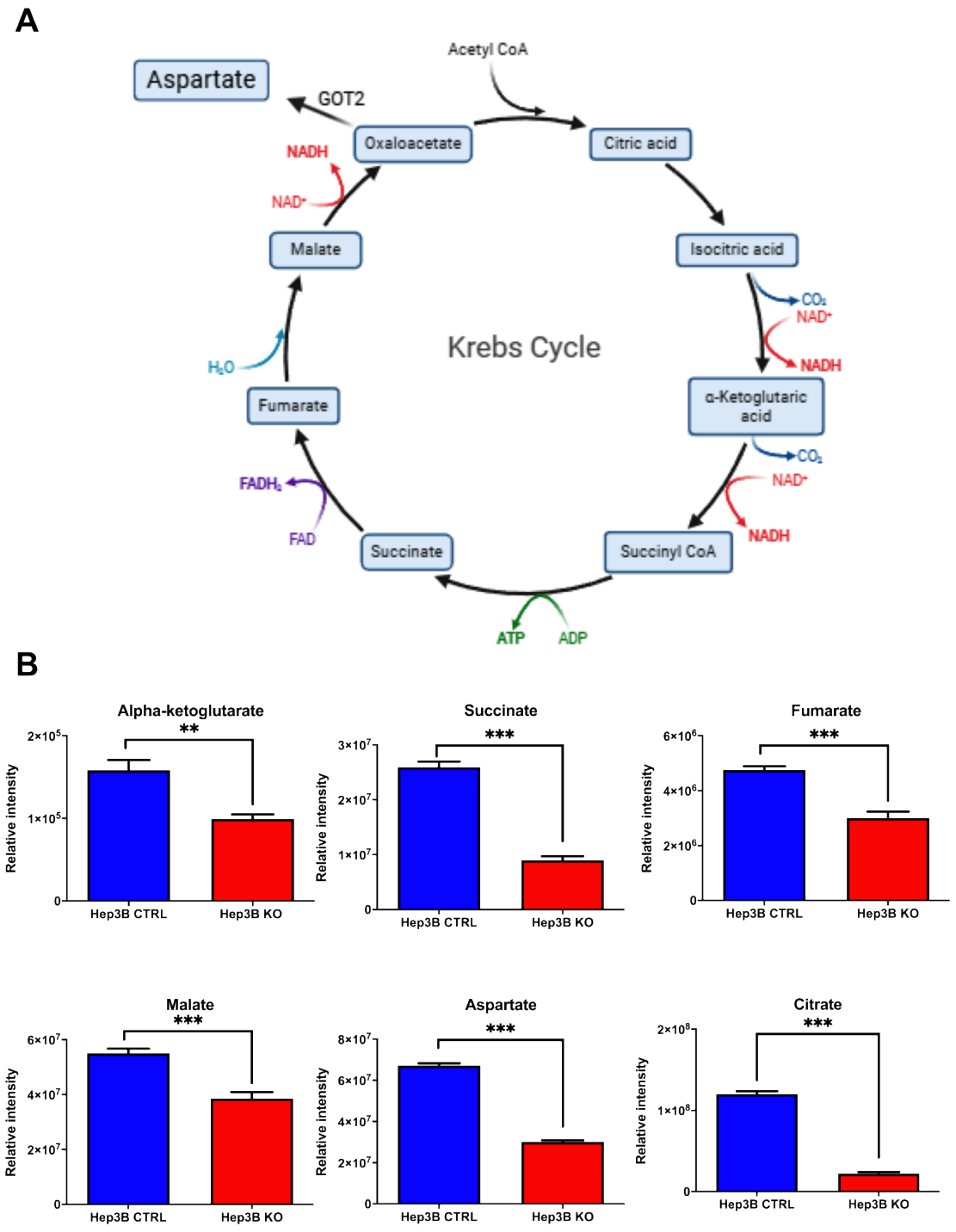

Figure. 3-17 A) Model and key component of TCA cycle (Figure generated using BioRender). B) Analysis of change of alpha-ketoglutarate, succinate, fumarate, malate, aspartate and citrate level in Hep3B CTRL and KO cells. **, $P < 0.05$; ***, $P<0.001$ (by t - test).

Although our biochemical measurement showed that there was a significant induction of PEP levels in Hep3B KO cells, compared with Hep3B CTRL (Fig. 3-14A), biochemical measurement of pyruvate showed that it is presence at a similar level in Hep3B CTRL and KO cells respectively (Fig. 3-18A). These data suggested that elevated PEP in Hep3B cells might be directed to gluconeogenesis. Consistent with our speculation, we found that the level of intracellular glucose is significantly elevated in the Hep3B KO cells compared to the Hep3B CTRL cells (Fig. 3-18B). The increase in glucose level was not due to enhanced cellular glucose uptake, as there was no difference in the rate of cellular glucose uptake between Hep3B KO and CTRL cells (Fig. 3-18C). Moreover, gluconeogenesis assay using lactate as energy source revealed that there is no significant difference in the extracellular glucose level between the Hep3B KO and CTRL cells (Fig. 3-18D). Together these data suggested that gluconeogenesis is activated, while glycolytic pathway was inhibited in Hep3B KO cells.

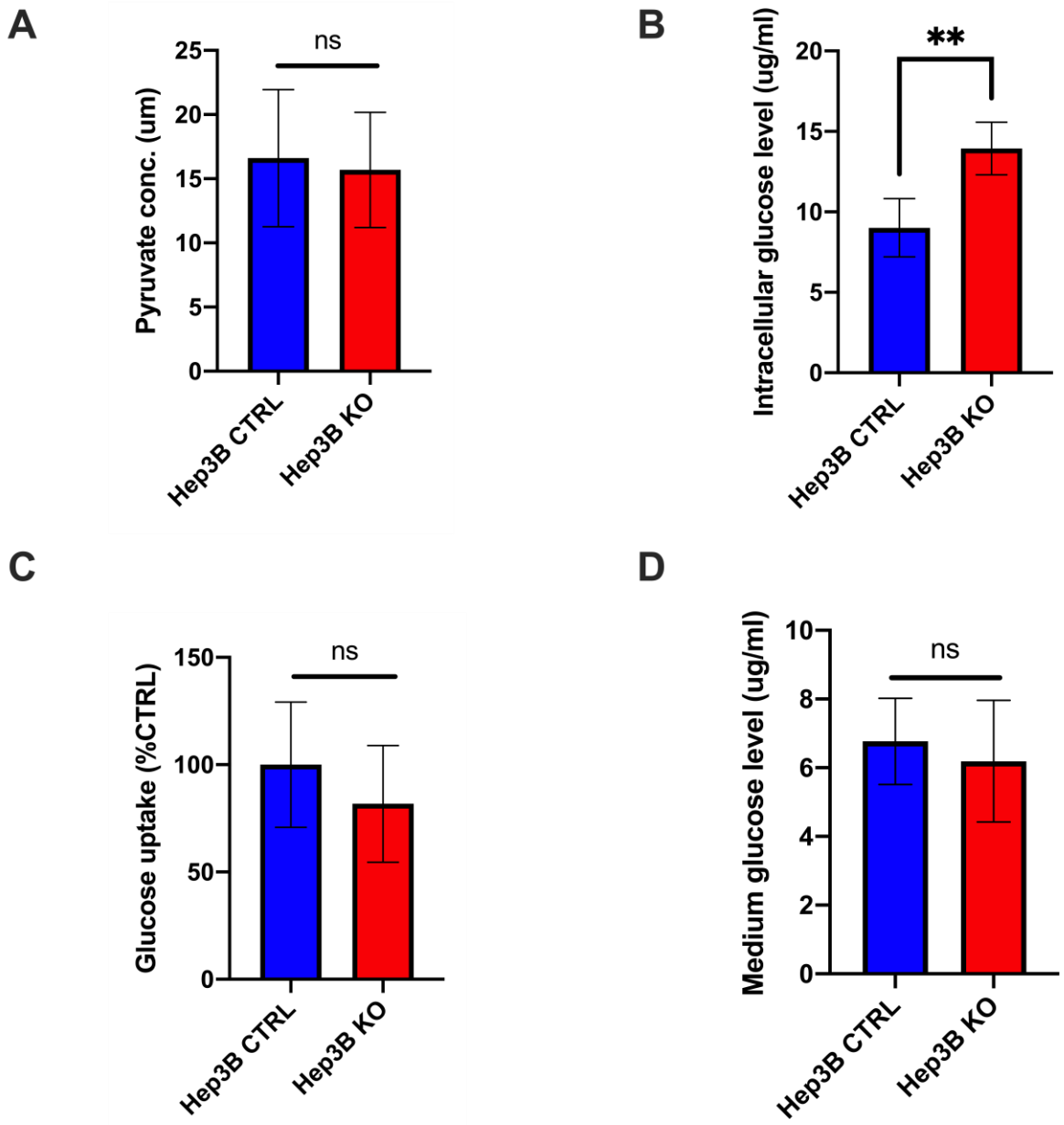

Figure. 3-18 A) Pyruvate level in Hep3B KO versus CTRL cells. ns, no significant difference (by t - test). B) Intra-cellular glucose level of Hep3B KO versus CTRL cells. **, $P < 0.05$ (by t - test). C) Glucose uptake by Hep3B KO versus CTRL cells. ns, no significant difference (by t - test). D) Extracellular glucose level of Hep3B KO versus CTRL cells. ns, no significant difference (by t - test).

Biochemical and metabolic analysis above suggested that there is a reduction in glycolysis and TCA metabolites when CBX2 is depleted. However, whether the reduction in TCA metabolites represents reduced metabolic flux through the TCA cycle flux remains elusive. To address this question, uniformly ^{13}C-labeled glutamine ($U^{13}C_5$-Glutamine) was used as an isotopic tracer to analyze the TCA metabolism in Hep3B CTRL and KO cells (Fig. 3-19A).

Cells were cultured in DMEM without glutamine for 6 hours to remove background signals and were then collected after one hour and three hours of incubation with $U^{13}C_5$-Glutamine respectively, followed by metabolic analysis using mass spectrometry. We found that there is a similar level of ^{13}C-labeled alpha-ketoglutarate in Hep3B KO and CTRL cells after three hours of incubation, suggesting that there was a stable supply of $U^{13}C_5$-Glutamine over the period of treatment. However, there was a significant reduction in the level of ^{13}C-labeled succinate, fumarate, malate, aspartate and citrate in the Hep3B KO cells after three hours of tracing (Fig. 3-19B). These data suggested that there is a significant reduction in the flux through the TCA in CBX2 KO cells.

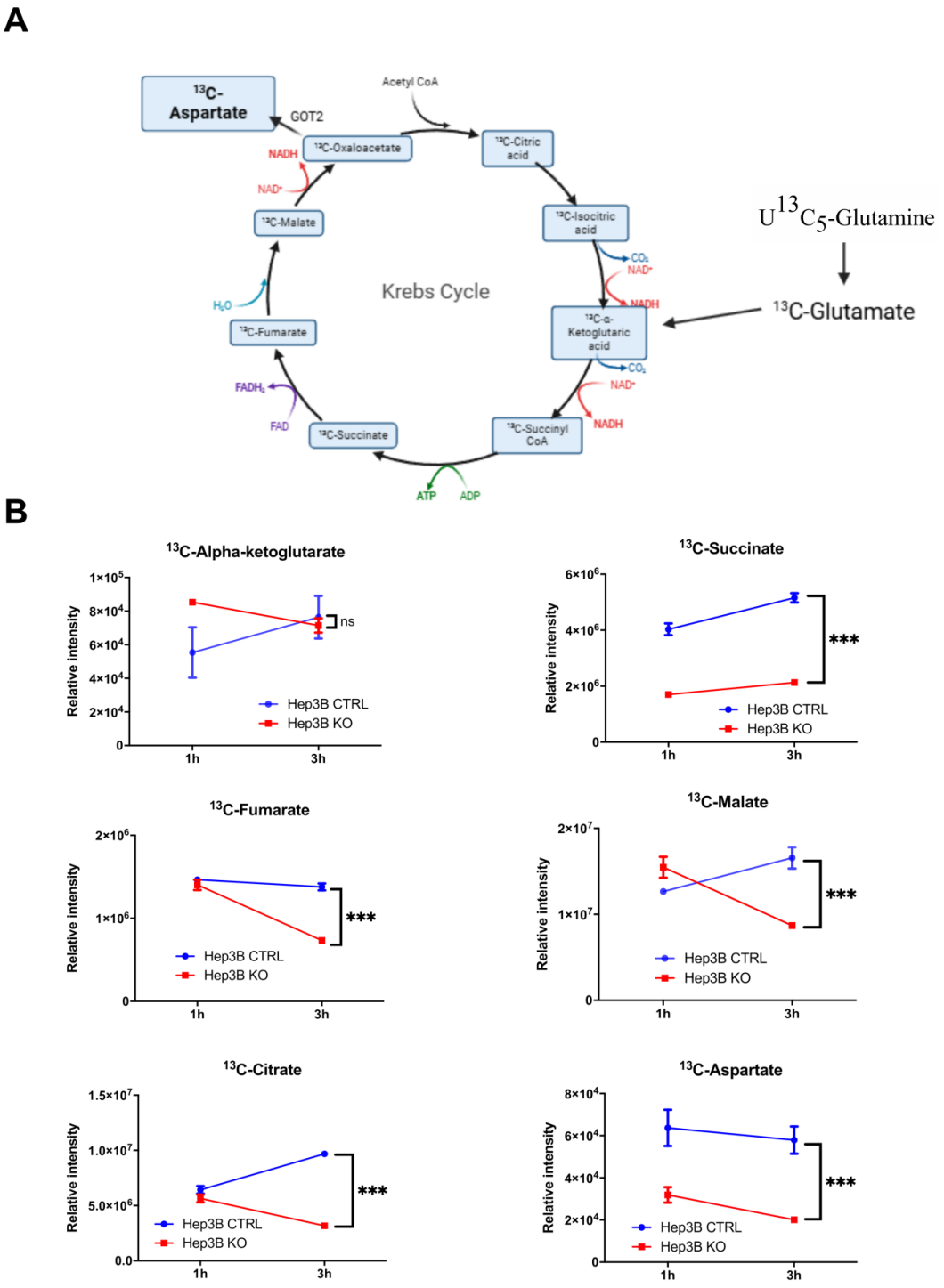

Figure. 3-19 A) Schematics illustration of the isotope labeling TCA intermediates in cells cultured with U$^{13}C_5$-Glutamine (Figure generated using BioRender). B) Quantification of ^{13}C-labeled alpha-ketoglutarate, succinate, fumarate, malate, citrate and aspartate level in Hep3B CTRL and KO cells cultured with U$^{13}C_5$-Glutamine for 1 hour (1h) and 3 hour (3h) respectively. ***, $P < 0.001$; ns, no significant difference (by 2 - way ANOVA), compared with Hep3B CTRL at 3h.

4. Discussion

It is well known that PRC proteins play a vital role in the pathogenesis of many cancers, but the function of each component of the complex remains largely elusive. Although previous studies have shown that CBX2 expression is associated with the development of prostate, breast, and lung cancers (174-176), CBX2 may elicit different functions in a tumor specific manner. In breast cancer, CBX2 promotes cell proliferation, invasion, and migration through the PI3K/AKT pathway(175). In contrast, in lung cancer, CBX2 and EZH2 cooperate to enhance tumor growth and metastasis by mediating the PPAR pathway (190). Additionally, it has been shown that CBX2 depletion induces cell apoptosis by activating the caspase-3 pathway in prostate cancer (174). Recent studies also suggest a clinical association between CBX2 expression and poor prognosis in HCC (178). . A recent analysis based on single RNA sequencing from the TCGA database and GSE revealed that CBX2 was one of 18 genes related to ligand receptors of hepatocytes and fibroblasts, and it was associated with hypoxia, glycolysis, and lactate metabolism(191). Furthermore, a novel HCC prognostic model, known as the super-enhancer-related risk model, indicated that CBX2 promotes metabolic reprogramming, such as glycolysis, and is regarded as a potential biomarker for predicting HCC prognosis(192). These findings suggest that CBX2 may mediate diverse regulatory pathways in a tissue- or cancer-specific manner.

The specific role of CBX2 in HCC pathogenesis remains largely unexplored. Using bioinformatics analysis, we started with analyzing TCGA database to elucidate the association between mutational frequency and gene amplification of cPRC1 components and HCCs, and discovered that CBX2 gene amplification is associated with poor prognosis of HCC. We further confirmed the overexpression of CBX2 in our collection of clinical samples, as well as in our collection of HCC cell lines. We also showed that CBX2 expression is very

low in normal hepatocytes, but became highly upregulated in HCC cell lines, suggesting that CBX2 plays a specific role in HCC pathogenesis.

Previous study had shown that CBX2 regulated proliferation and apoptosis in HCC cells (178). In our study, we found that CBX2 deletion profoundly inhibits proliferation in vitro and *in vivo*. Nevertheless, we failed to detect significant cell death in our cell model. It could possibly since while the previous repressed CBX2 expression through gene knockdown approach (178, 193), our study aimed to develop CBX2 gene knockout cell models. HCC cells that are highly susceptible to CBX2 depletion might have been eliminated during cell selection process, and the surviving cells developed phenotypes related to CBX2 depletion besides cell death. The critical role of CBX2 in HCC pathogenesis was further supported by the fact that ectopic expression of the gene in primary hepatocytes promotes cell proliferation and migration ability of the cells.

An earlier study indicated that CBX2 inhibits the expression of Wilms' tumor 1-interacting protein (WTIP), potentially leading to the inhibition of the Hippo pathway and inducing the phosphorylation of YAP1 in HCC (147). Another study also showed that CBX2 activates the accumulation of WNK1 protein to promote glycolysis in HCC (152). In agreement with previous findings, our study similarly revealed the role of CBX2 in regulating glycolysis of HCC cells. However, our bioinformatics analysis did not reveal significant enrichment of the Hippo pathway nor differential WTIP expression in CBX2-depleted HCC cells. The difference between these findings remains elusive at the moment. Our bioinformatics analysis of genes commonly regulated in Huh7 and Hep3B CBX2 KO cells suggested that CBX2 plays a central role in the regulation of metabolic pathways and energy metabolism in HCC cells. We found that CBX2 is essential for maintaining ECAR and OCR capability in HCC cells.

In addition, our analysis of CBX2 knockout cells further identified NAD^+ as an important link between CBX2 and energy metabolism. We found that CBX2 is important for the maintenance of NAD^+ level, and NAD^+/NADH ratio. Importantly, the supplementation of NAM, the NAD precursor, restored the growth and ATP level of CBX2 KO cells, suggesting that CBX2 regulates cellular processes related to NAD^+ metabolism, which in turns regulate energy homeostasis. NAD^+ is an essential coenzyme central to the glycolytic pathway, where the transfer of electrons from NAD^+ to NADH supports essential enzymatic conversions of glycolytic intermediates (194). The balance between NAD^+ and NADH levels is crucial for multiple metabolic pathways, including the maintenance of cellular redox conditions, energy metabolism, mitochondrial function, and various signaling pathways (195). Notably, increased NAD^+/NADH ratios have been observed in cancer cells compared to non-cancerous cells, suggesting that NAD^+ plays an essential role in metabolic pathways related to cancer development (196). Several studies have indicated that a decline in NAD^+ levels resulted in abnormal energy supply and a lower rate of glycolysis, subsequently leading to a reduction in TCA cycle activity (197).

How does CBX2 regulate NAD^+ level? Among the enriched gene list in the metabolic pathway identified by KEGG analysis, we made pivotal discovery that PCK2 overexpression is associated with cell growth inhibition, as well as NAD^+ level and ATP reduction in the CBX2-deficient HCC cells. We further showed that repression of PCK2 expression, but not its cytoplasmic isoform, PCK1, in CBX2 knockout cells effective restored cell growth, NAD^+ level and ECAR activity, suggesting that PCK2 plays a specific function in this process. The function role of PCK1 and PKC2 in HCC has not been in detail. PCK1 expression was found to be up-regulated under glucose-starved conditions and played a role in the cell death of HCC cells (198). The study showed that PCK1 overexpression resulted in metabolic

reprogramming by enhancing the abundance of TCA cycle intermediates, including citrate, fumarate, and malate, as well as the PEP(198). Based on our findings, it is interesting that PCK2, but not PCK1, is activated in the CBX2-depleted cells. Besides, under adequate nutritional conditions, overexpression of PCK1 did not impact on the proliferation of HCC cells, while ectopic expression of PCK2 showed obvious inhibitory activity in HCC cells in our study, suggesting that PCK2 plays a specific function in HCC cell growth. Overexpression of PCK2 was shown to inhibit colony formation in lung cancer and was regarded as a cancer suppressor (199). The discrepancy between the activity of PCK2 in these two cancer types may be due to the difference in the functional role of these two organs in energy homeostasis. The liver, alongside the kidneys, are the main organs that up-regulate gluconeogenesis for glucose production in response to starvation (200). Nevertheless, our data did not support the role of PCK2 in cell growth inhibition through gluconeogenesis, because we failed to identify an increased level of extracellular glucose in the CBX2 knockout cells.

Depsite that we have demonstrated a crucial role of PCK2 in regulating NAD^+ metabolism and mediating growth inhibition of CBX2 knockout cells, the classical reaction catalyzed by PCK2 does not have a role in NAD^+ metabolism. Although enhancing PCK2 activity may possibly enhance gluconeogenesis and promote the conversion of NAD^+ to NADH, the overexpression of PCK1 did not produce similar effects. These findings suggested that PCK2 overexpression in CBX2 knockout cells may play a novel functional role in limiting HCC cell growth, rather than the direct promotion of gluconeogenesis. In fact, Recent studies have suggested that PCK2 has a novel role in regulating metabolic pathways through protein degradation via direct protein binding. It was found that PCK2 promotes breast cancer invasion by upregulating the transforming growth factor (TGF) pathway. Specifically,

cytoplasmic PCK2 directly binds to the tripartite motif containing 67 (TRIM67), leading to the inhibition of ubiquitination and proteasomal degradation of SMAD family member 3 (SMAD3). Consequently, PCK2 sustains the expression of SMAD3 and promotes EMT in triple-negative breast cancer cells via the TGF-β/SMAD3 signaling pathway (201). Additionally, another study suggested that PCK2 translocates from the mitochondria to the cytosol and mediates LPS-induced inflammation. In this context, PCK2 modulates the phosphorylation of nuclear factor kappa B subunit 1 and the AKT/MAPK signaling pathway (202), but the mechanism of phosphorylation by PCK2 regulation is still unknown.

5. Conclusion and Future Plan

In this study, through analyzing CBX2 using bioinformatics, clinical specimens, and cell analysis, we confirmed that CBX2 is overexpressed in a subset of HCC specimens, and its overexpression in HCC has been associated with a worse prognostic outcome. Using HCC cell models where CBX2 expression was eliminated by CRISPR/Cas9 gene knockdown, we further discovered novel functional role of CBX2 in the regulation of HCC cell growth and metastasis by controlling cellular energy metabolism through regulating the expression of PCK2. Importantly, we defined a critical role of PCK2 upregulation in mediating the growth suppression phenotype of CBX2 depletion, where repression of PCK2 expression could completely restore the growth of CBX2-depleted HCC cells.

However, how PCK2 elicits dominant control in cellular energy homeostasis in HCC cells remains elusive. Additionally, it will also be important to investigate if similar CBX2-PCK2 regulatory axis is operating in other cancer cell types, and whether this pathway represents a major cell growth regulatory pathway in other cancers. With regards to HCCs, it will be essential to further elucidate the function of PCK2, and the molecular pathways regulated by

this enzyme. Emerging evidence suggested that besides its role in the chemical conversion of metabolites, PCK1 and PCK2 may regulate cellular activities through protein-protein interaction or post-translational modifications of proteins. Therefore, one may explore and compare the proteome of CBX2 knockout cells with or without PCK2 knockdown. Because PCKs have been implicated in protein phosphorylation, the potential of post-translational modifications served as a good starting point for the analysis of novel PCK2 functions,its mechanisms in relation to CBX2 in the pathogenesis of HCC.

6. Reference List

1. Bray F, Laversanne M, Sung H, Ferlay J, Siegel RL, Soerjomataram I, Jemal A. Global cancer statistics 2022: GLOBOCAN estimates of incidence and mortality worldwide for 36 cancers in 185 countries. CA Cancer J Clin. 2024.
2. Hobeika C, Nault JC, Barbier L, Schwarz L, Lim C, Laurent A, et al. Influence of surgical approach and quality of resection on the probability of cure for early-stage HCC occurring in cirrhosis. JHEP Rep. 2020;2(6):100153.
3. Bruix J, Sherman M. Diagnosis of Small HCC. Gastroenterology. 2005;129(4):1364.
4. McGlynn KA, Petrick JL, El-Serag HB. Epidemiology of Hepatocellular Carcinoma. Hepatology. 2021;73 Suppl 1(Suppl 1):4-13.
5. Alfaiate D, Clement S, Gomes D, Goossens N, Negro F. Chronic hepatitis D and hepatocellular carcinoma: A systematic review and meta-analysis of observational studies. J Hepatol. 2020;73(3):533-9.
6. Singal AG, Lampertico P, Nahon P. Epidemiology and surveillance for hepatocellular carcinoma: New trends. J Hepatol. 2020;72(2):250-61.
7. Chen K, Sng WK, Quah JH, Liu J, Chong BY, Lee HK, et al. Clinical spectrum of non-alcoholic fatty liver disease in patients with diabetes mellitus. PLoS One. 2020;15(8):e0236977.
8. Xie B, Wang DH, Spechler SJ. Sorafenib for treatment of hepatocellular carcinoma: a systematic review. Dig Dis Sci. 2012;57(5):1122-9.
9. Kim NY, Sun JM, Kim YJ, Lee KW, Kim JH, Bang SM, et al. Cisplatin-Based Combination Chemotherapy for Advanced Hepatocellular Carcinoma: A Single Center Experience before the Sorafenib Era. Cancer Res Treat. 2010;42(4):203-9.
10. Park JY, Chae JR, Cho YL, Kim Y, Lee D, Lee JK, Kang WJ. Targeted Therapy of Hepatocellular Carcinoma Using Gemcitabine-Incorporated GPC3 Aptamer. Pharmaceutics. 2020;12(10).
11. Wu Q, Wang R, Yang Q, Hou X, Chen S, Hou Y, et al. Chemoresistance to gemcitabine in hepatoma cells induces epithelial-mesenchymal transition and involves activation of PDGF-D pathway. Oncotarget. 2013;4(11):1999-2009.
12. Xu XF, Yang XK, Song Y, Chen BJ, Yu X, Xu T, Chen ZL. Dysregulation of non-coding RNAs mediates cisplatin resistance in hepatocellular carcinoma and therapeutic strategies. Pharmacol Res. 2022;176:105906.
13. Tang W, Chen Z, Zhang W, Cheng Y, Zhang B, Wu F, et al. The mechanisms of sorafenib resistance in hepatocellular carcinoma: theoretical basis and therapeutic aspects. Signal Transduct Target Ther. 2020;5(1):87.
14. Mihajlovic K, Milosavljevic I, Jeremic J, Savic M, Sretenovic J, Srejovic I, et al. Redox and apoptotic potential of novel ruthenium complexes in rat blood and heart. Can J Physiol Pharmacol. 2021;99(2):207-17.
15. Ueno H, Kiyosawa K, Kaniwa N. Pharmacogenomics of gemcitabine: can genetic studies lead to tailor-made therapy? Br J Cancer. 2007;97(2):145-51.
16. Liu L, Cao Y, Chen C, Zhang X, McNabola A, Wilkie D, et al. Sorafenib blocks the RAF/MEK/ERK pathway, inhibits tumor angiogenesis, and induces tumor cell apoptosis in hepatocellular carcinoma model PLC/PRF/5. Cancer Res. 2006;66(24):11851-8.
17. Pang Y, Eresen A, Zhang Z, Hou Q, Wang Y, Yaghmai V, Zhang Z. Adverse events of sorafenib in hepatocellular carcinoma treatment. Am J Cancer Res. 2022;12(6):2770-82.
18. Ogunwobi OO, Harricharran T, Huaman J, Galuza A, Odumuwagun O, Tan Y, et al. Mechanisms of hepatocellular carcinoma progression. World J Gastroenterol. 2019;25(19):2279-93.
19. Kensler TW, Qian GS, Chen JG, Groopman JD. Translational strategies for cancer prevention in liver. Nat Rev Cancer. 2003;3(5):321-9.
20. Farazi PA, DePinho RA. Hepatocellular carcinoma pathogenesis: from genes to environment. Nat Rev Cancer. 2006;6(9):674-87.

21. Xu J, Lin H, Wu G, Zhu M, Li M. IL-6/STAT3 Is a Promising Therapeutic Target for Hepatocellular Carcinoma. Front Oncol. 2021;11:760971.
22. Brinzea A, Nedelcu RI, Turcu G, Antohe M, Zurac SA, Ion DA. TIMPs expression in lentigo maligna/lentigo maligna melanoma versus aged skin - a review of the literature and personal experience. Rom J Morphol Embryol. 2017;58(3):717-21.
23. Shibue T, Weinberg RA. EMT, CSCs, and drug resistance: the mechanistic link and clinical implications. Nat Rev Clin Oncol. 2017;14(10):611-29.
24. Jablonska-Trypuc A, Matejczyk M, Rosochacki S. Matrix metalloproteinases (MMPs), the main extracellular matrix (ECM) enzymes in collagen degradation, as a target for anticancer drugs. J Enzyme Inhib Med Chem. 2016;31(sup1):177-83.
25. Scheau C, Badarau IA, Costache R, Caruntu C, Mihai GL, Didilescu AC, et al. The Role of Matrix Metalloproteinases in the Epithelial-Mesenchymal Transition of Hepatocellular Carcinoma. Anal Cell Pathol (Amst). 2019;2019:9423907.
26. Li TE, Wang S, Shen XT, Zhang Z, Chen M, Wang H, et al. PKM2 Drives Hepatocellular Carcinoma Progression by Inducing Immunosuppressive Microenvironment. Front Immunol. 2020;11:589997.
27. Schulte LA, Lopez-Gil JC, Sainz B, Jr., Hermann PC. The Cancer Stem Cell in Hepatocellular Carcinoma. Cancers (Basel). 2020;12(3).
28. Radu P, Zurzu M, Paic V, Bratucu M, Garofil D, Tigora A, et al. CD34-Structure, Functions and Relationship with Cancer Stem Cells. Medicina (Kaunas). 2023;59(5).
29. Baylin SB, Jones PA. A decade of exploring the cancer epigenome - biological and translational implications. Nat Rev Cancer. 2011;11(10):726-34.
30. Nowell PC. The clonal evolution of tumor cell populations. Science. 1976;194(4260):23-8.
31. Tanabe S, Quader S, Cabral H, Ono R. Interplay of EMT and CSC in Cancer and the Potential Therapeutic Strategies. Front Pharmacol. 2020;11:904.
32. Calcagno AM, Salcido CD, Gillet JP, Wu CP, Fostel JM, Mumau MD, et al. Prolonged drug selection of breast cancer cells and enrichment of cancer stem cell characteristics. J Natl Cancer Inst. 2010;102(21):1637-52.
33. Maugeri-Sacca M, Vigneri P, De Maria R. Cancer stem cells and chemosensitivity. Clin Cancer Res. 2011;17(15):4942-7.
34. Bracker TU, Giebel B, Spanholtz J, Sorg UR, Klein-Hitpass L, Moritz T, Thomale J. Stringent regulation of DNA repair during human hematopoietic differentiation: a gene expression and functional analysis. Stem Cells. 2006;24(3):722-30.
35. Fan ST, Yang ZF, Ho DW, Ng MN, Yu WC, Wong J. Prediction of posthepatectomy recurrence of hepatocellular carcinoma by circulating cancer stem cells: a prospective study. Ann Surg. 2011;254(4):569-76.
36. Ji J, Wang XW. Clinical implications of cancer stem cell biology in hepatocellular carcinoma. Semin Oncol. 2012;39(4):461-72.
37. Sun YF, Xu Y, Yang XR, Guo W, Zhang X, Qiu SJ, et al. Circulating stem cell-like epithelial cell adhesion molecule-positive tumor cells indicate poor prognosis of hepatocellular carcinoma after curative resection. Hepatology. 2013;57(4):1458-68.
38. Rawal P, Siddiqui H, Hassan M, Choudhary MC, Tripathi DM, Nain V, et al. Endothelial Cell-Derived TGF-beta Promotes Epithelial-Mesenchymal Transition via CD133 in HBx-Infected Hepatoma Cells. Front Oncol. 2019;9:308.
39. Song W, Li H, Tao K, Li R, Song Z, Zhao Q, et al. Expression and clinical significance of the stem cell marker CD133 in hepatocellular carcinoma. Int J Clin Pract. 2008;62(8):1212-8.
40. Zhang Y, Li W, Bian Y, Li Y, Cong L. Multifaceted roles of aerobic glycolysis and oxidative phosphorylation in hepatocellular carcinoma. PeerJ. 2023;11:e14797.
41. Pokrzywinski KL, Biel TG, Kryndushkin D, Rao VA. Therapeutic Targeting of the Mitochondria Initiates Excessive Superoxide Production and Mitochondrial Depolarization Causing Decreased mtDNA Integrity. PLoS One. 2016;11(12):e0168283.

42. Kuznetsov AV, Javadov S, Saks V, Margreiter R, Grimm M. Synchronism in mitochondrial ROS flashes, membrane depolarization and calcium sparks in human carcinoma cells. Biochim Biophys Acta Bioenerg. 2017;1858(6):418-31.
43. Li Y, Xu S, Li J, Zheng L, Feng M, Wang X, et al. SIRT1 facilitates hepatocellular carcinoma metastasis by promoting PGC-1alpha-mediated mitochondrial biogenesis. Oncotarget. 2016;7(20):29255-74.
44. Schwartz L, Supuran CT, Alfarouk KO. The Warburg Effect and the Hallmarks of Cancer. Anticancer Agents Med Chem. 2017;17(2):164-70.
45. Liberti MV, Locasale JW. The Warburg Effect: How Does it Benefit Cancer Cells? Trends Biochem Sci. 2016;41(3):211-8.
46. Vander Heiden MG, Cantley LC, Thompson CB. Understanding the Warburg effect: the metabolic requirements of cell proliferation. Science. 2009;324(5930):1029-33.
47. Epstein T, Xu L, Gillies RJ, Gatenby RA. Separation of metabolic supply and demand: aerobic glycolysis as a normal physiological response to fluctuating energetic demands in the membrane. Cancer Metab. 2014;2:7.
48. Locasale JW, Grassian AR, Melman T, Lyssiotis CA, Mattaini KR, Bass AJ, et al. Phosphoglycerate dehydrogenase diverts glycolytic flux and contributes to oncogenesis. Nat Genet. 2011;43(9):869-74.
49. Page P. Advances and strategies in NADPH oxidase inhibitors and activators patents. Pharm Pat Anal. 2014;3(4):387-409.
50. Lunt SY, Vander Heiden MG. Aerobic glycolysis: meeting the metabolic requirements of cell proliferation. Annu Rev Cell Dev Biol. 2011;27:441-64.
51. Feng J, Li J, Wu L, Yu Q, Ji J, Wu J, et al. Emerging roles and the regulation of aerobic glycolysis in hepatocellular carcinoma. J Exp Clin Cancer Res. 2020;39(1):126.
52. Bartrons R, Rodriguez-Garcia A, Simon-Molas H, Castano E, Manzano A, Navarro-Sabate A. The potential utility of PFKFB3 as a therapeutic target. Expert Opin Ther Targets. 2018;22(8):659-74.
53. Shang RZ, Qu SB, Wang DS. Reprogramming of glucose metabolism in hepatocellular carcinoma: Progress and prospects. World J Gastroenterol. 2016;22(45):9933-43.
54. Luo W, Semenza GL. Emerging roles of PKM2 in cell metabolism and cancer progression. Trends Endocrinol Metab. 2012;23(11):560-6.
55. Zhang J, Shang L, Jiang W, Wu W. Shikonin induces apoptosis and autophagy via downregulation of pyrroline-5-carboxylate reductase1 in hepatocellular carcinoma cells. Bioengineered. 2022;13(3):7904-18.
56. Afonso J, Goncalves C, Costa M, Ferreira D, Santos L, Longatto-Filho A, Baltazar F. Glucose Metabolism Reprogramming in Bladder Cancer: Hexokinase 2 (HK2) as Prognostic Biomarker and Target for Bladder Cancer Therapy. Cancers (Basel). 2023;15(3).
57. Tomizawa M, Shinozaki F, Motoyoshi Y, Sugiyama T, Yamamoto S, Ishige N. 2-Deoxyglucose and sorafenib synergistically suppress the proliferation and motility of hepatocellular carcinoma cells. Oncol Lett. 2017;13(2):800-4.
58. Porporato PE, Dhup S, Dadhich RK, Copetti T, Sonveaux P. Anticancer targets in the glycolytic metabolism of tumors: a comprehensive review. Front Pharmacol. 2011;2:49.
59. Ricotti L, Tesei A, De Paola F, Milandri C, Amadori D, Frassineti GL, et al. Potentiation of antiproliferative drug activity by lonidamine in hepatocellular carcinoma cells. J Chemother. 2003;15(5):480-7.
60. Lage R, Dieguez C, Vidal-Puig A, Lopez M. AMPK: a metabolic gauge regulating whole-body energy homeostasis. Trends Mol Med. 2008;14(12):539-49.
61. Rui L. Energy metabolism in the liver. Compr Physiol. 2014;4(1):177-97.
62. Ma R, Zhang W, Tang K, Zhang H, Zhang Y, Li D, et al. Switch of glycolysis to gluconeogenesis by dexamethasone for treatment of hepatocarcinoma. Nat Commun. 2013;4:2508.
63. Hers HG, Hue L. Gluconeogenesis and related aspects of glycolysis. Annu Rev Biochem. 1983;52:617-53.

64. Wang Z, Dong C. Gluconeogenesis in Cancer: Function and Regulation of PEPCK, FBPase, and G6Pase. Trends Cancer. 2019;5(1):30-45.
65. Nye C, Kim J, Kalhan SC, Hanson RW. Reassessing triglyceride synthesis in adipose tissue. Trends Endocrinol Metab. 2008;19(10):356-61.
66. Grasmann G, Smolle E, Olschewski H, Leithner K. Gluconeogenesis in cancer cells - Repurposing of a starvation-induced metabolic pathway? Biochim Biophys Acta Rev Cancer. 2019;1872(1):24-36.
67. Yong J, Cai S, Zeng Z. Targeting NAD(+) metabolism: dual roles in cancer treatment. Front Immunol. 2023;14:1269896.
68. Liu L, Su X, Quinn WJ, 3rd, Hui S, Krukenberg K, Frederick DW, et al. Quantitative Analysis of NAD Synthesis-Breakdown Fluxes. Cell Metab. 2018;27(5):1067-80 e5.
69. Chiarugi A, Dolle C, Felici R, Ziegler M. The NAD metabolome--a key determinant of cancer cell biology. Nat Rev Cancer. 2012;12(11):741-52.
70. Chowdhry S, Zanca C, Rajkumar U, Koga T, Diao Y, Raviram R, et al. NAD metabolic dependency in cancer is shaped by gene amplification and enhancer remodelling. Nature. 2019;569(7757):570-5.
71. Srivastava S. Emerging therapeutic roles for NAD(+) metabolism in mitochondrial and age-related disorders. Clin Transl Med. 2016;5(1):25.
72. Palmieri F, Rieder B, Ventrella A, Blanco E, Do PT, Nunes-Nesi A, et al. Molecular identification and functional characterization of Arabidopsis thaliana mitochondrial and chloroplastic NAD+ carrier proteins. J Biol Chem. 2009;284(45):31249-59.
73. Todisco S, Agrimi G, Castegna A, Palmieri F. Identification of the mitochondrial NAD+ transporter in Saccharomyces cerevisiae. J Biol Chem. 2006;281(3):1524-31.
74. Kory N, Uit de Bos J, van der Rijt S, Jankovic N, Gura M, Arp N, et al. MCART1/SLC25A51 is required for mitochondrial NAD transport. Sci Adv. 2020;6(43).
75. Luongo TS, Eller JM, Lu MJ, Niere M, Raith F, Perry C, et al. SLC25A51 is a mammalian mitochondrial NAD(+) transporter. Nature. 2020;588(7836):174-9.
76. Fletcher RS, Lavery GG. The emergence of the nicotinamide riboside kinases in the regulation of NAD+ metabolism. J Mol Endocrinol. 2018;61(3):R107-R21.
77. Chatterjee S, Daenthanasanmak A, Chakraborty P, Wyatt MW, Dhar P, Selvam SP, et al. CD38-NAD(+)Axis Regulates Immunotherapeutic Anti-Tumor T Cell Response. Cell Metab. 2018;27(1):85-100 e8.
78. Guo X, Dilidaxi D, Li L, Wang C, Ma X, Sang F, et al. Aspirin protects human trophoblast HTR-8/SVneo cells from H(2)O(2)-Induced oxidative stress via NADPH/ROS pathway. Placenta. 2023;144:55-63.
79. Bonora M, Morganti C, van Gastel N, Ito K, Calura E, Zanolla I, et al. A mitochondrial NADPH-cholesterol axis regulates extracellular vesicle biogenesis to support hematopoietic stem cell fate. Cell Stem Cell. 2024;31(3):359-77 e10.
80. Hayes JD, Dinkova-Kostova AT, Tew KD. Oxidative Stress in Cancer. Cancer Cell. 2020;38(2):167-97.
81. Moloney JN, Cotter TG. ROS signalling in the biology of cancer. Semin Cell Dev Biol. 2018;80:50-64.
82. Cha C, Dematteo RP. Molecular mechanisms in hepatocellular carcinoma development. Best Pract Res Clin Gastroenterol. 2005;19(1):25-37.
83. Wang Y, Deng B. Hepatocellular carcinoma: molecular mechanism, targeted therapy, and biomarkers. Cancer Metastasis Rev. 2023;42(3):629-52.
84. Bhat V, Srinathan S, Pasini E, Angeli M, Chen E, Baciu C, Bhat M. Epigenetic basis of hepatocellular carcinoma: A network-based integrative meta-analysis. World J Hepatol. 2018;10(1):155-65.
85. Zheng Y, Hlady RA, Joyce BT, Robertson KD, He C, Nannini DR, et al. DNA methylation of individual repetitive elements in hepatitis C virus infection-induced hepatocellular carcinoma. Clin Epigenetics. 2019;11(1):145.

86. Braghini MR, Lo Re O, Romito I, Fernandez-Barrena MG, Barbaro B, Pomella S, et al. Epigenetic remodelling in human hepatocellular carcinoma. J Exp Clin Cancer Res. 2022;41(1):107.
87. Woodcock CL, Ghosh RP. Chromatin higher-order structure and dynamics. Cold Spring Harb Perspect Biol. 2010;2(5):a000596.
88. Talbert PB, Henikoff S. Histone variants--ancient wrap artists of the epigenome. Nat Rev Mol Cell Biol. 2010;11(4):264-75.
89. Jin C, Felsenfeld G. Nucleosome stability mediated by histone variants H3.3 and H2A.Z. Genes Dev. 2007;21(12):1519-29.
90. Cavanaugh A, Juengst B, Sheridan K, Danella JF, Williams H. Combined inhibition of heat shock proteins 90 and 70 leads to simultaneous degradation of the oncogenic signaling proteins involved in muscle invasive bladder cancer. Oncotarget. 2015;6(37):39821-38.
91. Wu Q, Lian JB, Stein JL, Stein GS, Nickerson JA, Imbalzano AN. The BRG1 ATPase of human SWI/SNF chromatin remodeling enzymes as a driver of cancer. Epigenomics. 2017;9(6):919-31.
92. Hargreaves DC, Crabtree GR. ATP-dependent chromatin remodeling: genetics, genomics and mechanisms. Cell Res. 2011;21(3):396-420.
93. Wang J, Wang F, Wang N, Zhang MY, Wang HY, Huang GL. Diagnostic and Prognostic Value of Protein Post-translational Modifications in Hepatocellular Carcinoma. J Clin Transl Hepatol. 2023;11(5):1192-200.
94. Greer EL, Shi Y. Histone methylation: a dynamic mark in health, disease and inheritance. Nat Rev Genet. 2012;13(5):343-57.
95. Byvoet P, Shepherd GR, Hardin JM, Noland BJ. The distribution and turnover of labeled methyl groups in histone fractions of cultured mammalian cells. Arch Biochem Biophys. 1972;148(2):558-67.
96. Shi Y, Lan F, Matson C, Mulligan P, Whetstine JR, Cole PA, et al. Histone demethylation mediated by the nuclear amine oxidase homolog LSD1. Cell. 2004;119(7):941-53.
97. Shi X, Hong T, Walter KL, Ewalt M, Michishita E, Hung T, et al. ING2 PHD domain links histone H3 lysine 4 methylation to active gene repression. Nature. 2006;442(7098):96-9.
98. Hoeijmakers JH. Genome maintenance mechanisms for preventing cancer. Nature. 2001;411(6835):366-74.
99. Cao J, Yan Q. Histone ubiquitination and deubiquitination in transcription, DNA damage response, and cancer. Front Oncol. 2012;2:26.
100. Lin Y, Qiu Y, Xu C, Liu Q, Peng B, Kaufmann GF, et al. Functional role of asparaginyl endopeptidase ubiquitination by TRAF6 in tumor invasion and metastasis. J Natl Cancer Inst. 2014;106(4):dju012.
101. Prenzel T, Begus-Nahrmann Y, Kramer F, Hennion M, Hsu C, Gorsler T, et al. Estrogen-dependent gene transcription in human breast cancer cells relies upon proteasome-dependent monoubiquitination of histone H2B. Cancer Res. 2011;71(17):5739-53.
102. Zhu P, Zhou W, Wang J, Puc J, Ohgi KA, Erdjument-Bromage H, et al. A histone H2A deubiquitinase complex coordinating histone acetylation and H1 dissociation in transcriptional regulation. Mol Cell. 2007;27(4):609-21.
103. Graff J, Tsai LH. Histone acetylation: molecular mnemonics on the chromatin. Nat Rev Neurosci. 2013;14(2):97-111.
104. McGhee JD, Felsenfeld G. Nucleosome structure. Annu Rev Biochem. 1980;49:1115-56.
105. Goelet P, Castellucci VF, Schacher S, Kandel ER. The long and the short of long-term memory--a molecular framework. Nature. 1986;322(6078):419-22.
106. Allaire M, El Hajj W, Brichler S, Diallo K, Fanica D, Blaise L, et al. Prior surveillance and antiviral treatment improve the prognosis of HCC developed in HBV patients in the West. Clin Res Hepatol Gastroenterol. 2021;45(1):101436.
107. Downs JA, Lowndes NF, Jackson SP. A role for Saccharomyces cerevisiae histone H2A in DNA repair. Nature. 2000;408(6815):1001-4.

108. Garcia Fernandez F, Lemos B, Khalil Y, Batrin R, Haber JE, Fabre E. Modified chromosome structure caused by phosphomimetic H2A modulates the DNA damage response by increasing chromatin mobility in yeast. J Cell Sci. 2021;134(6).
109. Redon C, Pilch DR, Bonner WM. Genetic analysis of Saccharomyces cerevisiae H2A serine 129 mutant suggests a functional relationship between H2A and the sister-chromatid cohesion partners Csm3-Tof1 for the repair of topoisomerase I-induced DNA damage. Genetics. 2006;172(1):67-76.
110. Gajos-Michniewicz A, Czyz M. WNT/beta-catenin signaling in hepatocellular carcinoma: The aberrant activation, pathogenic roles, and therapeutic opportunities. Genes Dis. 2024;11(2):727-46.
111. Tian LY, Smit DJ, Jucker M. The Role of PI3K/AKT/mTOR Signaling in Hepatocellular Carcinoma Metabolism. Int J Mol Sci. 2023;24(3).
112. Liu J, Xiao Q, Xiao J, Niu C, Li Y, Zhang X, et al. Wnt/beta-catenin signalling: function, biological mechanisms, and therapeutic opportunities. Signal Transduct Target Ther. 2022;7(1):3.
113. Perugorria MJ, Olaizola P, Labiano I, Esparza-Baquer A, Marzioni M, Marin JJG, et al. Wnt-beta-catenin signalling in liver development, health and disease. Nat Rev Gastroenterol Hepatol. 2019;16(2):121-36.
114. Fan J, Wei Q, Liao J, Zou Y, Song D, Xiong D, et al. Noncanonical Wnt signaling plays an important role in modulating canonical Wnt-regulated stemness, proliferation and terminal differentiation of hepatic progenitors. Oncotarget. 2017;8(16):27105-19.
115. Wakizaka K, Kamiyama T, Wakayama K, Orimo T, Shimada S, Nagatsu A, et al. Role of Wnt5a in suppressing invasiveness of hepatocellular carcinoma via epithelial-mesenchymal transition. Oncol Lett. 2020;20(5):268.
116. Choudhary HB, Mandlik SK, Mandlik DS. Role of p53 suppression in the pathogenesis of hepatocellular carcinoma. World J Gastrointest Pathophysiol. 2023;14(3):46-70.
117. Kew MC. Hepatitis B virus x protein in the pathogenesis of hepatitis B virus-induced hepatocellular carcinoma. J Gastroenterol Hepatol. 2011;26 Suppl 1:144-52.
118. Anzola M, Burgos JJ. Hepatocellular carcinoma: molecular interactions between hepatitis C virus and p53 in hepatocarcinogenesis. Expert Rev Mol Med. 2003;5(28):1-16.
119. Wetzker R, Bohmer FD. Transactivation joins multiple tracks to the ERK/MAPK cascade. Nat Rev Mol Cell Biol. 2003;4(8):651-7.
120. Li L, Zhao GD, Shi Z, Qi LL, Zhou LY, Fu ZX. The Ras/Raf/MEK/ERK signaling pathway and its role in the occurrence and development of HCC. Oncol Lett. 2016;12(5):3045-50.
121. Huang P, Xu X, Wang L, Zhu B, Wang X, Xia J. The role of EGF-EGFR signalling pathway in hepatocellular carcinoma inflammatory microenvironment. J Cell Mol Med. 2014;18(2):218-30.
122. Moon H, Ro SW. MAPK/ERK Signaling Pathway in Hepatocellular Carcinoma. Cancers (Basel). 2021;13(12).
123. Fruman DA, Rommel C. PI3K and cancer: lessons, challenges and opportunities. Nat Rev Drug Discov. 2014;13(2):140-56.
124. Buontempo F, Ersahin T, Missiroli S, Senturk S, Etro D, Ozturk M, et al. Inhibition of Akt signaling in hepatoma cells induces apoptotic cell death independent of Akt activation status. Invest New Drugs. 2011;29(6):1303-13.
125. Hara K, Maruki Y, Long X, Yoshino K, Oshiro N, Hidayat S, et al. Raptor, a binding partner of target of rapamycin (TOR), mediates TOR action. Cell. 2002;110(2):177-89.
126. Nebbioso A, Tambaro FP, Dell'Aversana C, Altucci L. Cancer epigenetics: Moving forward. PLoS Genet. 2018;14(6):e1007362.
127. Zheng Z, Li L, Li G, Zhang Y, Dong C, Ren F, et al. EZH2/EHMT2 Histone Methyltransferases Inhibit the Transcription of DLX5 and Promote the Transformation of Myelodysplastic Syndrome to Acute Myeloid Leukemia. Front Cell Dev Biol. 2021;9:619795.
128. Nachiyappan A, Gupta N, Taneja R. EHMT1/EHMT2 in EMT, cancer stemness and drug resistance: emerging evidence and mechanisms. FEBS J. 2022;289(5):1329-51.

129. Ringrose L, Paro R. Epigenetic regulation of cellular memory by the Polycomb and Trithorax group proteins. Annu Rev Genet. 2004;38:413-43.
130. Eckert RL, Adhikary G, Rorke EA, Chew YC, Balasubramanian S. Polycomb group proteins are key regulators of keratinocyte function. J Invest Dermatol. 2011;131(2):295-301.
131. Lyko F, Paro R. Chromosomal elements conferring epigenetic inheritance. Bioessays. 1999;21(10):824-32.
132. Maurange C, Paro R. A cellular memory module conveys epigenetic inheritance of hedgehog expression during Drosophila wing imaginal disc development. Genes Dev. 2002;16(20):2672-83.
133. Horard B, Tatout C, Poux S, Pirrotta V. Structure of a polycomb response element and in vitro binding of polycomb group complexes containing GAGA factor. Mol Cell Biol. 2000;20(9):3187-97.
134. Wang W, Qin JJ, Voruganti S, Nag S, Zhou J, Zhang R. Polycomb Group (PcG) Proteins and Human Cancers: Multifaceted Functions and Therapeutic Implications. Med Res Rev. 2015;35(6):1220-67.
135. Beisel C, Paro R. Silencing chromatin: comparing modes and mechanisms. Nat Rev Genet. 2011;12(2):123-35.
136. Schuettengruber B, Cavalli G. Recruitment of polycomb group complexes and their role in the dynamic regulation of cell fate choice. Development. 2009;136(21):3531-42.
137. Sparmann A, van Lohuizen M. Polycomb silencers control cell fate, development and cancer. Nat Rev Cancer. 2006;6(11):846-56.
138. Reik W. Stability and flexibility of epigenetic gene regulation in mammalian development. Nature. 2007;447(7143):425-32.
139. Piunti A, Shilatifard A. The roles of Polycomb repressive complexes in mammalian development and cancer. Nat Rev Mol Cell Biol. 2021;22(5):326-45.
140. Wu KJ, Grandori C, Amacker M, Simon-Vermot N, Polack A, Lingner J, Dalla-Favera R. Direct activation of TERT transcription by c-MYC. Nat Genet. 1999;21(2):220-4.
141. Agherbi H, Gaussmann-Wenger A, Verthuy C, Chasson L, Serrano M, Djabali M. Polycomb mediated epigenetic silencing and replication timing at the INK4a/ARF locus during senescence. PLoS One. 2009;4(5):e5622.
142. Bracken AP, Helin K. Polycomb group proteins: navigators of lineage pathways led astray in cancer. Nat Rev Cancer. 2009;9(11):773-84.
143. Shen X, Liu Y, Hsu YJ, Fujiwara Y, Kim J, Mao X, et al. EZH1 mediates methylation on histone H3 lysine 27 and complements EZH2 in maintaining stem cell identity and executing pluripotency. Mol Cell. 2008;32(4):491-502.
144. Chen T, Dent SY. Chromatin modifiers and remodellers: regulators of cellular differentiation. Nat Rev Genet. 2014;15(2):93-106.
145. Kuzmichev A, Nishioka K, Erdjument-Bromage H, Tempst P, Reinberg D. Histone methyltransferase activity associated with a human multiprotein complex containing the Enhancer of Zeste protein. Genes Dev. 2002;16(22):2893-905.
146. Brown JL, Fritsch C, Mueller J, Kassis JA. The Drosophila pho-like gene encodes a YY1-related DNA binding protein that is redundant with pleiohomeotic in homeotic gene silencing. Development. 2003;130(2):285-94.
147. Lanzuolo C, Orlando V. Memories from the polycomb group proteins. Annu Rev Genet. 2012;46:561-89.
148. Iwata S, Takenobu H, Kageyama H, Koseki H, Ishii T, Nakazawa A, et al. Polycomb group molecule PHC3 regulates polycomb complex composition and prognosis of osteosarcoma. Cancer Sci. 2010;101(7):1646-52.
149. Kirmizis A, Bartley SM, Kuzmichev A, Margueron R, Reinberg D, Green R, Farnham PJ. Silencing of human polycomb target genes is associated with methylation of histone H3 Lys 27. Genes Dev. 2004;18(13):1592-605.

150. Morin RD, Johnson NA, Severson TM, Mungall AJ, An J, Goya R, et al. Somatic mutations altering EZH2 (Tyr641) in follicular and diffuse large B-cell lymphomas of germinal-center origin. Nat Genet. 2010;42(2):181-5.
151. Lee ST, Li Z, Wu Z, Aau M, Guan P, Karuturi RK, et al. Context-specific regulation of NF-kappaB target gene expression by EZH2 in breast cancers. Mol Cell. 2011;43(5):798-810.
152. Wu H, Zeng H, Dong A, Li F, He H, Senisterra G, et al. Structure of the catalytic domain of EZH2 reveals conformational plasticity in cofactor and substrate binding sites and explains oncogenic mutations. PLoS One. 2013;8(12):e83737.
153. Liu Y, Yang Q. The roles of EZH2 in cancer and its inhibitors. Med Oncol. 2023;40(6):167.
154. Gonzalez ME, Moore HM, Li X, Toy KA, Huang W, Sabel MS, et al. EZH2 expands breast stem cells through activation of NOTCH1 signaling. Proc Natl Acad Sci U S A. 2014;111(8):3098-103.
155. Wang J, Yu X, Gong W, Liu X, Park KS, Ma A, et al. EZH2 noncanonically binds cMyc and p300 through a cryptic transactivation domain to mediate gene activation and promote oncogenesis. Nat Cell Biol. 2022;24(3):384-99.
156. Jeong GY, Park MK, Choi HJ, An HW, Park YU, Choi HJ, et al. NSD3-Induced Methylation of H3K36 Activates NOTCH Signaling to Drive Breast Tumor Initiation and Metastatic Progression. Cancer Res. 2021;81(1):77-90.
157. Wang Y, Hou N, Cheng X, Zhang J, Tan X, Zhang C, et al. Ezh2 Acts as a Tumor Suppressor in Kras-driven Lung Adenocarcinoma. Int J Biol Sci. 2017;13(5):652-9.
158. Fischle W, Wang Y, Jacobs SA, Kim Y, Allis CD, Khorasanizadeh S. Molecular basis for the discrimination of repressive methyl-lysine marks in histone H3 by Polycomb and HP1 chromodomains. Genes Dev. 2003;17(15):1870-81.
159. Gao Z, Zhang J, Bonasio R, Strino F, Sawai A, Parisi F, et al. PCGF homologs, CBX proteins, and RYBP define functionally distinct PRC1 family complexes. Mol Cell. 2012;45(3):344-56.
160. Nielsen SJ, Schneider R, Bauer UM, Bannister AJ, Morrison A, O'Carroll D, et al. Rb targets histone H3 methylation and HP1 to promoters. Nature. 2001;412(6846):561-5.
161. Lachner M, O'Carroll D, Rea S, Mechtler K, Jenuwein T. Methylation of histone H3 lysine 9 creates a binding site for HP1 proteins. Nature. 2001;410(6824):116-20.
162. Jangal M, Lebeau B, Witcher M. Beyond EZH2: is the polycomb protein CBX2 an emerging target for anti-cancer therapy? Expert Opin Ther Targets. 2019;23(7):565-78.
163. Iqbal MA, Siddiqui S, Ur Rehman A, Siddiqui FA, Singh P, Kumar B, Saluja D. Multiomics integrative analysis reveals antagonistic roles of CBX2 and CBX7 in metabolic reprogramming of breast cancer. Mol Oncol. 2021;15(5):1450-65.
164. Morey L, Pascual G, Cozzuto L, Roma G, Wutz A, Benitah SA, Di Croce L. Nonoverlapping functions of the Polycomb group Cbx family of proteins in embryonic stem cells. Cell Stem Cell. 2012;10(1):47-62.
165. Dai T, Liu Y, Cao R, Cao J. CBX7 regulates metastasis of basal-like breast cancer through Twist1/EphA2 pathway. Transl Oncol. 2022;24:101468.
166. Kagey MH, Melhuish TA, Wotton D. The polycomb protein Pc2 is a SUMO E3. Cell. 2003;113(1):127-37.
167. Li J, Xu Y, Long XD, Wang W, Jiao HK, Mei Z, et al. Cbx4 governs HIF-1alpha to potentiate angiogenesis of hepatocellular carcinoma by its SUMO E3 ligase activity. Cancer Cell. 2014;25(1):118-31.
168. Jiao HK, Xu Y, Li J, Wang W, Mei Z, Long XD, Chen GQ. Prognostic significance of Cbx4 expression and its beneficial effect for transarterial chemoembolization in hepatocellular carcinoma. Cell Death Dis. 2015;6(3):e1689.
169. Jia Y, Wang Y, Zhang C, Chen MY. Upregulated CBX8 Promotes Cancer Metastasis via the WNK2/MMP2 Pathway. Mol Ther Oncolytics. 2020;19:188-96.

170. Chen H, Su Y, Yang L, Xi L, Li X, Lan B, et al. CBX8 promotes lung adenocarcinoma growth and metastasis through transcriptional repression of CDKN2C and SCEL. J Cell Physiol. 2023;238(11):2710-23.
171. Fonfria-Subiros E, Acosta-Reyes F, Saperas N, Pous J, Subirana JA, Campos JL. Crystal structure of a complex of DNA with one AT-hook of HMGA1. PLoS One. 2012;7(5):e37120.
172. Tardat M, Albert M, Kunzmann R, Liu Z, Kaustov L, Thierry R, et al. Cbx2 targets PRC1 to constitutive heterochromatin in mouse zygotes in a parent-of-origin-dependent manner. Mol Cell. 2015;58(1):157-71.
173. Kawaguchi T, Machida S, Kurumizaka H, Tagami H, Nakayama JI. Phosphorylation of CBX2 controls its nucleosome-binding specificity. J Biochem. 2017;162(5):343-55.
174. Clermont PL, Crea F, Chiang YT, Lin D, Zhang A, Wang JZ, et al. Identification of the epigenetic reader CBX2 as a potential drug target in advanced prostate cancer. Clin Epigenetics. 2016;8:16.
175. Zheng S, Lv P, Su J, Miao K, Xu H, Li M. Overexpression of CBX2 in breast cancer promotes tumor progression through the PI3K/AKT signaling pathway. Am J Transl Res. 2019;11(3):1668-82.
176. Wheeler LJ, Watson ZL, Qamar L, Yamamoto TM, Post MD, Berning AA, et al. CBX2 identified as driver of anoikis escape and dissemination in high grade serous ovarian cancer. Oncogenesis. 2018;7(11):92.
177. Liao X, Wang X, Huang K, Han C, Deng J, Yu T, et al. Integrated analysis of competing endogenous RNA network revealing potential prognostic biomarkers of hepatocellular carcinoma. J Cancer. 2019;10(14):3267-83.
178. Mao J, Tian Y, Wang C, Jiang K, Li R, Yao Y, et al. CBX2 Regulates Proliferation and Apoptosis via the Phosphorylation of YAP in Hepatocellular Carcinoma. J Cancer. 2019;10(12):2706-19.
179. van den Boom V, Rozenveld-Geugien M, Bonardi F, Malanga D, van Gosliga D, Heijink AM, et al. Nonredundant and locus-specific gene repression functions of PRC1 paralog family members in human hematopoietic stem/progenitor cells. Blood. 2013;121(13):2452-61.
180. Zhao Y, Hu Q, Cheng F, Su N, Wang A, Zou Y, et al. SoNar, a Highly Responsive NAD+/NADH Sensor, Allows High-Throughput Metabolic Screening of Anti-tumor Agents. Cell Metab. 2015;21(5):777-89.
181. McLaughlin KJ, Strain-Damerell CM, Xie K, Brekasis D, Soares AS, Paget MS, Kielkopf CL. Structural basis for NADH/NAD+ redox sensing by a Rex family repressor. Mol Cell. 2010;38(4):563-75.
182. Hu Q, Wu D, Walker M, Wang P, Tian R, Wang W. Genetically encoded biosensors for evaluating NAD(+)/NADH ratio in cytosolic and mitochondrial compartments. Cell Rep Methods. 2021;1(7).
183. Otte AP, Kwaks TH. Gene repression by Polycomb group protein complexes: a distinct complex for every occasion? Curr Opin Genet Dev. 2003;13(5):448-54.
184. Abate E, Mehdi M, Addisu S, Degef M, Tebeje S, Kelemu T. Emerging roles of cytosolic phosphoenolpyruvate kinase 1 (PCK1) in cancer. Biochem Biophys Rep. 2023;35:101528.
185. Mendez-Lucas A, Hyrossova P, Novellasdemunt L, Vinals F, Perales JC. Mitochondrial phosphoenolpyruvate carboxykinase (PEPCK-M) is a pro-survival, endoplasmic reticulum (ER) stress response gene involved in tumor cell adaptation to nutrient availability. J Biol Chem. 2014;289(32):22090-102.
186. DeBerardinis RJ, Mancuso A, Daikhin E, Nissim I, Yudkoff M, Wehrli S, Thompson CB. Beyond aerobic glycolysis: transformed cells can engage in glutamine metabolism that exceeds the requirement for protein and nucleotide synthesis. Proc Natl Acad Sci U S A. 2007;104(49):19345-50.
187. Hasunuma T, Matsuda M, Kato Y, Vavricka CJ, Kondo A. Temperature enhanced succinate production concurrent with increased central metabolism turnover in the cyanobacterium Synechocystis sp. PCC 6803. Metab Eng. 2018;48:109-20.
188. Ito S, Hakamada T, Ogino T, Osanai T. Reconstitution of oxaloacetate metabolism in the tricarboxylic acid cycle in Synechocystis sp. PCC 6803: discovery of important factors that directly affect the conversion of oxaloacetate. Plant J. 2021;105(6):1449-58.

189. Knoop H, Grundel M, Zilliges Y, Lehmann R, Hoffmann S, Lockau W, Steuer R. Flux balance analysis of cyanobacterial metabolism: the metabolic network of Synechocystis sp. PCC 6803. PLoS Comput Biol. 2013;9(6):e1003081.
190. Hu FF, Chen H, Duan Y, Lan B, Liu CJ, Hu H, et al. CBX2 and EZH2 cooperatively promote the growth and metastasis of lung adenocarcinoma. Mol Ther Nucleic Acids. 2022;27:670-84.
191. Qin X, Sun H, Hu S, Pan Y, Wang S. A hypoxia-glycolysis-lactate-related gene signature for prognosis prediction in hepatocellular carcinoma. BMC Med Genomics. 2024;17(1):88.
192. Wu Q, Li P, Tao X, Lin N, Mao B, Xie X. A novel super-enhancer-related risk model for predicting prognosis and guiding personalized treatment in hepatocellular carcinoma. BMC Cancer. 2024;24(1):1087.
193. Zeng M, Li B, Yang L, Guan Q. CBX2 depletion inhibits the proliferation, invasion and migration of gastric cancer cells by inactivating the YAP/beta-catenin pathway. Mol Med Rep. 2021;23(2).
194. Pacl HT, Chinta KC, Reddy VP, Nadeem S, Sevalkar RR, Nargan K, et al. NAD(H) homeostasis underlies host protection mediated by glycolytic myeloid cells in tuberculosis. Nat Commun. 2023;14(1):5472.
195. Lee M, Yoo JH, Kim I, Kang S, Lee W, Kim S, Han KS. The compartment-specific manipulation of the NAD(+)/NADH ratio affects the metabolome and the function of glioblastoma. Sci Rep. 2024;14(1):20575.
196. Moreira JD, Hamraz M, Abolhassani M, Bigan E, Peres S, Pauleve L, et al. The Redox Status of Cancer Cells Supports Mechanisms behind the Warburg Effect. Metabolites. 2016;6(4).
197. Canto C, Menzies KJ, Auwerx J. NAD(+) Metabolism and the Control of Energy Homeostasis: A Balancing Act between Mitochondria and the Nucleus. Cell Metab. 2015;22(1):31-53.
198. Liu MX, Jin L, Sun SJ, Liu P, Feng X, Cheng ZL, et al. Metabolic reprogramming by PCK1 promotes TCA cataplerosis, oxidative stress and apoptosis in liver cancer cells and suppresses hepatocellular carcinoma. Oncogene. 2018;37(12):1637-53.
199. Bluemel G, Planque M, Madreiter-Sokolowski CT, Haitzmann T, Hrzenjak A, Graier WF, et al. PCK2 opposes mitochondrial respiration and maintains the redox balance in starved lung cancer cells. Free Radic Biol Med. 2021;176:34-45.
200. Nordlie RC, Foster JD, Lange AJ. Regulation of glucose production by the liver. Annu Rev Nutr. 1999;19:379-406.
201. Chang TM, Fang WY, Hsu HP, Chu PY, Jiang SS, Huang KW, et al. PCK2 promotes invasion and epithelial-to-mesenchymal transition in triple-negative breast cancer by promoting TGF-beta/SMAD3 signaling through inhibiting TRIM67-mediated SMAD3 ubiquitination. Cancer Biol Ther. 2025;26(1):2478670.
202. Dong H, Feng Y, Yang Y, Hu Y, Jia Y, Yang S, et al. A Novel Function of Mitochondrial Phosphoenolpyruvate Carboxykinase as a Regulator of Inflammatory Response in Kupffer Cells. Front Cell Dev Biol. 2021;9:726931.